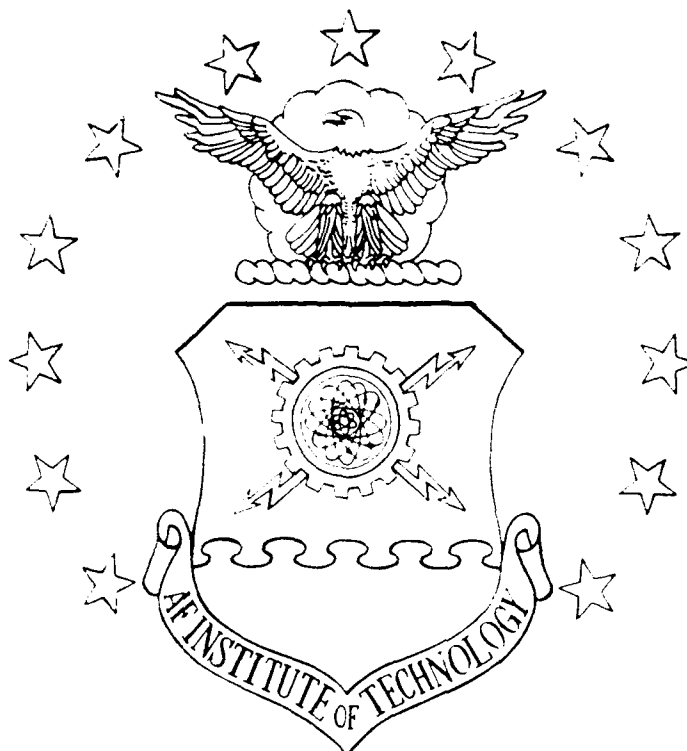


AD-A230 555



NUMERICAL ANALYSIS OF AN
AXISYMMETRIC THRUST AUGMENTING
EJECTOR

THESIS

Kenneth R. Gage, Captain, USAF
AFIT/GAE/ENY/89D-10

DEPARTMENT OF THE AIR FORCE
AIR UNIVERSITY

AIR FORCE INSTITUTE OF TECHNOLOGY

DTIC
ELECTE
JAN 09 1991

S **E** **D**

Wright-Patterson Air Force Base, Ohio

DISTRIBUTION STATEMENT A

Approved for public release;
Distribution Unlimited

94 1 3 096

1

AFIT/GAE/ENY/89D-10

NUMERICAL ANALYSIS OF AN
AXISYMMETRIC THRUST AUGMENTING
EJECTOR

THESIS
Kenneth R. Gage, Captain, USAF
AFIT/GAE/ENY/89D-10

DTIC
68-10000-1
1-1

DISTRIBUTION STATEMENT A
Approved for public release
Distribution Unlimited

AFIT/GAE/ENY/89D-10

NUMERICAL ANALYSIS OF AN AXISYMMETRIC THRUST
AUGMENTING EJECTOR

THESIS

Presented to the Faculty of the School of Engineering
of the Air Force Institute of Technology
Air University
In Partial Fulfillment of the
Requirements for the Degree of
Master of Science in Aeronautical Engineering

Kenneth R. Gage, B.S.
Captain, USAF

December 1990

Approved for public release; distribution unlimited

Acknowledgments

This project has been a long time in work and has been full of ups and downs, more than I care to recall. Through it all, the support of a few people have kept it, and me, all going. I would like to take this opportunity to thank them.

To my advisor, Dr. Franke, for supporting me in taking on a project which interested me although it was somewhat out of his field.

To Dr. Joe Shang, for giving me access to the resources and personnel to help me along and for the guiding hand when I needed it most.

To Dr. Don Rizzetta, for helping me iron out the little technicalities.

Especially to Dr. Kervyn Mach, for setting up and guiding me through the myriad complexities of working on an unfamiliar system and for helping me to understand the program I had to modify!

But mostly to my wife Barbara, who had to put up with what seemed like an interminable wait.

Accession For	
NTIS GRA&I	<input checked="checked" type="checkbox"/>
DTIC TAB	<input type="checkbox"/>
Unannounced	<input type="checkbox"/>
Justification	
By	
Distribution/	
Availability Codes	
Dist	Avail and/or Special
A-1	

Table of Contents

	Page
Acknowledgments	ii
List of Figures	v
List of Tables	vii
Notation	viii
Abstract	x
I. INTRODUCTION	1
Background	1
Purpose and Objectives	8
Scope	9
II. COMPUTATIONAL APPROACH AND PROCEDURES	11
Ejector Geometry	11
Grid	12
Flowfield Initialization	13
Flow Solver	15
Incorporation of Nozzle Structure	20
Boundary Conditions	22
Turbulence Model	26
Procedure	27
III. RESULTS AND DISCUSSION	29
Cases Investigated	29

Table of Contents (cont.)

	Page
Primary Objectives	30
Comparison With Experimental Data	30
Data Visualization	35
Flexibility	40
Secondary Objectives	40
Injection Angle	41
Nozzle Position	45
Nozzle Area Ratio	50
IV. CONCLUSIONS	53
V. SUGGESTIONS AND RECOMMENDATIONS	55
APPENDIX A: GRID GENERATING PROGRAMS AND TABLES	A-1
A-1: <i>EJECGRD</i>	A-2
A-2: <i>DEHNEN</i>	A-8
A-3: <i>EJECVRT</i>	A-10
A-4: <i>EJECHRZ</i>	A-12
APPENDIX B: FLOW SOLVING PROGRAM: <i>JSIAXK</i>	B-1
APPENDIX C: POST-PROCESSING PROGRAM: <i>AUGMENT</i>	C-1
Bibliography	
Vita	

List of Figures

Figure		Page
1.	Ejector Concept	2
2.	Ideal Thrust Augmentation vs. α	2
3.	Ejector with Diffuser	4
4.	Thrust Augmentation as a Function of α and β	6
5.	Ejector with Coanda Nozzles	6
6.	Control Volume	10
7.	Ejector Geometry	11
8.	Plane of Modeled Flow	12
9.	Computational Grid	14
10.	Identification of Nozzle Exit Corners	21
11.	Identification of Nozzle Walls	22
12.	Application of Boundary Conditions	23
13.	Nozzle Locations	31
14.	Exit Velocity Profile - Numerical	32
15.	Exit Velocity Profile - Experimental	32
16.	Thrust Augmentation vs. Injection Angle Numerical	33
17.	Thrust Augmentation vs. Injection Angle Experimental	34
18.	Total Velocity Contours	36
19.	Streamlines	37
20.	Velocity Vectors - Nozzle Area	38
21.	Inlet Velocity Profiles	38
22.	Mixing Chamber Velocity Profiles	39
23.	Diffuser Velocity Profiles	40
24.	Velocity Contours: $\alpha_1 = 64$ degrees	42
25.	Exit Velocity Profiles: $\alpha_1 = 52$ and 64 degrees	42

List of Figures (cont.)

Figure		Page
26.	Velocity Contours: $\alpha_1 = 36$ degrees	43
27.	Exit Velocity Profiles: $\alpha_1 = 52$ and 36 degrees	44
28.	Reference Injection Angles	45
29.	Optimum Injection Angle with Relation to Reference Angles	46
30.	Augmentation vs. Position Angle	47
31.	Nozzle Velocity Profile: Configuration 3	47
32.	Nozzle Velocity Profile: Configuration 0	48
33.	Pressure Contours: Configuration 3	49
34.	Pressure Contours: Configuration 0	49
35.	Augmentation vs. Nozzle Area Ratio (α) .	40
36.	Augmentation vs. Nozzle Area Ratio ($1/\alpha$) Numerical and Experimental	41

List of Tables

Table		Page
I.	Nozzle Geometries	30
II.	Thrust Augmentation Comparison	34
III.	Augmentation with Changing Injection Angle (α_1)	41
IV.	Augmentation with Changing Nozzle Area Ratio (α)	50

Notation

A	Cross-Sectional Area of Mixing Region
A _E	Cross-Sectional Area of (Diffuser) Exit
A _J	Cross-Sectional Area of Jet
A*	Critical Area
c _v	Specific Heat of Constant Volume
D	Van Driest Damping Factor
e	Energy
F	Thrust Force
F _{noz isen}	Isentropic Thrust of Primary Nozzle
F _{wake}	Wake Function
j	Radial Grid Index
k	Axial Grid Index
L	Scaling Length
L ₁ , L ₂	Diffuser Section Lengths
L ₁	Nozzle Position
M, N	Integers
P	Static Pressure
P _{o noz}	Nozzle Stagnation Pressure
P ₁	Static Pressure at Jet Exit Plane
P _a	Ambient Pressure
P _{rat}	Pressure Ratio
Pr	Prandtl Number
Pr _t	Turbulent Prandtl Number
R	Gas Constant for Air
r	Radial Cylindrical Coordinate
T	Static Temperature
T _a	Ambient Temperature
T _w	Constant Wall Temperature
t	Time
u	Axial Component of Velocity
U _{ref}	Reference Velocity

Notation (cont.)

V	Total Velocity
V_1	Secondary Flow Velocity at Jet Exit Plane
V_E	Velocity at Exit
V_J	Jet Velocity
v	Radial Component of Velocity
x	Axial Cylindrical Coordinate
y^*	Critical Distance from Wall
α	Nozzle Area Ratio A_J / A
α_1	Flow Injection Angle
β	Diffuser Area Ratio A_E / A
γ	Ratio of Specific Heats
ϵ	Turbulent Viscosity
ζ	'Axial' Curvilinear Coordinate
η	'Radial' Curvilinear Coordinate
θ	Nozzle Position Angle
μ	Viscosity
ρ	Density
σ	Normal Stresses
τ	Shear Stresses
\emptyset	Thrust Augmentation Ratio
γ_1, γ_2	Diffuser Angles
ω	Vorticity

Abstract

Use of an ejector is an effective way to increase the thrust produced by a jet. In this thesis project an axisymmetric ejector concept which had been previously explored by experiment was numerically modeled. An existing axisymmetric, internal flow code based on the explicit MacCormack method was modified to incorporate primary nozzle structure and flow injection within the flowfield. Results were compared qualitatively and quantitatively with experimental results to verify the validity of the model. Internal flow structure, difficult to obtain in experiment, is easily examined. This code may be used for parametric analysis of such ejector performance parameters as primary nozzle location, flow injection angle, diffuser area ratio, and inlet geometry to optimize future hardware configurations.

NUMERICAL ANALYSIS OF AN AXISYMMETRIC THRUST

AUGMENTING EJECTOR

I Introduction

Background

Ejectors provide an attractive solution to a problem which has plagued designers of jet powered Vertical/Short Takeoff and Landing (V/STOL) aircraft since they were conceived. The problem being, that in order to get thrust greater than the weight of the vehicle such that vertical takeoff or landing can be achieved, an aircraft must be equipped with a powerplant which is larger (sometimes substantially) than that which is needed for its primary mission. Ejectors, due to their thrust augmenting characteristics, provide a means for achieving thrust to weight ratios greater than unity with a more reasonably sized powerplant.

In an ejector, a jet flow is directed into an open duct of somewhat larger cross-sectional area. A secondary flow is induced through the duct by viscous entrainment (Figure 1). A simple analysis developed by Von Karman (18:461-62) shows that the thrust theoretically achievable by such a process is up to twice that of the primary nozzle alone (Figure 2).

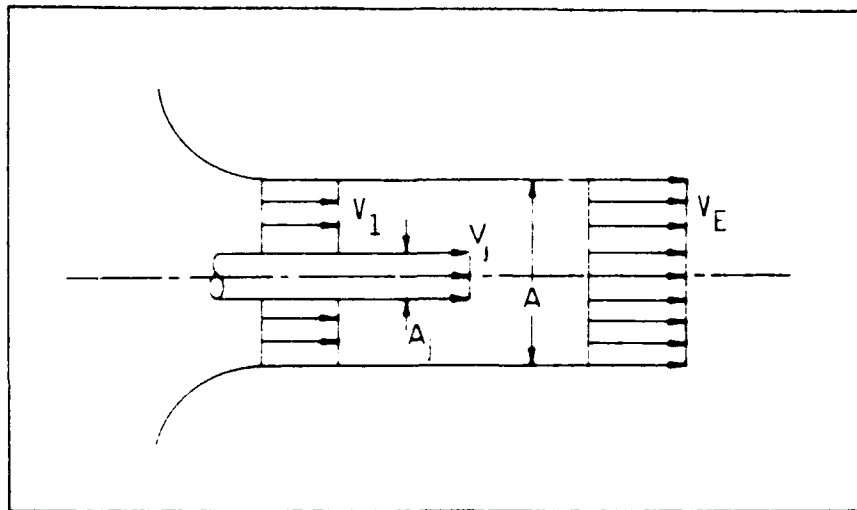


Fig. 1. Ejector Concept (9:281)

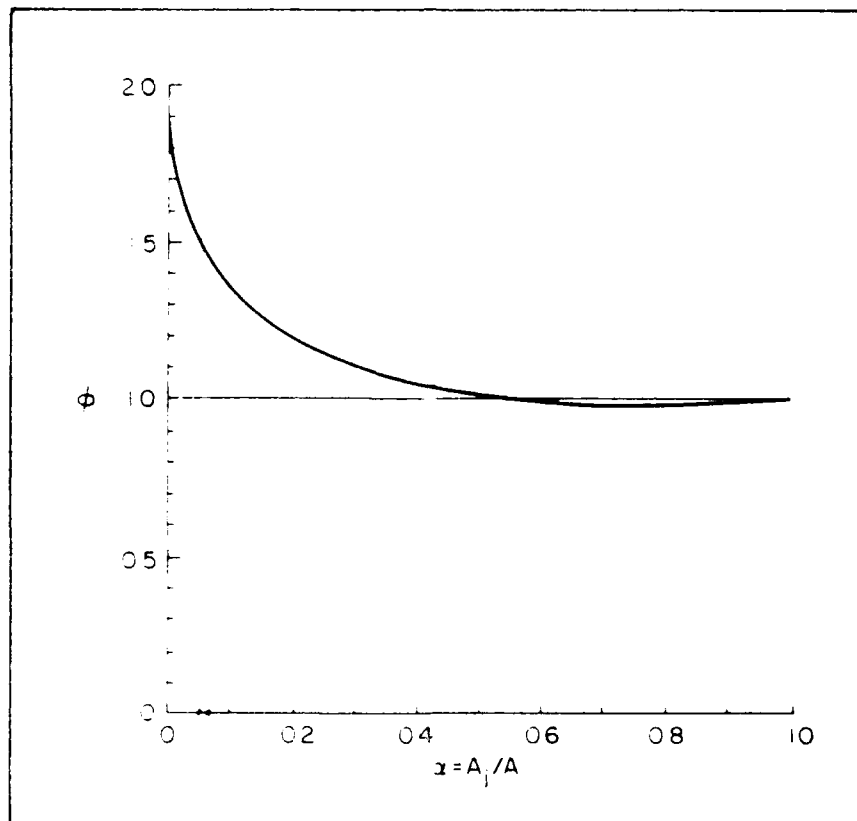


Fig. 2. Ideal Thrust Augmentation vs. α (9:281)

The thrust augmentation ratio (ϕ) is defined as the ratio of the total thrust of the ejector (F) to the isentropic thrust of the primary nozzle alone (assuming incompressible flow):

$$\phi = F / F_{noz isen}$$

$$\phi = \rho V_E^2 A / \rho V_j^2 A_j$$

$$\phi = (V_E/V_j)^2 / \alpha \quad (1)$$

where α is the ratio of the area of the jet (A_j) to the area of the mixing chamber (A)

$$\alpha = A_j/A$$

and V_E/V_j is the ratio of the flow velocity following complete mixing (V_E) to the flow velocity of the primary nozzle (V_j) found by applying continuity from the jet exit plane to the exit of the ejector:

$$V_1 (A - A_j) + V_j A_j = V_E A \quad (2)$$

and applying conservation of momentum:

$$A (P_1 - P_0) = \rho A V_E^2 - \rho A_j V_j^2 - \rho (A - A_j) V_1^2 \quad (3)$$

Applying Bernoulli's equation from ahead of the inlet to the jet exit plane:

$$P_0 = P_1 + \frac{1}{2} \rho V_1^2 \quad (4)$$

gives three equations in three unknowns, V_E , V_1 , and P_1 .

Eliminating V_1 and P_1 , the velocity ratio, V_E/V_J , is found to be:

$$V_E/V_J = \frac{[-a(1-2a) + (2a-6a^2+6a^3-2a^4)^{1/2}]}{(1-2a+2a^2)} \quad (5)$$

(7:28)

The thrust augmentation achieved may be further increased through the use of a diffuser (Figure 3).

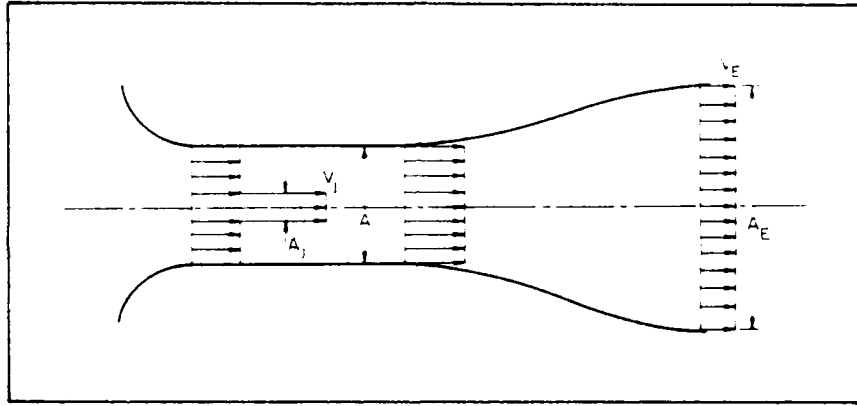


Fig. 3. Ejector with Diffuser (9:283)

Through a similar analysis, the modified equation for a diffuser equipped ejector is found to be:

$$(V_E/V_J)^2 + (V_E/V_J) \left[\frac{2a\beta(1-2a)}{1-2a+a^2(1+\beta^2)} \right] - \left[\frac{2a-3a^2}{1-2a+a^2(1+\beta^2)} \right] = 0 \quad (6)$$

(9:282)

with ϕ now given by (assuming incompressible flow):

$$\phi = \rho V_E^2 A_E / \rho V_J^2 A_J$$

$$\phi = (V_E/V_J)^2 (A_E/A) (A/A_J)$$

$$\phi = (V_E/V_J)^2 (\beta/\alpha) \quad (7)$$

where:

$$\beta = A_E/A$$

with V_E and A_E as defined in Figure 3 (9:282-3).

Plotting the thrust augmentation ratio shows that for every primary nozzle to mixing chamber area ratio (A_J/A) there is an optimum diffuser area ratio (A_E/A) which provides the maximum thrust augmentation (Figure 4). Within the practical limit of area ratios, it can be seen that thrust augmentations of up to 3 times the primary jet thrust are theoretically achievable.

These theoretical values, however, assume that the ejector is long enough that complete mixing of the primary and secondary flows takes place. In practice, the size of the ejector is limited by aircraft installation constraints and frictional effects, which lead to separations in long diffusers. In such short ejectors mixing is incomplete and coanda nozzles, in which the jet flow is injected along the wall (Figure 5), have proven to be more effective due to the greater mixing surface area of the primary jet. (9:286)

Coanda nozzles provide an additional benefit for ejectors equipped with a diffuser in that the high energy flow along the wall helps to prevent separation in the diffuser allowing greater area ratios to be achieved.

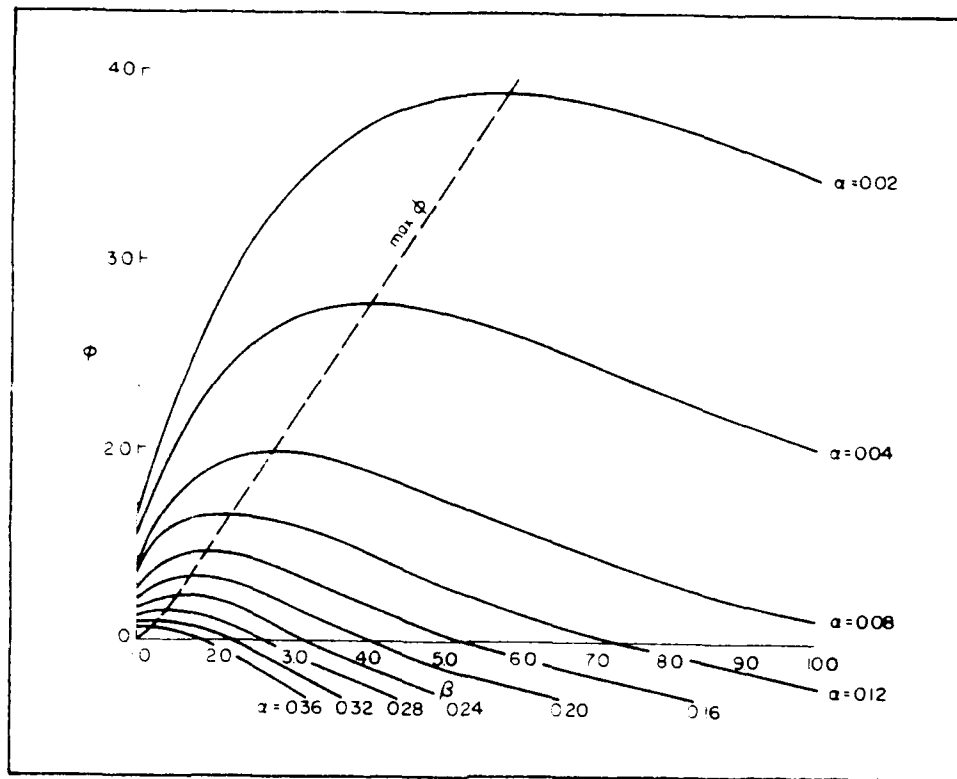


Fig. 4. Thrust Augmentation as a Function of α and β . (9:284)

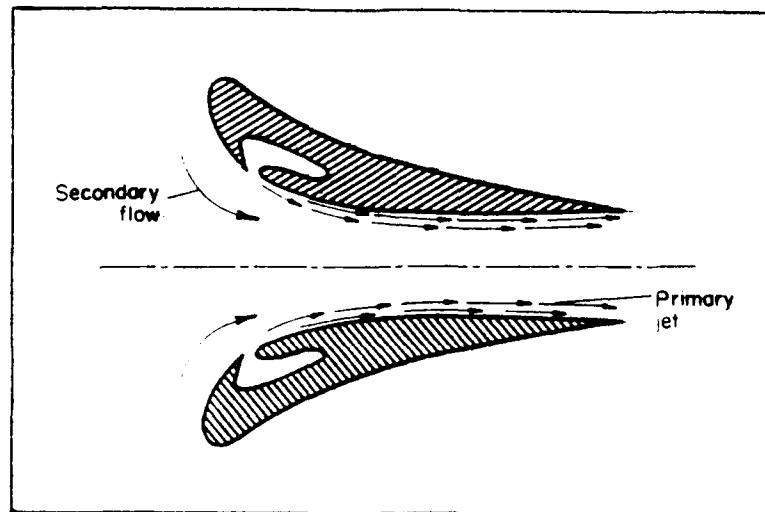


Fig. 5. Ejector with Coanda Nozzles (9:285)

In a previous study, Kedem, (6) experimentally investigated a two dimensional ejector with center and coanda nozzles and found that coanda nozzles did provide better performance (6:51). Reznick (11) and later Unnever (17) expanded on these results by testing both two dimensional and circular ejectors with coanda nozzles. The circular ejectors provided the best performance, achieving a thrust augmentation ratio of 2.09. This was accomplished through the use of discrete jets located about the periphery of the inlet which are referred to as 'hook nozzles' because of their hook-like shape (11:44). This approach was further investigated by Lewis (8) and later Uhuad (16). Hardware limitations necessarily constrained the various configurations which could be tested. It is desirable to have a computational model of a circular ejector which is free of such limitations. With this model a full range of inlet and diffuser geometries, nozzle sizes and positions, and nozzle plenum pressures can be investigated. The computational solutions also provide complete data on the behavior of the flow within the ejector, which is difficult, if not impossible, to obtain experimentally. This model has, however, been constrained to an axisymmetric case to reduce complexity and required computational power. This eliminates the possibility of modeling the hook nozzles used to achieve the high thrust augmentation observed by Reznick. This model is therefore constrained to the case of an annular nozzle, which was also one of the configurations tested by both Reznick and Unnever.

Purpose and Objectives

The primary objectives of this study are:

1. Develop a numerical algorithm that models a coanda flow axisymmetric ejector of the type tested by Reznick and Unnever.
2. Validate the model by demonstrating agreement with experimental results.
3. Provide data visualization of internal flow characteristics.
4. Provide sufficient flexibility to accomplish secondary objectives.
5. Begin preliminary investigation of secondary objectives.

The secondary objectives are:

1. Investigate the geometrical and fluid injection parameters which effect ejector performance. The parameters which may be investigated include:

- a) Fluid injection angle
- b) Nozzle position
- c) Nozzle area ratio
- d) Diffuser area ratio
- e) Diffuser geometry
- f) Pressure ratio ($P_{o\ noz} / P_a$)

2. From this parametric analysis, define new ejector configurations which may merit further experimental investigation.

Scope

A generic axisymmetric, internal, Navier-Stokes flow solver based on the explicit MacCormack method provided by WRDC/FIMM was modified to incorporate primary nozzle structure and flow injection within the flowfield (program JSIAXK, App B). A diffuser geometry, nozzle pressure ratio, and nozzle exit area and location were chosen for each run. The program was then run to a steady-state solution for a given flow injection angle (α_1). The injection angle was then varied and the run continued to new steady-state solutions to collect data on α_1 - variation of augmentation. Additional runs were made with different nozzle locations holding pressure ratio, nozzle area, and nozzle distance from the wall constant to provide data on nozzle location effects on augmentation. Also, runs were made with different nozzle areas for the same location to provide data on area ratio effects. Runs with different geometries and pressure ratios could provide data on variations with these parameters.

The achieved thrust was calculated by a control volume analysis (Figure 6). This analysis results in the equation:

$$F = \int_A \rho u^2 dA \quad (8)$$

where the right side of the equation is the integral of the x - momentum at the exit (5:12-13). The achieved thrust was compared to the isentropic thrust of the primary nozzle alone to calculate the thrust augmentation ratio as in equation (5). Thrust augmentation ratios were compared directly with experimental data for similar configurations and the differences analyzed. Exit plane velocity distributions and variation of thrust augmentation with α_1

and position were compared qualitatively with available experimental results.

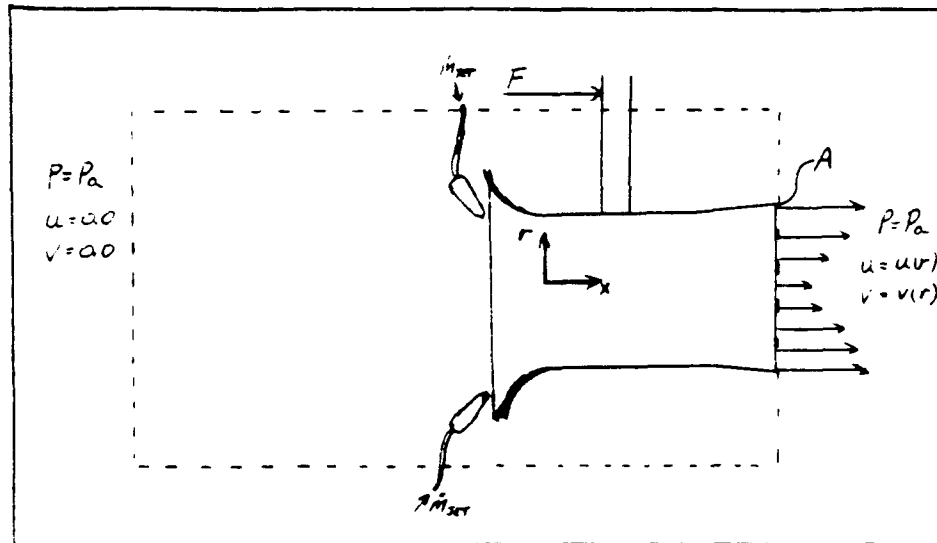


Fig. 6. Control Volume

II COMPUTATIONAL APPROACH AND PROCEDURES

Ejector Geometry

The geometry of the axisymmetric ejector which was investigated by Reznick and Unnever and was modeled in this study is portrayed in Figure 7. The mixing chamber was 4.4 inches in diameter and 3 inches in length, the inlet lip had a 2-inch radius of curvature, and the multi-section diffuser could be changed to alter the diffuser angles (ψ_1, ψ_2, \dots) and lengths (L_1, L_2, \dots), up to three sections, and thus the area ratio A_E/A . The annular exit of the nozzle had a gap of 0.065 inches and a radius of 3.0025 inches and could be positioned at any distance (L_1) from the ejector throat (constant area mixing chamber). (17:52)

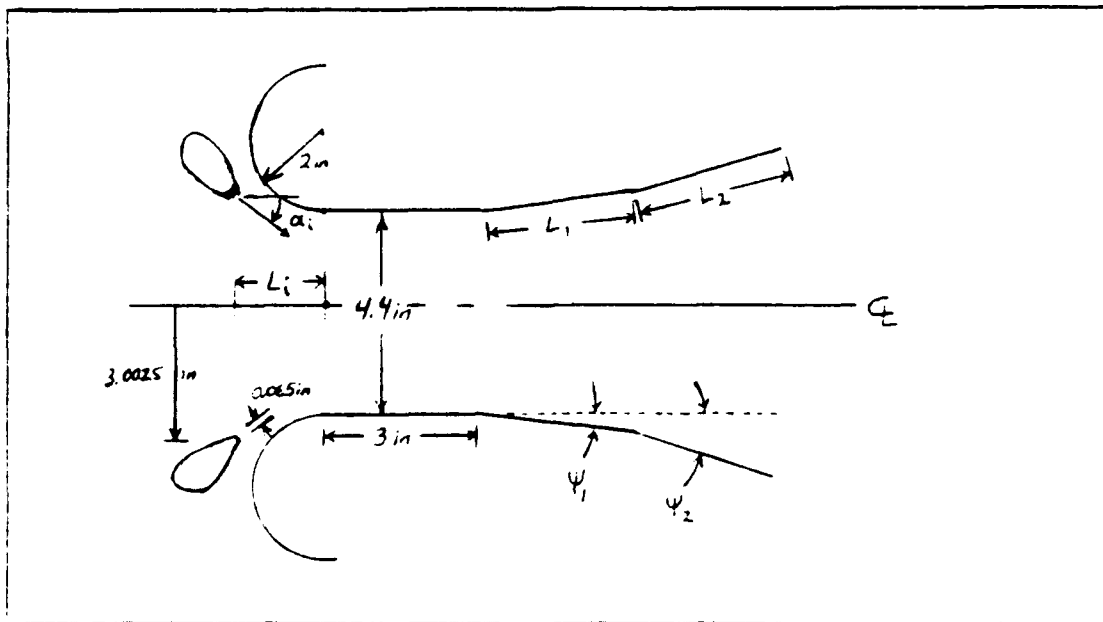


Fig. 7. Ejector Geometry

Grid

The computational grid was generated using the program EJEGRD (Appendix A-1) provided by WRDC/FIMM and modified for the required geometry. Taking advantage of axial symmetry, the grid models a single radial/axial plane from the centerline to the wall (Figure 8).

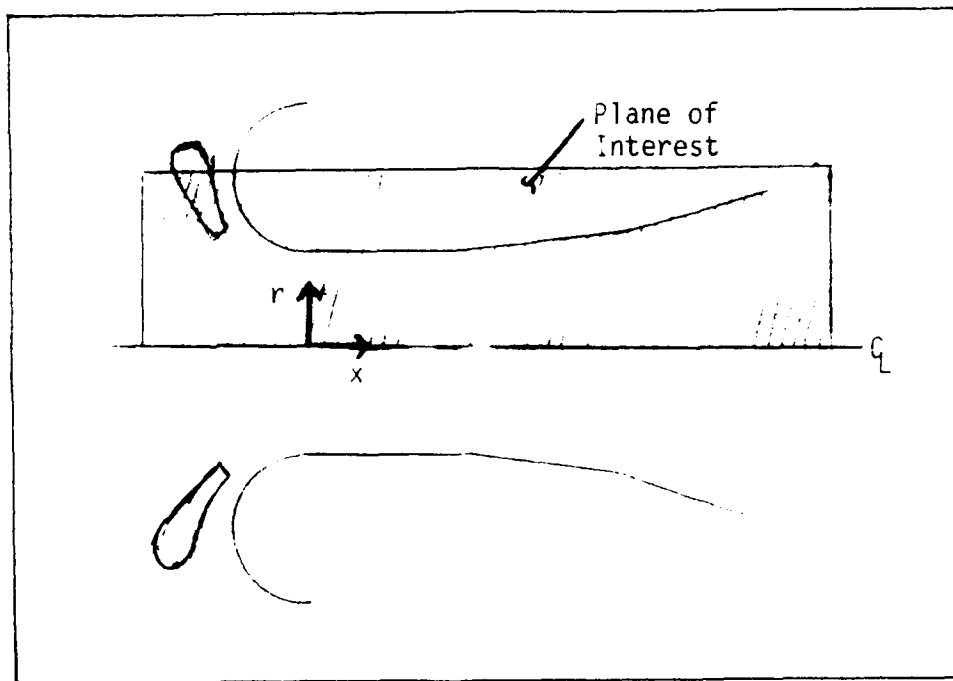


Fig. 8. Plane of Modeled Flow

The vertical (radial) grid lines are defined as follows:

For the inlet, by circular arcs perpendicular to the wall and centerline.

For the mixing area and diffuser, by parabolas perpendicular to the wall and centerline (which degenerate to straight lines for the mixing area).

Spacing between horizontal grid lines was varied exponentially to refine the grid near the wall where large gradients are found due to the jet. The grid was also refined near the centerline to minimize the effects of the boundary conditions. Spacing between vertical grid lines was varied exponentially to refine the grid in the vicinity of the inlet (and the jet exit) to help offset the tendency of the grid to spread out due to the increasing radii of the circular arcs in the inlet and also to concentrate on the larger gradients upstream. The exponential spacing was accomplished using the program DEHNEN (Appendix A-2) also provided by WRDC/FIMM which was used to produce vertical and horizontal grid spacing tables, EJE CVRT and EJE CHRZ (Appendices A-3,-4). Once a nozzle location was identified, the grid was refined both vertically and horizontally in the area of the nozzle exit. An example of the grid is shown in Figure 9. Note that only every fourth grid line has been drawn for the purpose of clarity.

Flowfield Initialization

The program EJE CGRD also calculates an initial flowfield based on a simple one-dimensional flow area ratio formula given a value of the critical area (A^*), the duct area through which the flow would theoretically be sonic. This critical area was chosen to provide a reference Mach number at the diffuser exit of 0.1 (111.7 ft/sec). This program was modified to overlay a high-speed jet flow over the low speed duct flow calculated by this procedure. This

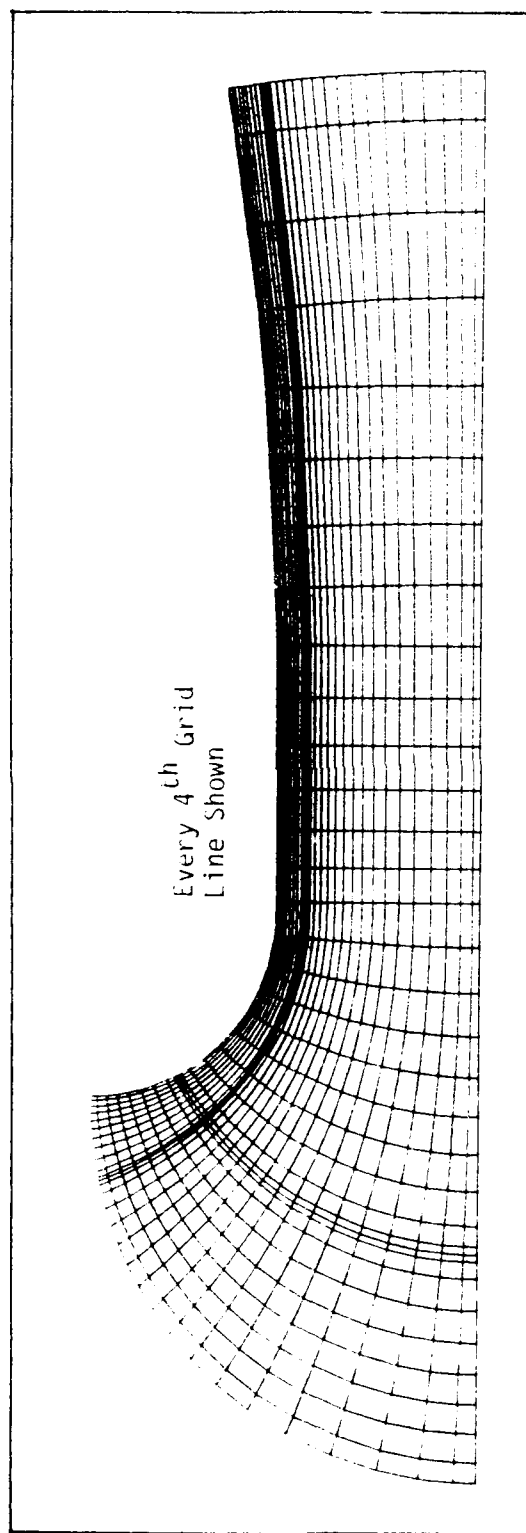


Fig. 9. Computational Grid

was necessary because the formula used assumes a mass flow balance between the beginning and end of the duct. If the jet flow is not accounted for, this provides an extremely poor initial flowfield which can lead to extended processing time or even cause the solution to 'blow up', or diverge, as the flowfield tries to adapt to the increased mass flow injected by the primary nozzle.

Flow Solver

The flow solving program JSIAXK (Appendix B) solves the conservative form of the Navier-Stokes equations using the explicit MacCormack scheme. The conservative Navier-Stokes equations in axisymmetric coordinates are (3:3):

Equation of Mass

$$\frac{\partial}{\partial t}(\rho) + \frac{\partial}{\partial x}(\rho u) + (1/r) \frac{\partial}{\partial r}(\rho v r) = 0 \quad (9)$$

Equation of Axial Motion

$$\frac{\partial}{\partial t}(\rho u) + \frac{\partial}{\partial x}(\rho u^2) + (1/r) \frac{\partial}{\partial r}(\rho u v r) = \frac{\partial}{\partial x}(\sigma_{xx}) + (1/r) \frac{\partial}{\partial r}(r \tau_{xr}) \quad (10)$$

Equation of Radial Motion

$$\frac{\partial}{\partial t}(\rho v) + \frac{\partial}{\partial x}(\rho u v) + (1/r) \frac{\partial}{\partial r}(\rho v^2 r) = \frac{\partial}{\partial x}(\tau_{xr}) + (1/r) \frac{\partial}{\partial r}(r \sigma_{rr}) - \sigma_H \quad (11)$$

Energy Equation

$$\begin{aligned} \frac{\partial}{\partial t}(\rho e) + \frac{\partial}{\partial x}(\rho u e) + (1/r) \frac{\partial}{\partial r}(\rho v e r) = \frac{\partial}{\partial x} \left[\gamma \frac{\partial e}{\partial x} \left(\frac{\mu}{Pr} + \frac{\epsilon}{Pr_t} \right) - (u \sigma_{xx} + v \tau_{xr}) \right] \\ + (1/r) \frac{\partial}{\partial r} \left[r \gamma \frac{\partial e}{\partial r} \left(\frac{\mu}{Pr} + \frac{\epsilon}{Pr_t} \right) - r (u \tau_{xr} + v \sigma_{rr}) \right] \quad (12) \end{aligned}$$

These equations are written in vector form as (4:17):

$$\frac{\partial \vec{U}}{\partial t} + \frac{\partial \vec{F}}{\partial x} + (1/r) \frac{\partial \vec{G}}{\partial r} = (1/r) \vec{H} \quad (13)$$

where:

$$\vec{U} = \begin{bmatrix} \rho \\ \rho u \\ \rho v \\ \rho e \end{bmatrix}$$

$$\vec{F} = \begin{bmatrix} \rho u \\ \rho u^2 - \sigma_{xx} \\ \rho uv - \tau_{xr} \\ \rho u e - \gamma \frac{\partial e}{\partial x} \left(\frac{\mu}{Pr} + \frac{\epsilon}{Pr_t} \right) - (u \sigma_{xx} + v \tau_{xr}) \end{bmatrix}$$

$$\vec{G} = \begin{bmatrix} \rho v r \\ \rho u v r - \tau_{xr} r \\ \rho v^2 r - \sigma_{rr} r \\ \rho v e r - r \gamma \frac{\partial e}{\partial r} \left(\frac{\mu}{Pr} + \frac{\epsilon}{Pr_t} \right) - r (u \tau_{xr} + v \sigma_{rr}) \end{bmatrix}$$

$$\vec{H} = \begin{bmatrix} 0 \\ 0 \\ -\sigma_H \\ 0 \end{bmatrix}$$

The transformed vector equation for general curvilinear coordinates is:

$$\frac{\partial \vec{U}}{\partial t} + \frac{\partial \vec{F}}{\partial \xi} \frac{\partial \xi}{\partial x} + \frac{\partial \vec{F}}{\partial \eta} \frac{\partial \eta}{\partial x} + (1/r) \left[\frac{\partial \vec{G}}{\partial \xi} \frac{\partial \xi}{\partial r} + \frac{\partial \vec{G}}{\partial \eta} \frac{\partial \eta}{\partial r} \right] = (1/r) \vec{H} \quad (14)$$

Applying the explicit MacCormack scheme to the vector equation results in the following algorithm (4:27):

$$\vec{U}(\xi, \eta, t + \Delta t) = L(\Delta t) \vec{U}(\xi, \eta, t) \quad (15)$$

where $L(\Delta t)$ is the two-dimensional numerical operator representing MacCormack's algorithm acting on the transformed conservation equations. Through use of time-splitting, this two-dimensional operator is separated into two one-dimensional sweep operators in the ξ - and η - directions. The operator $L_\xi(\Delta t)$ represents the solution of the equation:

$$\frac{\partial \vec{U}}{\partial t} + \frac{\partial \vec{F}}{\partial \xi} \frac{\partial \xi}{\partial x} + (1/r) \frac{\partial \vec{G}}{\partial \xi} \frac{\partial \xi}{\partial r} = 0 \quad (16)$$

in the ξ - direction by a time increment of Δt seconds. In a like manner, the operator $L_\eta(\Delta t)$ represents the solution of:

$$\frac{\partial \vec{U}}{\partial t} + \frac{\partial \vec{F}}{\partial \eta} \frac{\partial \eta}{\partial x} + (1/r) \frac{\partial \vec{G}}{\partial \eta} \frac{\partial \eta}{\partial r} = (1/r) \vec{H} \quad (17)$$

in the η - direction by a time increment of Δt seconds.

The dependent variable vector $U(\zeta, \eta, t)$ can then be advanced in time as:

$$\tilde{U}(\zeta, \eta, t + \Delta t) = [L_{\zeta}^{M/2}(\Delta t/M) L_{\eta}(\Delta t) L_{\zeta}^{M/2}(\Delta t/M)] \tilde{U}(\zeta, \eta, t) \quad (18)$$

with $\Delta t = \Delta t_{\zeta}$ if $\Delta t_{\zeta} < \Delta t_{\eta}$

or as:

$$\tilde{U}(\zeta, \eta, t + \Delta t) = [L_{\eta}^{N/2}(\Delta t/N) L_{\zeta}(\Delta t) L_{\eta}^{N/2}(\Delta t/N)] \tilde{U}(\zeta, \eta, t) \quad (19)$$

with $\Delta t = \Delta t_{\eta}$ if $\Delta t_{\eta} < \Delta t_{\zeta}$

where M and N are the smallest even integers of the quotients $(\Delta t_{\eta}/\Delta t_{\zeta})$ and $(\Delta t_{\zeta}/\Delta t_{\eta})$ respectively. The timesteps Δt_{ζ} and Δt_{η} are the maximum allowable timesteps in the ζ - and η - directions as determined by stability requirements.

The finite difference form of these sweep operators consist of a two step predictor - corrector procedure which uses one-sided differencing in the direction of sweep and central differencing in the direction perpendicular to the direction of sweep. When complete, this method is equivalent to a second order central differencing scheme in two dimensions.

The $L_{\zeta}(\Delta t)$ sweep operator represents the following numerical procedure (4:29):

PREDICTOR

$$\begin{aligned}
 (\vec{U}_{k,j})^{n+1/2} = & (\vec{U}_{k,j})^n - \frac{\Delta t}{\Delta \zeta} [(\vec{F}_{k,j})^n - (\vec{F}_{k-1,j})^n] \left(\frac{\partial \zeta}{\partial x} \right)_{k,j} \\
 & - (1/r) \frac{\Delta t}{\Delta \zeta} [r_{k,j} (\vec{G}_{k,j})^n - r_{k,j} (\vec{G}_{k-1,j})^n] \left(\frac{\partial \zeta}{\partial r} \right)_{k,j}
 \end{aligned} \tag{20}$$

CORRECTOR

$$\begin{aligned}
 (\vec{U}_{k,j})^{n+1} = & 1/2 \{ (\vec{U}_{k,j})^n + (\vec{U}_{k,j})^{n+1/2} - \frac{\Delta t}{\Delta \zeta} [(\vec{F}_{k+1,j})^{n+1/2} - (\vec{F}_{k,j})^{n+1/2}] \left(\frac{\partial \zeta}{\partial x} \right)_{k,j} \\
 & - (1/r) \frac{\Delta t}{\Delta \zeta} [r_{k,j} (\vec{G}_{k+1,j})^{n+1/2} - r_{k,j} (\vec{G}_{k,j})^{n+1/2}] \left(\frac{\partial \zeta}{\partial r} \right)_{k,j} \}
 \end{aligned} \tag{21}$$

Similarly, the $L_{\eta}(\Delta t)$ operator represents the following predictor - corrector steps (4:29,31):

PREDICTOR

$$\begin{aligned}
 (\vec{U}_{k,j})^{n+1/2} = & (\vec{U}_{k,j})^n - \frac{\Delta t}{\Delta \eta} [(\vec{F}_{k,j})^n - (\vec{F}_{k,j-1})^n] \left(\frac{\partial \eta}{\partial x} \right)_{k,j} \\
 & - (1/r) \frac{\Delta t}{\Delta \eta} [r_{k,j} (\vec{G}_{k,j})^n - r_{k,j} (\vec{G}_{k,j-1})^n] \left(\frac{\partial \eta}{\partial r} \right)_{k,j} + (1/r) \Delta t (\vec{H}_{k,j})^n
 \end{aligned} \tag{22}$$

CORRECTOR

$$\begin{aligned}
 (\bar{U}_{k,j})^{n+1} = & \frac{1}{2} \{ (\bar{U}_{k,j})^n + (\bar{U}_{k,j})^{n+1/2} - \frac{\Delta t}{\Delta \eta} [(\bar{F}_{k,j+1})^{n+1/2} - (\bar{F}_{k,j})^{n+1/2}] \left(\frac{\partial \eta}{\partial x} \right)_{k,j} \\
 & - (1/r) \frac{\Delta t}{\Delta \eta} [r_{k,j} (\bar{G}_{k,j+1})^{n+1/2} - r_{k,j} (\bar{G}_{k,j})^{n+1/2}] \left(\frac{\partial \eta}{\partial r} \right)_{k,j} + (1/r) \Delta t (\bar{H}_{k,j})^n \}
 \end{aligned}
 \tag{23}$$

where n and $n+1$ designate values at time t and $t + \Delta t$ respectively and $n+1/2$ indicates a temporary, predicted value. The values $\frac{\partial \xi}{\partial x}$, $\frac{\partial \xi}{\partial r}$, $\frac{\partial \eta}{\partial x}$, and $\frac{\partial \eta}{\partial r}$ depend only on the grid geometry and are calculated only once for each grid point.

Variants of this program for two-dimensional internal flow and three-dimensional external flow have been used in studies by Olson, McGowan, and MacCormack (10); Shang, Hankey and Smith (13); and Shang and MacCormack (14). The internal axisymmetric version of the code was developed for in-office use by WRDC/FIMM.

Incorporation of Nozzle Structure

In order to model the ejector geometry desired, it was necessary to identify boundary conditions which accounted for the nozzle structure and the flow injection at the nozzle exit in addition to the usual wall and centerline conditions. Once the desired location of the nozzle exit was selected, the grid was refined in that area to better handle the large gradients which exist at the nozzle exit. Then, the grid points which best approximated the corners of the desired nozzle exit were identified (Figure 10).

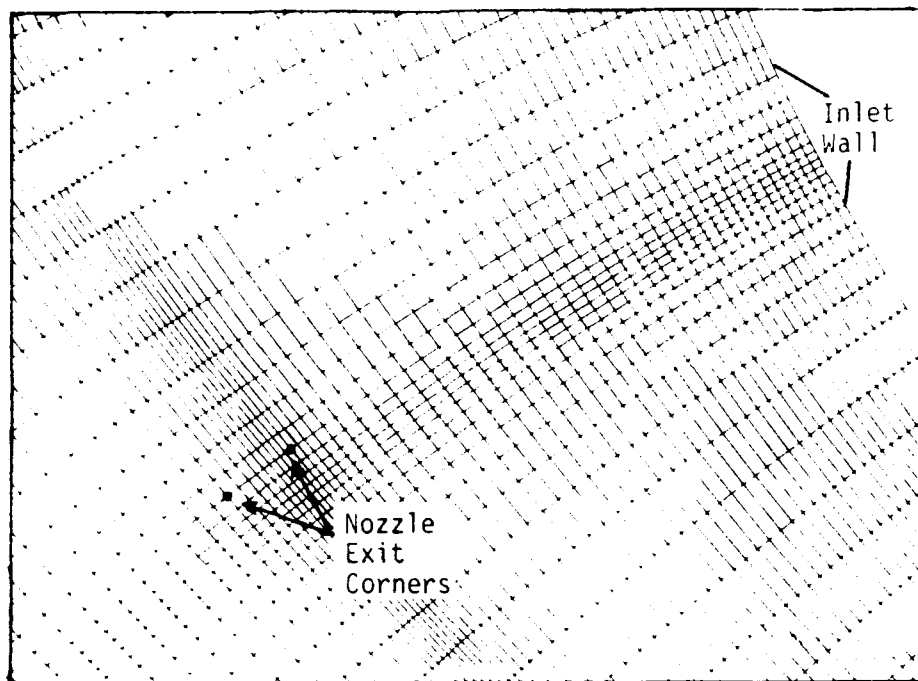


Fig. 10. Identification of Nozzle Exit Corners

The outside walls of the nozzle structure were defined as being three grid lines outside the nozzle exit. The outside walls and ends of the nozzle structure were defined as SOLID WALLS for the boundary conditions (Figure 11).

The grid points in the gap were defined as the NOZZLE EXIT for the boundary conditions. The area enclosed within the nozzle structure did not effect the computation of the flowfield and was set to zero velocity. Figure 12 shows a diagram of the grid boundaries with the types of boundary conditions applied identified.

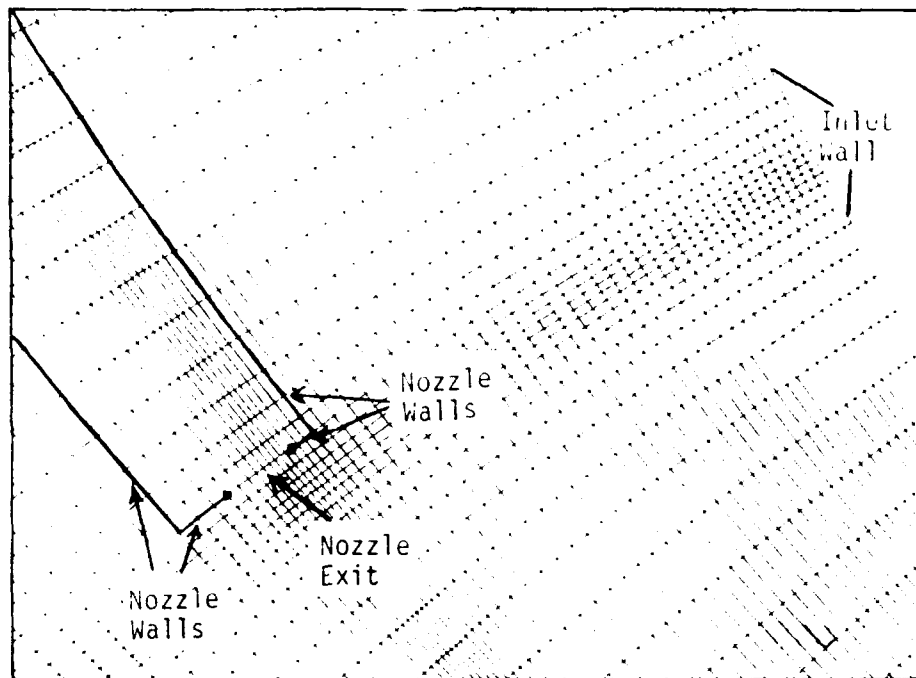


Fig. 11. Identification of Nozzle Walls

Boundary Conditions

Boundary conditions were imposed to accommodate the geometrical restrictions on the flowfield by defining the solid surfaces, to incorporate primary nozzle flow based on a constant plenum pressure, and to provide the necessary upstream and downstream conditions to achieve closure.

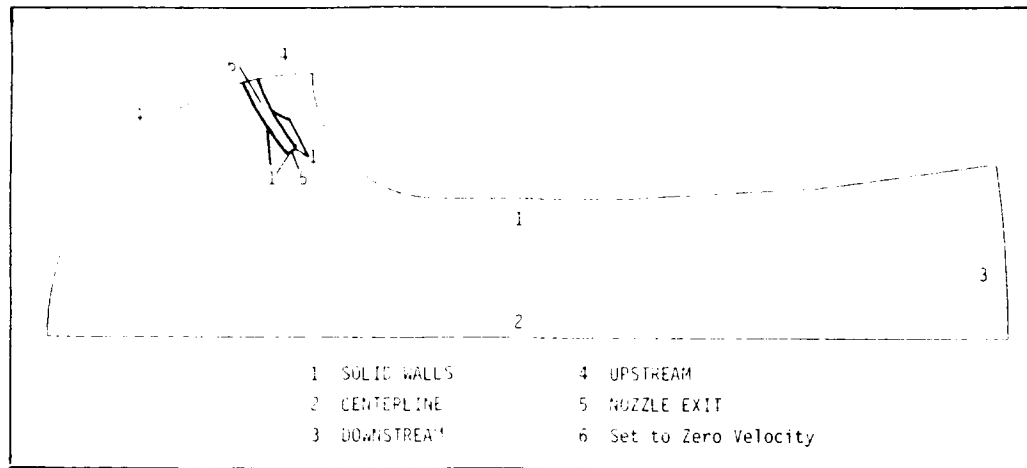


Fig. 12. Application of Boundary Conditions

Solid Walls. For the wall of the ejector and the inner and outer walls of the primary nozzle, applying the conditions of no penetration and no slip provides:

$$(\rho u)_w = 0 \quad (24)$$

$$(\rho v)_w = 0 \quad (25)$$

Allowing no normal pressure gradient ($\frac{\partial P}{\partial \eta} = 0$) leads to:

$$(\rho e)_w = \rho_1 [e_1 - \frac{1}{2} (u_1^2 + v_1^2)] \quad (26)$$

Applying a constant wall temperature T_w :

$$(\rho)_w = (\rho e)_w / (c_v T_w) \quad (27)$$

where the subscript w indicates the value at the wall and the subscript 1 indicates a value taken one grid point away from the wall.

Centerline. Since the centerline is the axis of symmetry, there can be no cross velocity. This results in the equation:

$$(\rho v)_{CL} = 0 \quad (28)$$

Also, there can be no radial gradients of u , ρ , or T ($\frac{\partial u}{\partial \eta} = \frac{\partial \rho}{\partial \eta} = \frac{\partial T}{\partial \eta} = 0$), resulting in the following equations:

$$\rho_{CL} = \rho_1 \quad (29)$$

$$(\rho u)_{CL} = (\rho u)_1 \quad (30)$$

$$(\rho e)_{CL} = (\rho e)_1 - \frac{1}{2} (\rho v)_1^2 / \rho_{CL} \quad (31)$$

where the subscript CL indicates the value at the centerline and the subscript 1 indicates a value taken one grid point away from the centerline.

Downstream. Enforcing conservation of mass in the ζ - direction ($\frac{\partial \rho u}{\partial \zeta} + 1/r \frac{\partial \rho v r}{\partial \zeta} = 0$) by allowing $\frac{\partial \rho u}{\partial \zeta} = 0$ and $\frac{\partial \rho v r}{\partial \zeta} = 0$ gives:

$$(\rho u)_K = (\rho u)_{K-1} \quad (32)$$

$$(\rho v)_K = (\rho v r)_{K-1} / r_K \quad (33)$$

where the subscript K indicates the value at the downstream boundary and the subscript K-1 indicates a value taken one grid point upstream. Since the flow in the ejector modeled is exclusively subsonic, the exit static pressure must equal

the ambient pressure P_a . Applying this constraint and allowing temperature to propagate downstream leads to:

$$(\rho)_K = P_a / RT_{K-1} \quad (34)$$

$$(\rho e)_K = \rho_K [(c_v T_{K-1}) + \frac{1}{2} (u_K^2 + v_K^2)] \quad (35)$$

Upstream. Enforcing conservation of mass in the ζ - direction as was done on the downstream boundary leads to:

$$(\rho u)_1 = (\rho u)_2 \quad (36)$$

$$(\rho v)_1 = (\rho v)_2 / r_1 \quad (37)$$

where the subscript 1 indicates the value at the upstream boundary and the subscript 2 indicates a value taken one grid point downstream. Additionally, assuming incompressible, isentropic flow from ambient stagnation conditions results in the equations:

$$(\rho)_1 = P_a / RT_a \quad (38)$$

$$(\rho e)_1 = \rho_1 [(c_v T_a) + \frac{1}{2} (u_1^2 + v_1^2) (\gamma - 1) / \gamma] \quad (39)$$

where P_a and T_a are the ambient stagnation pressure and temperature respectively.

Nozzle Exit. The nozzle exit was treated the same as the upstream boundary except that the nozzle total pressure ($P_{0 \text{ noz}}$) was based on the defined pressure ratio (P_{rat}):

$$P_{0 \text{ noz}} = P_{rat}(P_a) \quad (40)$$

and the direction of the flow was constrained to the desired injection angle (α_1).

Turbulence model

The turbulence model used in the original program was a modified Baldwin-Lomax model based on the upper surface. This turbulence model uses a two region calculation of the eddy viscosity (14:4). The inner region calculation ϵ_i is used up to the distance y^* from the wall after which the outer region formulation ϵ_o is used. The distance y^* is the defined as the smallest distance from the wall at which ϵ_i and ϵ_o are equal.

The inner formulation is given by (14:4):

$$\epsilon_i = \rho (0.4 L D)^2 |\omega| \quad (41)$$

where the vorticity of the flow, ω , the Van Driest damping factor, D , and the scaling length, L , are given by:

$$\omega = \frac{1}{2} \nabla \times \vec{U} \quad (42)$$

$$D = 1 - \exp[(-\rho_w |\omega_w| / \mu_w)^{1/2} L / 26] \quad (43)$$

$$L = [(x - x_w)^2 + (r - r_w)^2]^{1/2} \quad (44)$$

and the subscript w represents the value at the wall. The outer formulation is given by (14:4):

$$\epsilon_o = 0.0336 \rho F_{wake} / [1 + 5.5 (0.3 L / L_{max})^6] \quad (45)$$

where the wake function, F_{wake} , is the minimum value of the following at any point in space:

$$F_{wake} = L_{max} F_{max}$$

or
$$F_{wake} = 0.25 L_{max} V_{max}^2 / F_{max} \quad (46)$$

and L_{\max} is the value of the length scale, L , where F :

$$F = L D |\omega| \quad (47)$$

reaches its maximum value, F_{\max} , within the turbulent shear layer.

To simplify this investigation, no attempt was made to identify better turbulence models for this type of wall jet flow. The turbulence model already incorporated in JSIAXK was not changed but was based on the nearest wall to include nozzle wall effects.

Procedure

Once the desired location of the nozzle exit was identified, the vertical and horizontal grid spacing tables, EJE CVRT and EJE CHRZ (Appendices A-3,A-4), were modified to refine the grid in that vicinity. EJE CGRD was then run to produce the grid and establish the initial flowfield. Setting the flow injection angle (α_1) to approximate the flow direction established by the simplified initial flowfield (to minimize extreme gradients) the flow solver JSIAXK could be started.

Initially, the timestep per iteration was kept small until the larger gradients could be smoothed out, then was increased to provide faster convergence to the steady state. Once the large gradients of the initial flowfield were smoothed out, it was also possible to change α_1 until the desired value was set. The program was then run until steady state was reached. Steady state was defined for the purpose of this investigation as a change of less than 0.001 ft/sec in total velocity at each of four critical locations in 3000 iterations. This process took approximately 90,000

iterations to complete at 0.151 CPU seconds per iteration on the CRAY XMP computer. This solution was then stored on the Central Datafile System. A new α_1 was then set to the next angle of interest. Convergence on a new steady state solution then took approximately 3600 iterations.

This process was continued until solutions were achieved for all desired injection angles for the configuration under investigation. For a new nozzle location, the process was restarted from the beginning. Configurations 1a, 1b, and 1c were able to be run consecutively because the changes to the flowfield were minimal in switching from one to the other.

The post-processing program AUGMENT was then run for each flowfield solution. This program integrates the x - momentum across the exit and compares it to the isentropic thrust of the nozzle alone to calculate the thrust augmentation per the control volume analysis described in section I. A sample comparison of mass flows in and out was also accomplished to ensure that conservation of mass was being satisfied.

III. Results and Discussion

Cases Investigated

The cases investigated consist of four nozzle location configurations for one ejector geometry. The geometry of the ejector was selected to be similar to one investigated by Unnever to allow for direct comparison. The dimensions of the ejector studied by Unnever (Figure 7) were (17:60):

$$L_1 = 3.5 \text{ in}$$

$$\psi_1 = 3^\circ$$

$$L_2 = 3.5 \text{ in}$$

$$\psi_2 = 8^\circ$$

resulting in a diffuser area ratio (β) of 1.71.

The dimensions of the annular nozzle of Unnever's experiment and those of the configurations investigated are tabulated in Table I. The dimensions of Unnever's nozzle indicate that it was 0.55 inches from the wall. Unnever's testing was carried out with a pressure ratio of 1.14 which was replicated for all configurations investigated.

Configuration 1a. The location and geometry of the nozzle for configuration 1 was chosen to approximate as closely as possible that of the annular nozzle tested by Unnever.

Configurations 0, 2, 3. The locations and geometries of the nozzles for configurations 0, 2, and 3 were chosen such that the distance from the wall and the nozzle area would be approximately the same as configuration 1a. This allowed investigation of the thrust augmentation effects of nozzle position angle, θ , only (Figure 13).

TABLE I
Nozzle Geometries

	L_1	Radius	Gap	A_J	θ	α
Unnever	2.25	3.00	0.065	1.226	61.9	0.081
Config 1a	2.25	2.96	0.072	1.349	61.9	0.089
Config 0	2.40	3.30	0.064	1.325	70.0	0.087
Config 2	1.96	2.51	0.081	1.296	50.0	0.085
Config 3	1.64	2.17	0.094	1.306	40.0	0.086
Config 1b	2.26	2.96	0.053	0.989	61.9	0.065
Config 1c	2.25	2.95	0.095	1.774	61.9	0.117

Configurations 1b, 1c. The locations of the nozzles for configurations 1b and 1c were chosen to be as close to that of configuration 1a as possible. The only change made was to the size of the gap and therefore the nozzle area. This was done to investigate nozzle area ratio effects on thrust augmentation.

Primary Objectives

Comparison with Experimental Data. Configuration 1a was designed to model as closely as possible the annular nozzle configuration used in Unnever's experimental investigation. A qualitative comparison of the exit velocity profile of configuration 1a with an experimentally measured profile from Reznick (Figs. 14 and 15) shows that

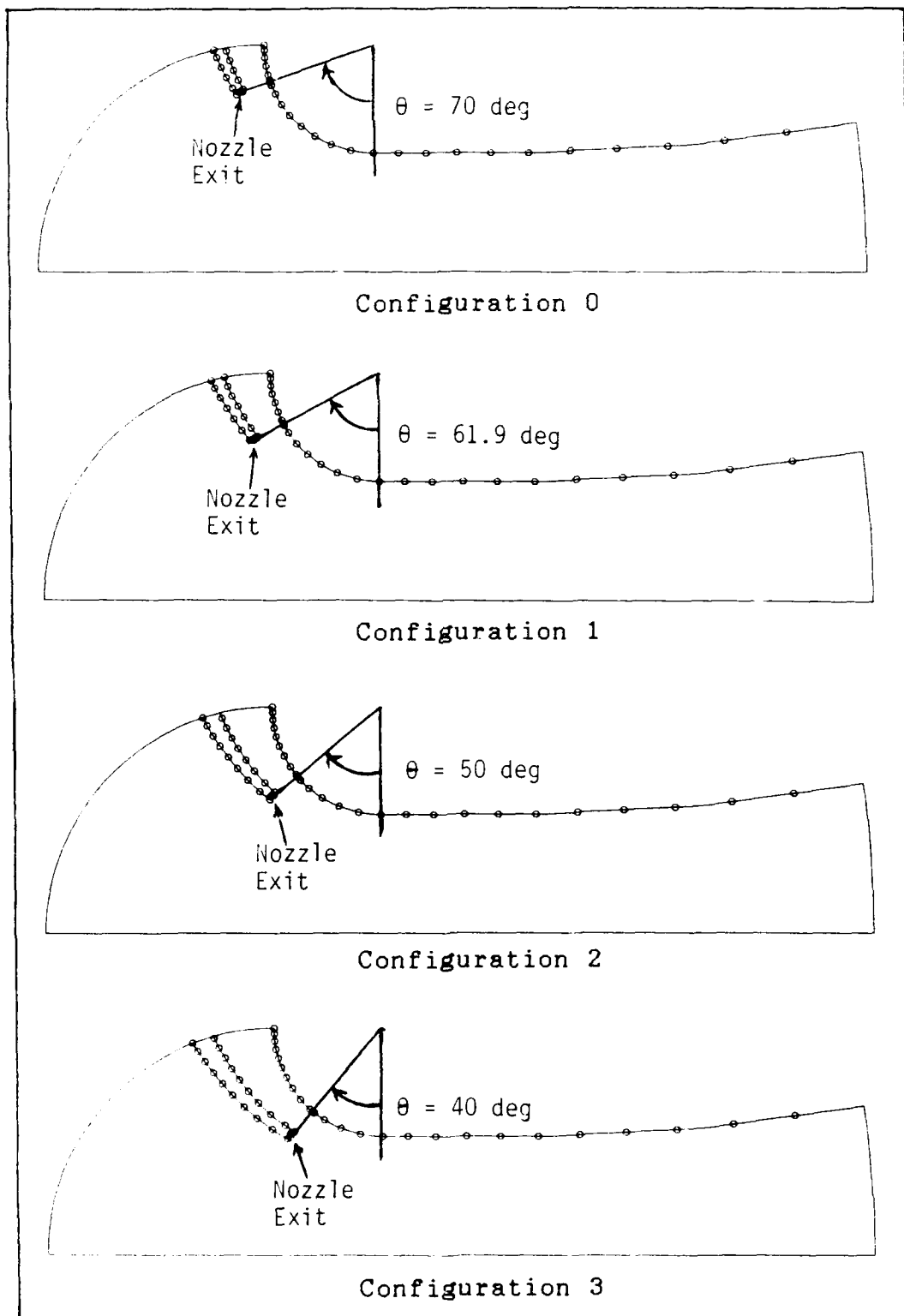


Fig. 13. Nozzle Locations

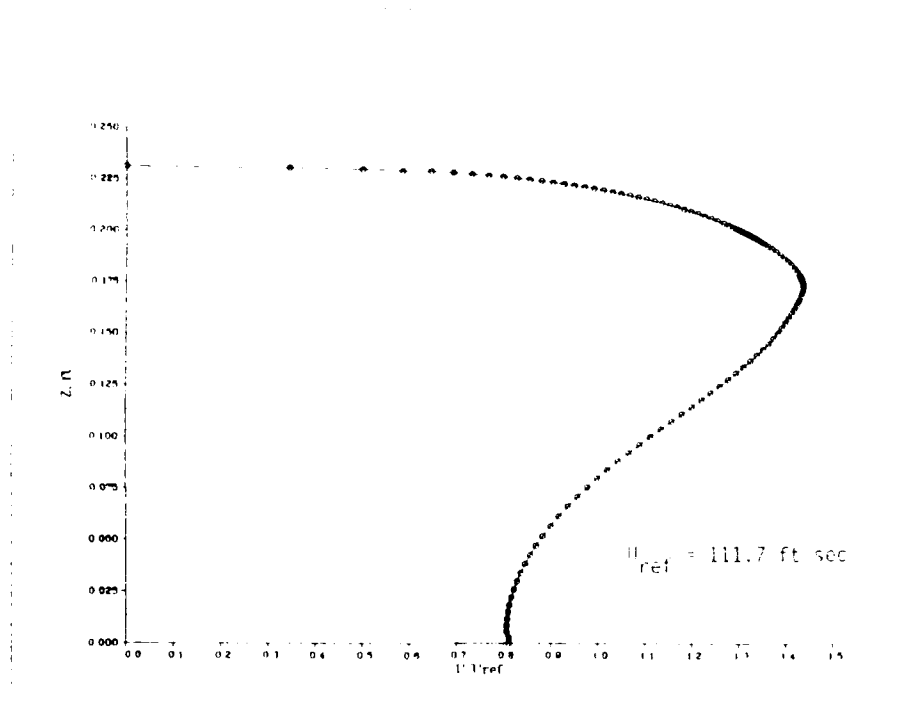


Fig. 14. Exit Velocity Profile - Numerical

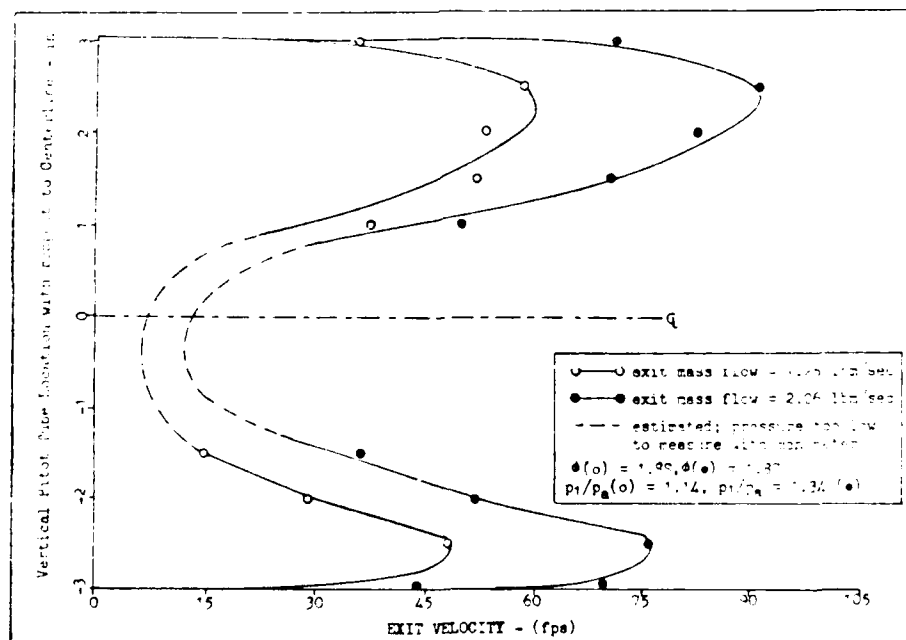


Fig. 15. Exit Velocity Profile - Experimental (11:48)

the shape of the profile is closely replicated by the model. This is an indication that the flow structure is indeed similar to that in the experimental ejector. However, since the experimental data was produced using the hook nozzles and is therefore only similar to the ejector modeled, the comparison cannot be exact.

Similarly, comparison of thrust augmentation vs. injection angle curves for the numerical model (Figure 16) with similar curves from Unnever (Figure 17) (17:46) show that the expected trends are indeed modeled. Again, since the experimental curves are from hook nozzle cases (by necessity, since the injection angle of the annular nozzle could not be varied) the comparison can only be qualitative, not quantitative.

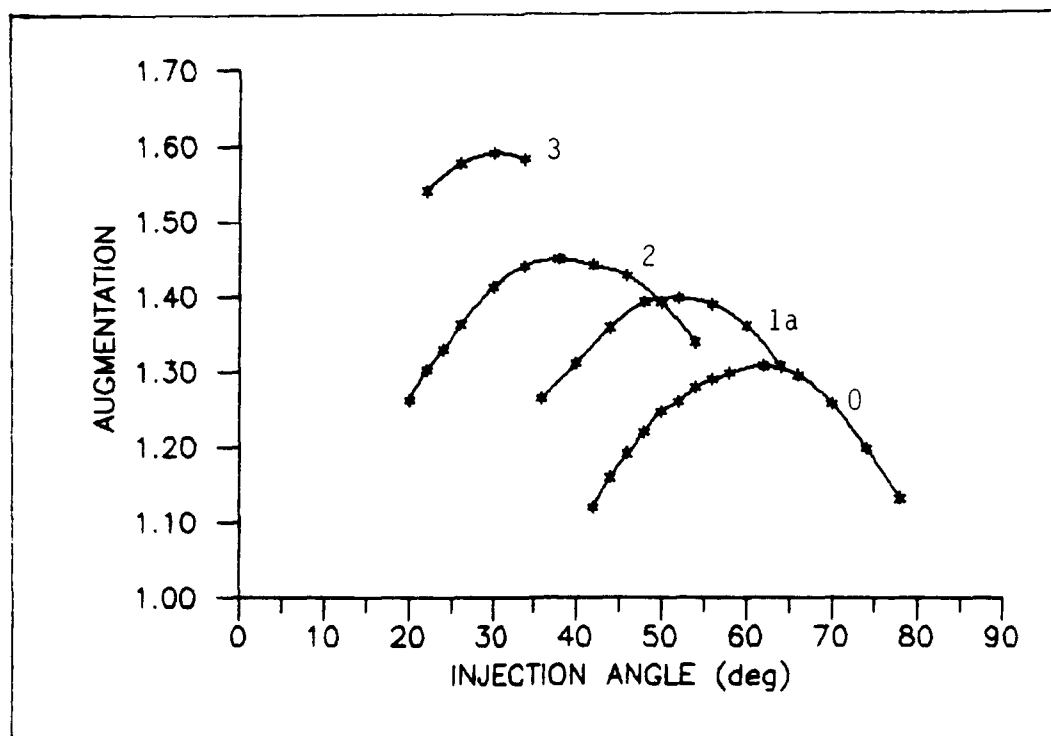


Fig. 16. Thrust Augmentation vs. Injection Angle
Numerical

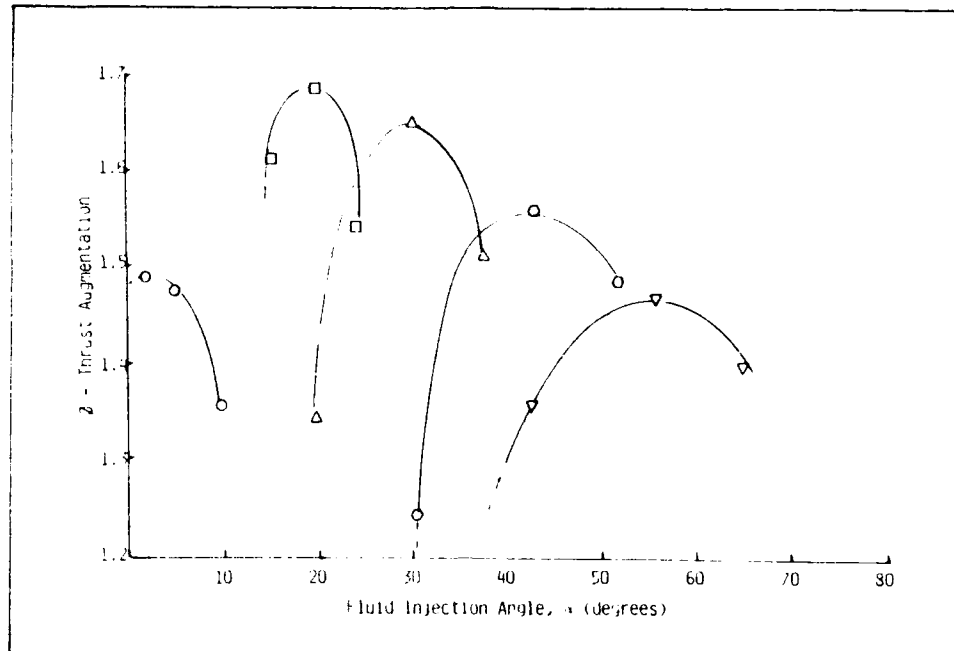


Fig. 17. Thrust Augmentation vs. Injection Angle
Experimental

However, a quantitative comparison of the thrust augmentation from configuration 1a with Unnever's annular nozzle configuration (Table II) (17:60) shows that the numerical model did not achieve the thrust augmentation measured experimentally.

Table II
Thrust Augmentation Comparison

Ejector	ϕ
Numerical Model	1.40
Experimental	1.48

Possible explanations for this difference include:

1. Turbulence modeling not optimized for a wall jet flow resulting in poorer mixing in the numerical model.
2. Three dimensional mixing or swirl in the experimental ejector which is not accounted for in the numerical model due to the assumption of axial symmetry.
3. Modeling the jet exiting the nozzle as perfectly parallel flow in the desired direction when there is likely some divergence in the actual jet experimentally.

Each of these lead to less complete mixing in the numerical model and would thus account for the lower thrust augmentation calculated. Additionally, other sources of error which would account for differences in experimental versus numerical results include:

4. Insufficient grid resolution.
5. Experimental error.

Using $\phi = 1.00$, or no augmentation, as a baseline, this results in a 16.7 percent error. This error indicates that the model, as it is, would not be a good predictor of the actual thrust augmentation which could be expected from an experimental setup. However, since trends determined with this model appear to be consistent with experimental results, analysis of different parameters should allow identification of values which maximize thrust augmentation which could be used to guide hardware development.

Data Visualization. One of the benefits of a numerical simulation is that the solution results in complete knowledge of the computed flowfield. This knowledge can be

used to provide insight into the behavior of the flow within the ejector which would be nearly impossible to determine experimentally. Plotting velocity contours (Figure 18) clearly shows the primary characteristics of the flowfield.

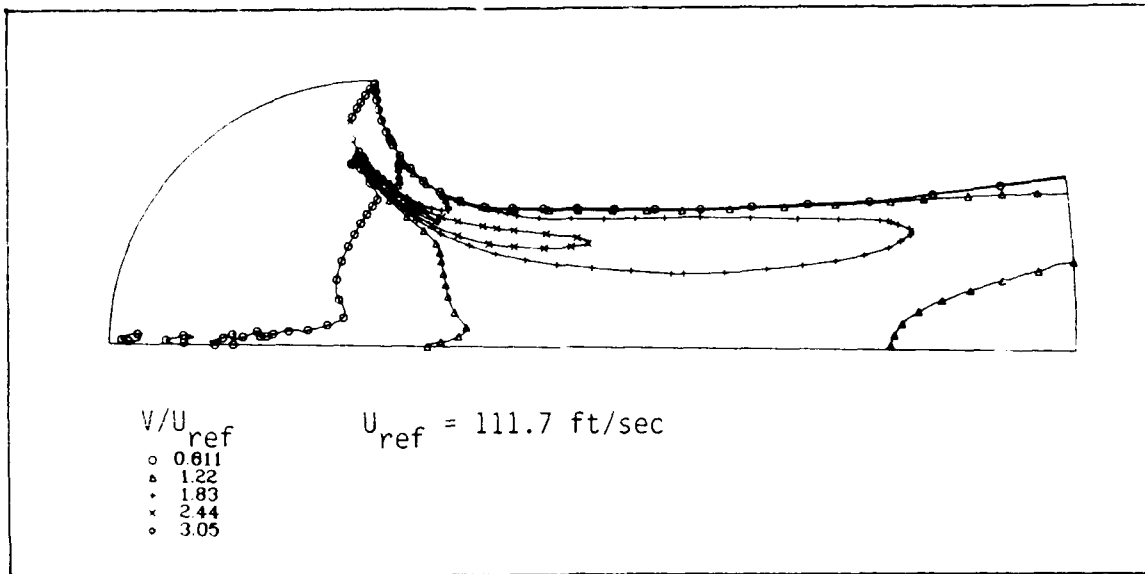


Fig. 18. Total Velocity Contours

First, (noting that the flow is from left to right) one can see how the jet hugs the wall and negotiates the curvature in the inlet due to the coanda effect. Second, one can see how the jet spreads out as it entrains more of the surrounding flow along with it. The increasing velocity of the entire flowfield as the cross-sectional area of the duct decreases can also be seen. Lastly, a relatively high velocity channel flow can be seen between the nozzle structure (and the jet) and the wall.

A streamline diagram of configuration 1a at its optimum injection angle (Figure 19) shows the smooth flow which characterizes the best performing injection angles.

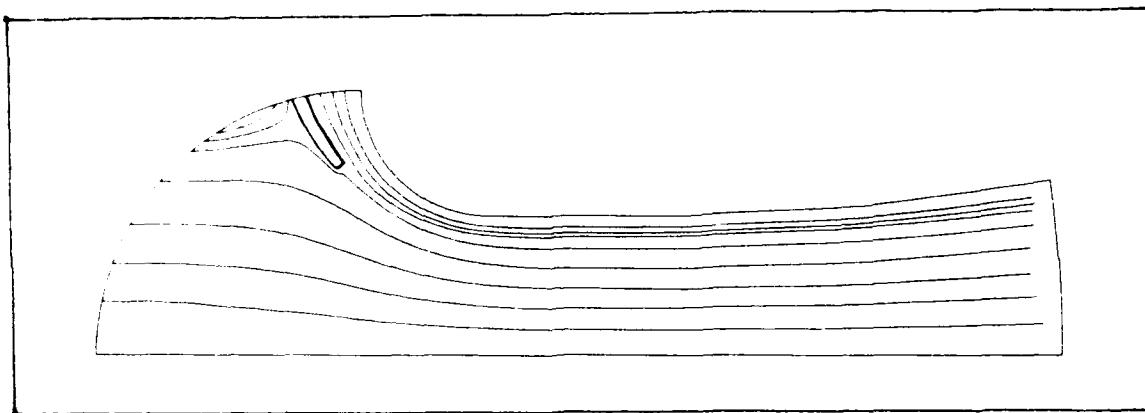


Fig. 19. Streamlines

One can also see, however, that a stagnation point exists on the nozzle structure upstream. Although the annular nozzle structure, as modeled, is thinner than that of the experimental apparatus, this diagram shows that significant flow blockage by the nozzle exists even in the numerical model just as was suspected in the experimental work by both Reznick and Unnever. A velocity vector plot of this region (Figure 20) clarifies the picture.

Finally, a sequence of plots of velocity profiles (Figures 21-23) shows how the jet mixes with the secondary flow as it progresses through the ejector. The first plot (Figure 21) shows the velocity profile at three grid stations ranging from the exit plane of the nozzle ($K = 32$) to a cross-section within the constant area mixing chamber, or throat, of the ejector ($K = 75$). These plots show clearly how the jet begins to mix with the secondary flow and how the entire flow accelerates as the inlet converges. It may further be determined from this plot is that the grid resolution at the upper surface appears to be barely sufficient to capture the boundary layer. However, it does not appear to be sufficient to capture boundary layer effects on the nozzle walls.

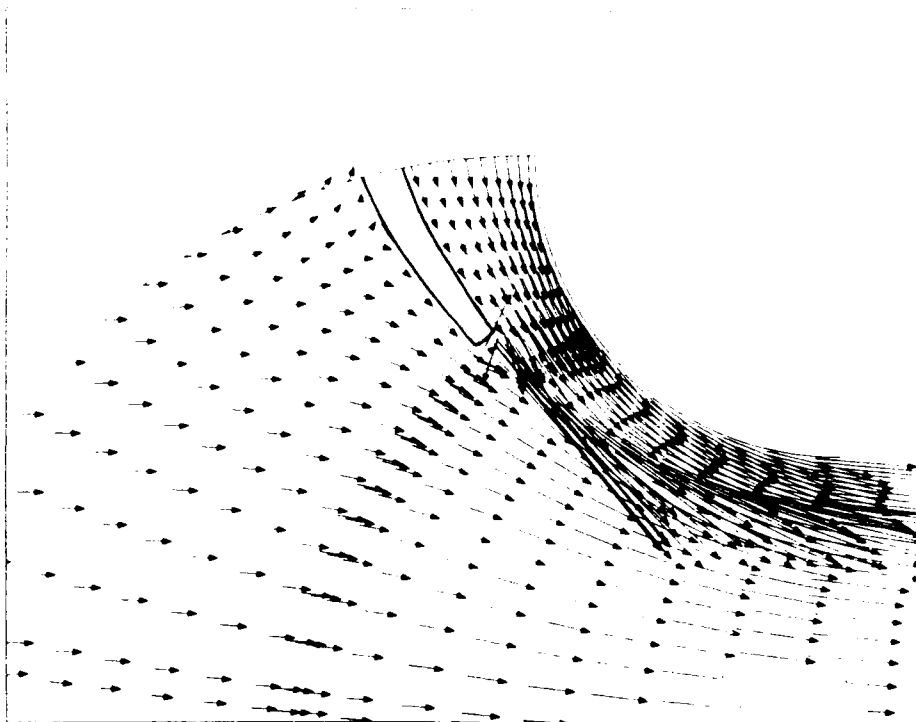


Fig. 20. Velocity Vectors - Nozzle Area

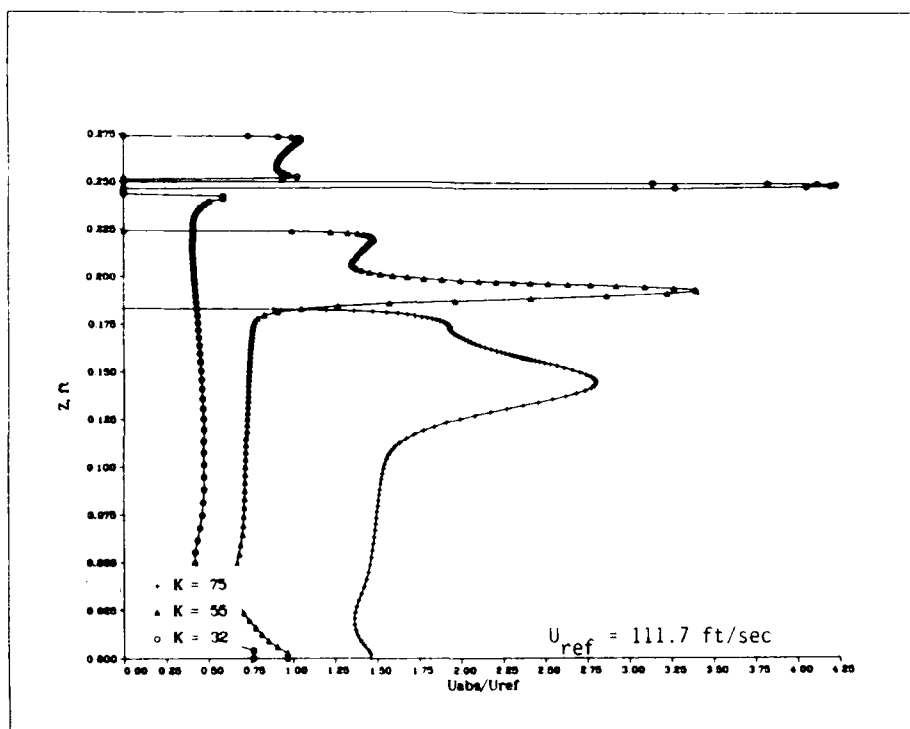


Fig. 21. Inlet Velocity Profiles

The second plot (Figure 22) shows how the jet continues to mix with the secondary flow as it progresses from the beginning ($K = 75$) to the end ($K = 100$) of the mixing chamber.

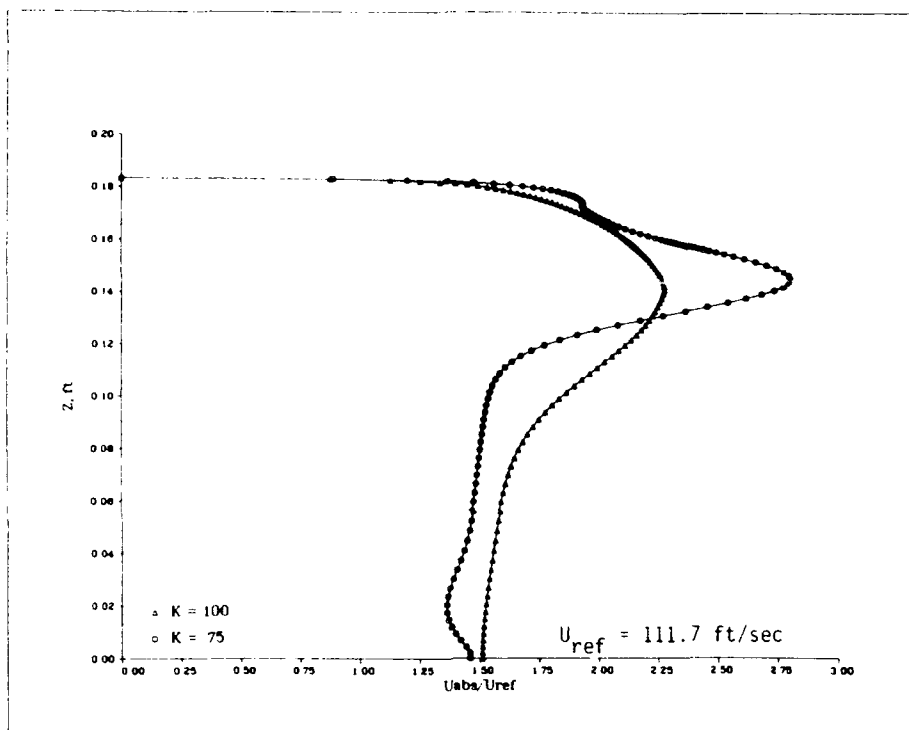


Fig. 22. Mixing Chamber Velocity Profiles

The last plot (Figure 23) portrays the changing profiles as the flow proceeds through the diffuser from the end of the mixing chamber ($K = 100$) to the exit ($K = 130$). The deceleration of the flow in the diffuser is evident. Also, the continued spreading of the jet as it mixes with the secondary flow is clearly visible. These basic flow features were consistent for all of the configurations modeled.

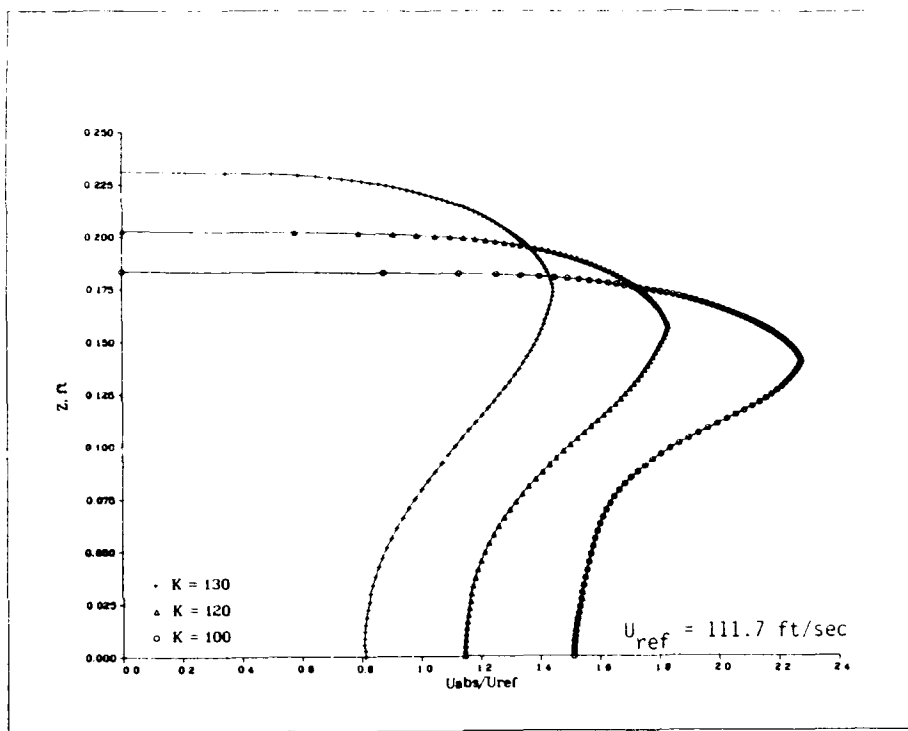


Fig. 23. Diffuser Velocity Profiles

Flexibility. This code, as modified for this investigation, is capable of handling variations of injection angle, nozzle position, nozzle gap (and therefore area) and pressure ratio. With some additional effort, diffuser and inlet geometries could be altered as well.

Secondary Objectives

Several of the secondary objectives were approached in the course of this investigation although all would require further work to provide the requisite parametrics to use for hardware design. The parameters studied include injector angle, nozzle position, and nozzle to throat area ratio.

Injection Angle. The effect of injection angle on the flowfield can be observed by comparing the optimum injection angle for configuration 1a to two off-nominal cases. For configuration 1a, the optimum injection angle was found to be $\alpha_1 = 52$ degrees. This is compared to the off-nominal cases of $\alpha_1 = 64$ degrees and $\alpha_1 = 36$ degrees. The thrust augmentation achieved by each of these cases is tabulated in Table III.

Table III
Augmentation with Changing Injection Angle (α_1)

α_1	ϕ
36	1.264
52	1.398
64	1.308

First, looking at velocity contours for the $\alpha_1 = 64$ degree case (Figure 24) one can see that the jet flow does not follow the wall closely but instead spreads out into the main mixing chamber. The improved mixing accomplished by the increased injection angle would seem to be desirable. But, as the exit velocity profiles indicate (Figure 25), the increased centerline flow is accomplished at the expense of a large drop in flow velocity near the wall. For a circular ejector, the region near the wall represents a much greater area in which momentum was sacrificed than the area near the centerline where momentum was gained. Also, it can be seen that the flow has begun to separate from the wall resulting in reversed flow.

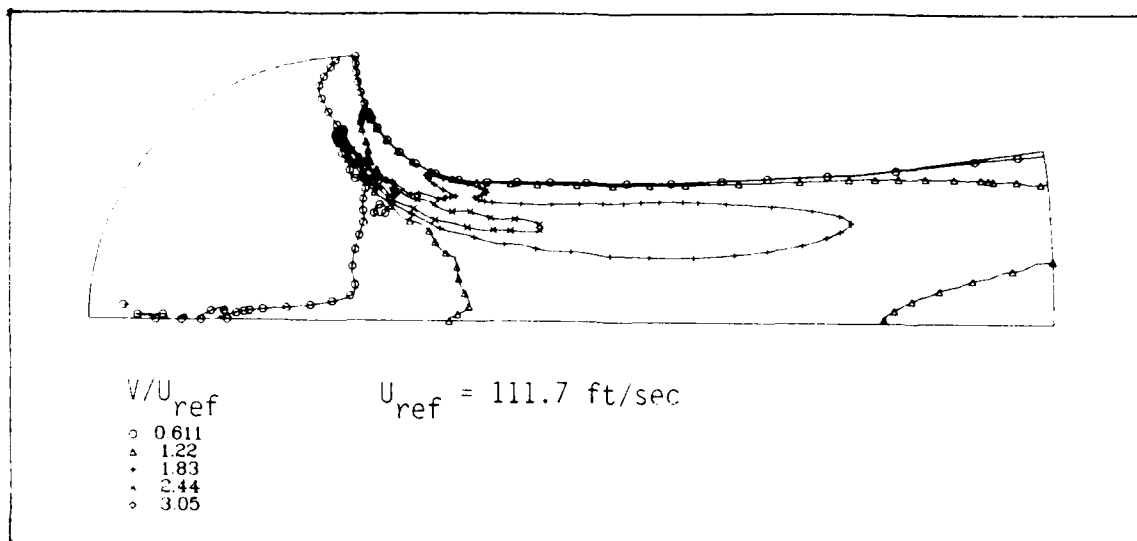


Fig. 24. Velocity Contours : $\alpha_1 = 64$ degrees

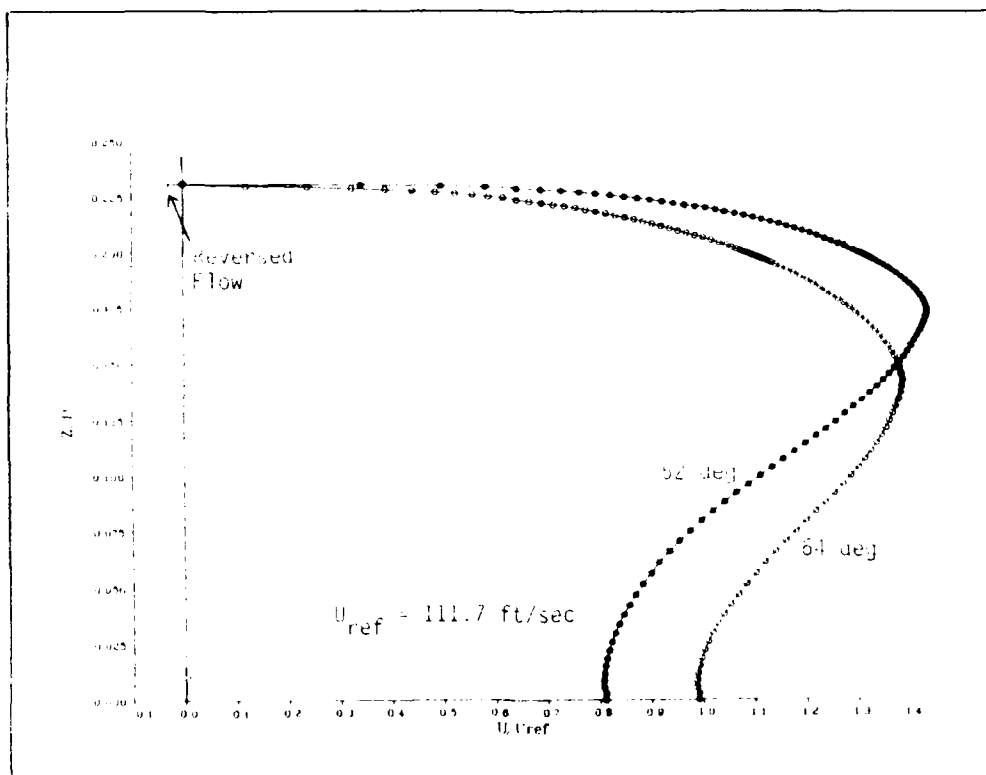


Fig. 25. Exit Velocity Profiles : $\alpha_1 = 52$ and 64 degrees

The second off-nominal case ($\alpha_1 = 36$ degrees) is one in which the jet is directed too near the wall. A first look at the velocity contours (Figure 26) shows the jet closely hugging the wall which by the above argument would seem to be desirable. However, a closer look at the area between the jet and the wall shows that, contrary to the optimum case (Figure 18), the flow through this channel is of relatively low velocity. Also, the high speed jet flow along the wall loses more momentum due to frictional effects.

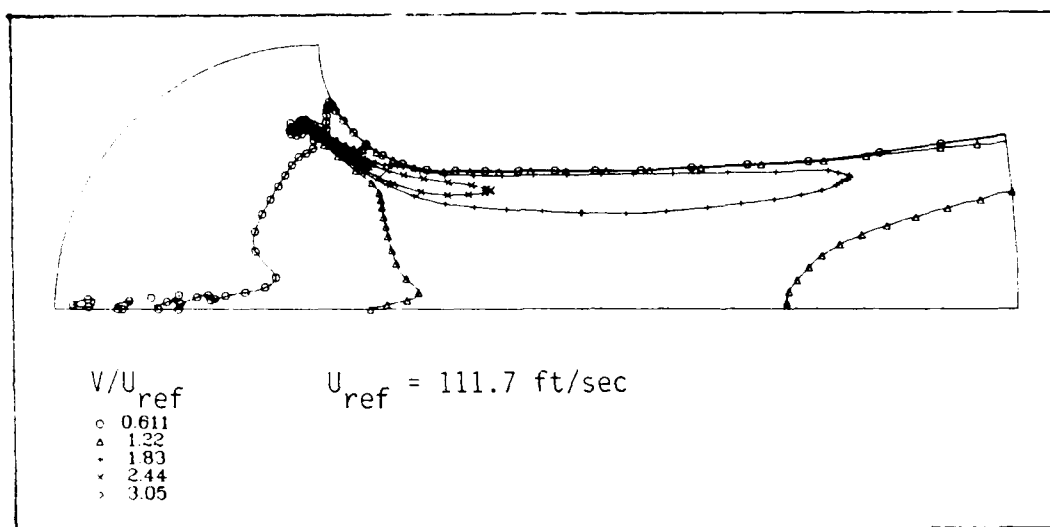


Fig. 26. Velocity Contours : $\alpha_1 = 36$ degrees

The effect of the blockage of this high energy flow source and frictional losses are reflected in the exit profile (Figure 27). Although the jet is more concentrated for the $\alpha_1 = 36$ degree case it is no more powerful than the optimal, $\alpha_1 = 52$ degree, case. The reduced mixing also results in a decrease in momentum across the majority of the

center section of the ejector. Apparently, the optimum case is one which balances these considerations by achieving maximum mixing without allowing the jet to separate from the wall.

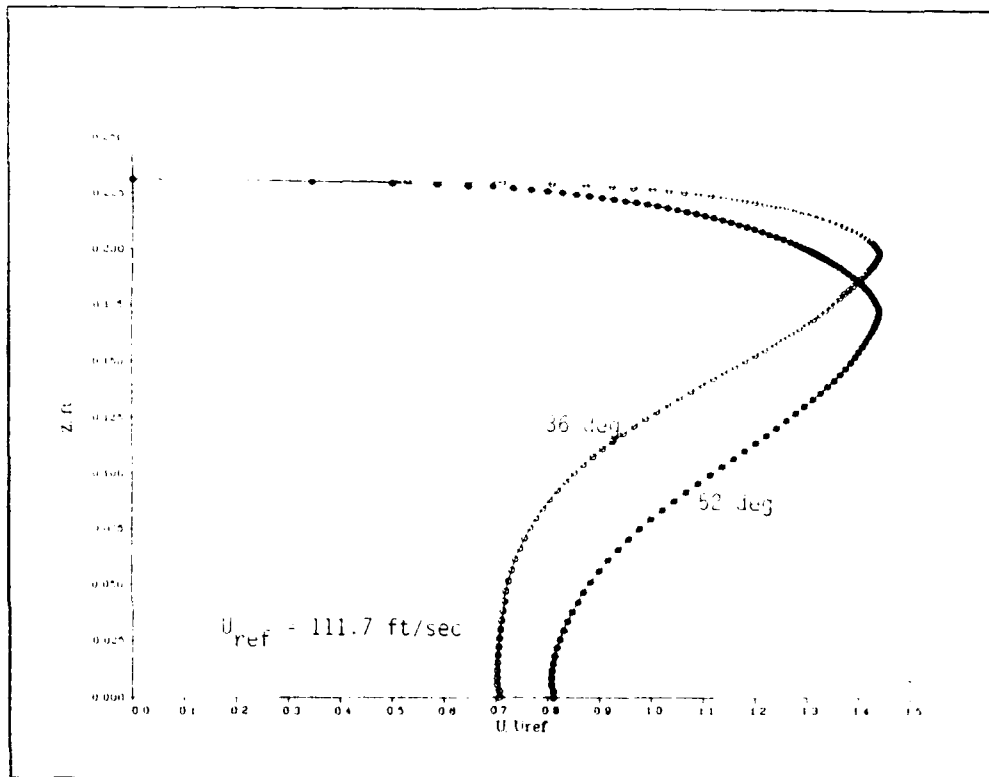


Fig. 27. Exit Velocity Profiles : $\alpha = 52$ and 36 degrees

Figure 28 defines a pair of angles which the injection angle of the nozzle can be referenced to. These angles are those representing injection parallel and tangent to the wall. Figure 29 shows the relationship of the injection angle for maximum thrust augmentation to those representing injection parallel to the wall and tangent to the wall for each of the four configurations investigated. In all cases, the optimum injection angle is approximately a quarter of

the way between parallel and tangent to the wall. This conclusion must be caveated by noting that, due to the circular inlet lip and the fact that all configurations were limited to be the same distance from the wall, the relative geometry between the nozzle and the wall is the same for all configurations. To fully investigate this parameter, additional data would need to be collected at different distances from the wall and (if desired) for different inlet geometries.

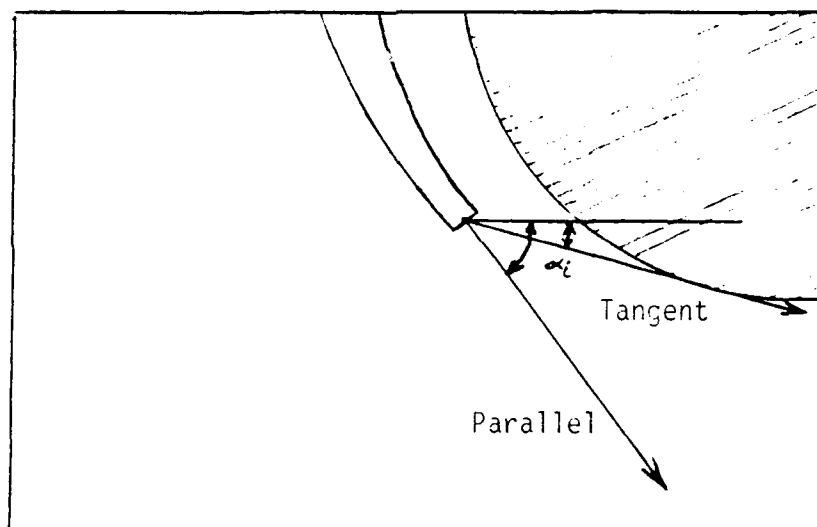


Fig. 28. Reference Injection Angles

Nozzle Position. In investigating the influence of nozzle position on thrust augmentation, it was necessary to isolate the effect of nozzle movement by constraining the configurations chosen. In order to eliminate changing wall effects, all configurations were set to have the nozzle the same distance from the wall as configuration 1a (0.55 in.).

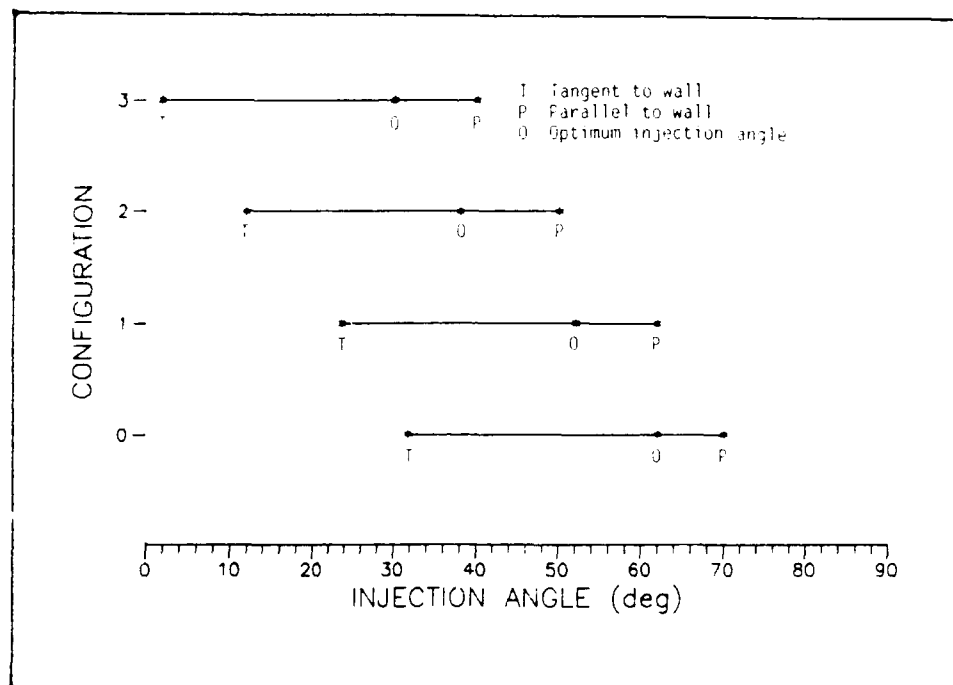


Fig. 29. Optimum Injection Angle with Relation to Reference Angles

The nozzle gap size was adjusted to achieve similar nozzle areas for all configurations to eliminate area ratio effects. This reduces the effect of location changes to only the effect of nozzle position angle, θ . Plotting the maximum augmentation achieved at each location vs. the position angle (Figure 30) a definite trend can be detected. Higher augmentation ratios are achieved with decreasing position angle, or in other words, placing the nozzle further into the inlet.

The effect of nozzle location can best be seen by comparing the two extremes studied, configuration 0 and configuration 3. By looking at velocity profiles of the jet itself (Figures 31 and 32) we can see that configuration 3 has a higher peak jet velocity than configuration 0.

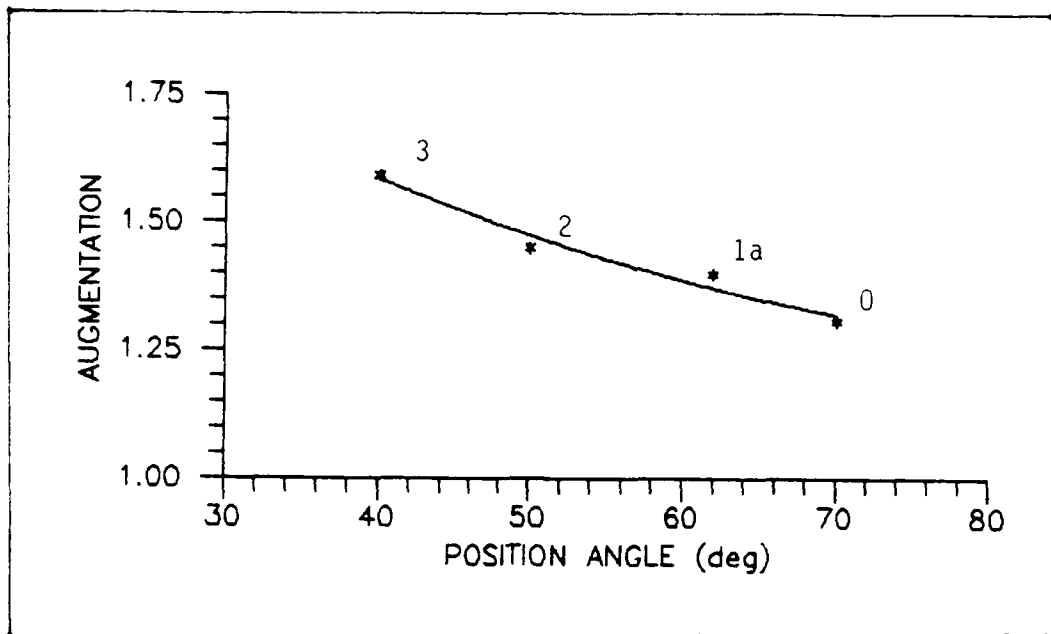


Fig. 30. Augmentation vs. Position Angle

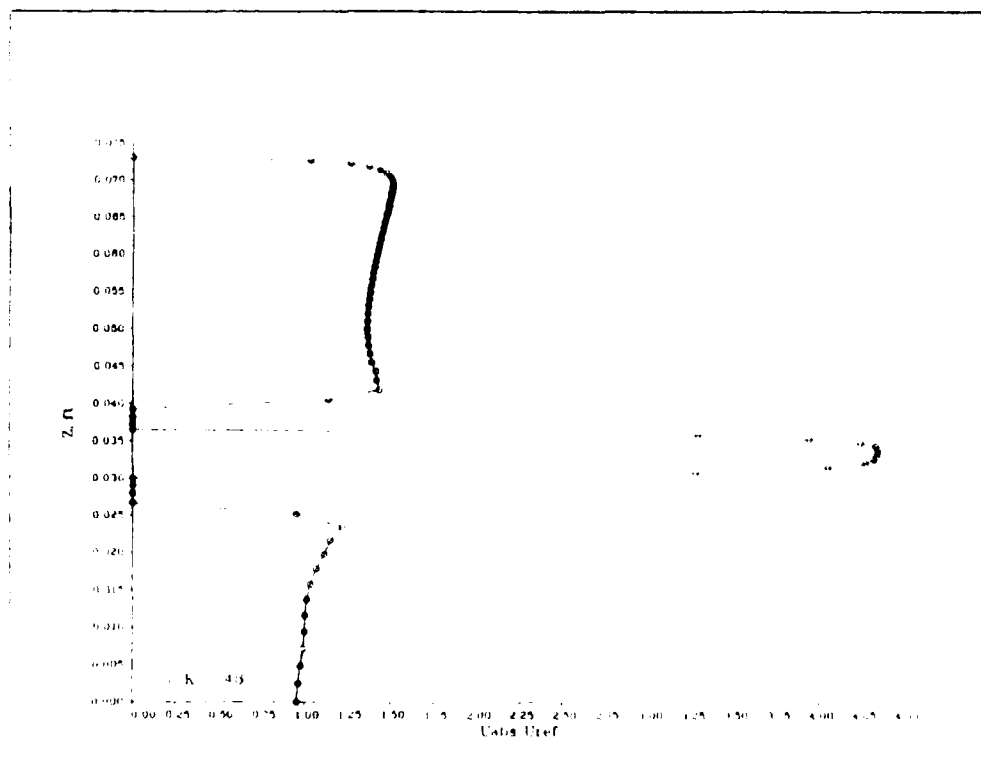


Fig. 31. Nozzle Velocity Profile : Configuration 3

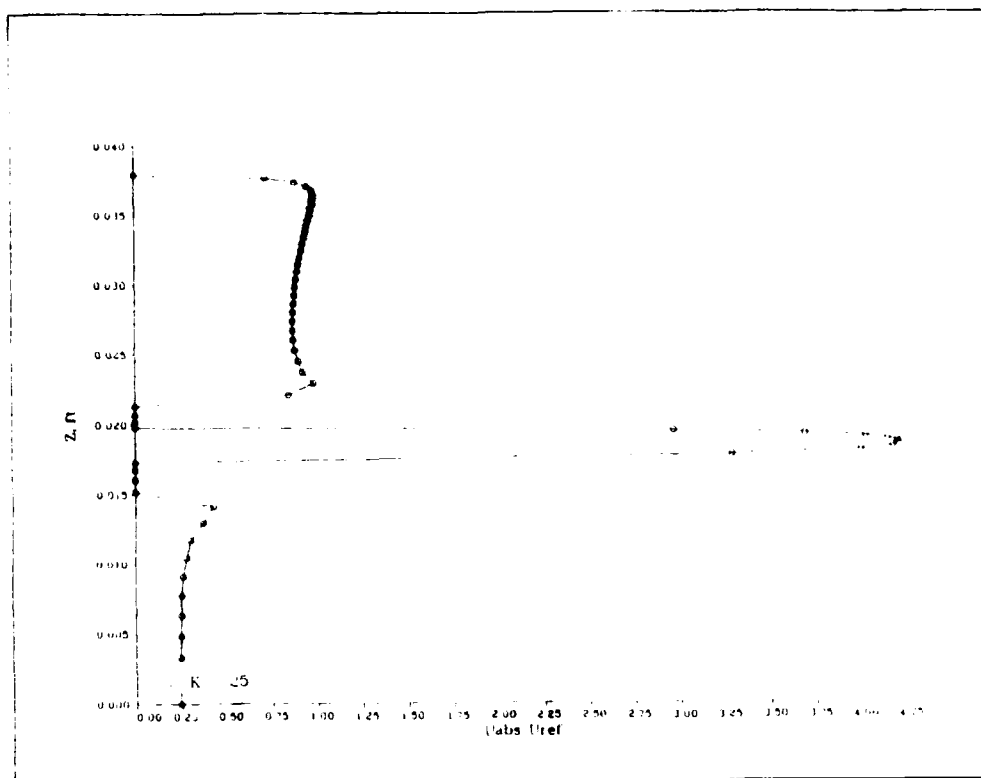


Fig. 32. Nozzle Velocity Profile : Configuration 0

This is due to the fact that the plenum pressure of both configurations is the same:

$$P_{o \text{ noz}} = P_{rat} (P_a) \quad (47)$$

but, as can be seen in Figures 33 and 34, the exit of configuration 3's nozzle is in the lower pressure region nearer the throat of the ejector. The pressure near the exit of configuration 3's nozzle (Figure 33) is about 0.990 P_a on the side nearer the wall and about 0.994 P_a on the opposite side. This is compared to configuration 0's nozzle (Figure 34) which is located where the pressures are approximately 0.996 P_a and P_a respectively. Since the exit

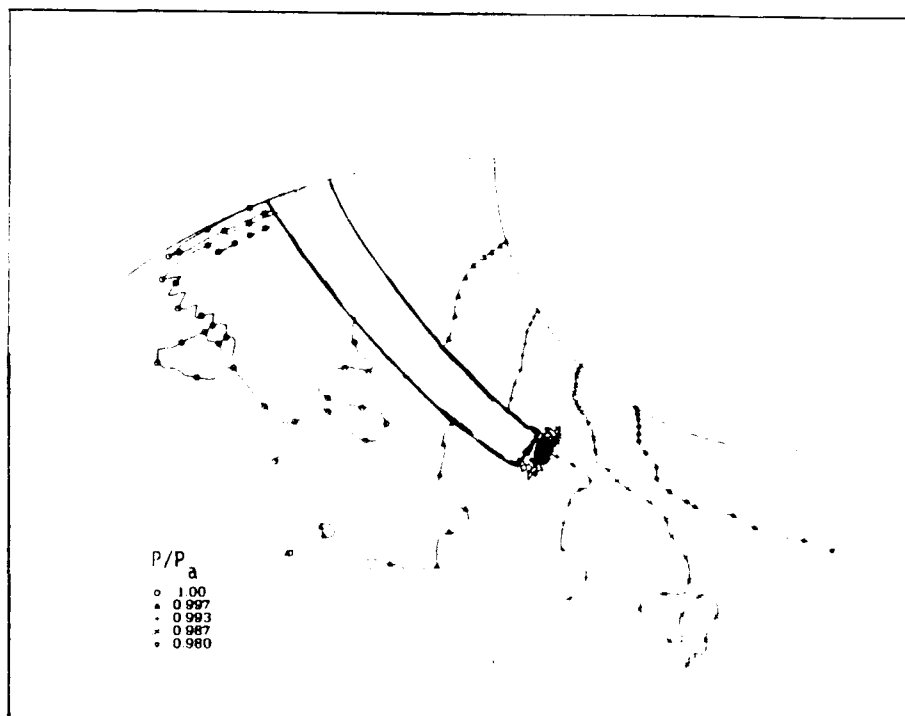


Fig. 33. Pressure Contours : Configuration 3

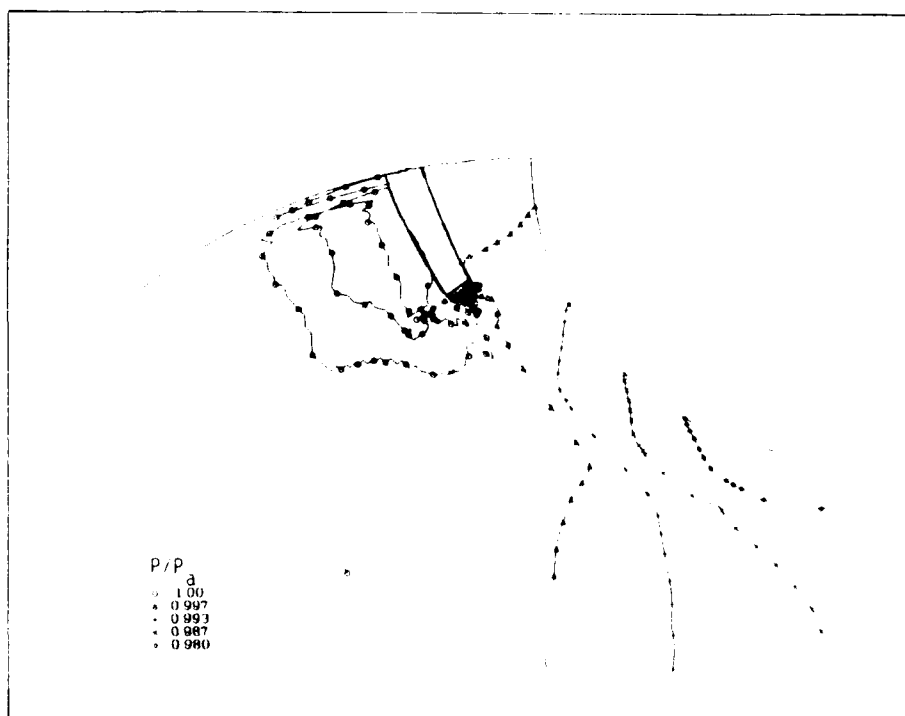


Fig. 34. Pressure Contours : Configuration 0

pressure is lower for configuration 3, the exit velocity is necessarily higher. Also, there is less momentum loss due to friction. This model does not, however, account for losses within the nozzle which would reduce the effectiveness of the longer nozzle structure of configuration 3. One would assume that there would be some point at which the advantages of moving the nozzle toward the throat would be outweighed by the reduced mixing length allowed. Further analysis would be necessary to define the optimum location. One can also see in these plots how a pressure difference is maintained across the jet it which forces the jet to turn. This is similar to the turning of the flow from a jet flap.

Nozzle Area Ratio. Configurations 1b and 1c were designed to keep all other factors the same as configuration 1a except the nozzle gap, and therefore the nozzle area, in order to investigate the effect of nozzle to throat area ratio changes. Configuration 1b had a reduced nozzle area and configuration 1c had an increased nozzle area relative to configuration 1a. The area ratios and achieved thrust augmentation were as in Table IV. The results are plotted in Figure 35.

Table IV
Augmentation with Changing Nozzle Area Ratio (α)

Config.	Nozzle Area Ratio	ϕ
1b	0.0650	1.407
1a	0.0887	1.398
1c	0.1167	1.353

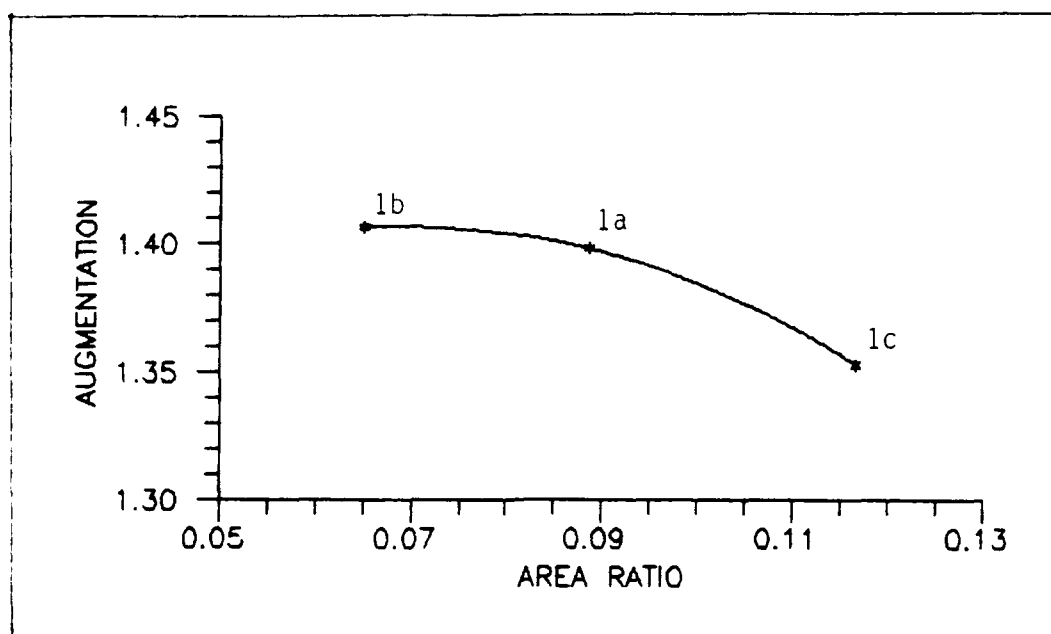


Fig. 35. Augmentation vs. Nozzle Area Ratio (α)

As can be seen from Figure 35, further reduction in area ratio would appear to be fruitless, contrary to the theoretical analysis presented earlier which predicted ever increasing augmentation with decreased area ratio. But, as Figure 36 shows, these results are in line with experimental results from Fought's MS Thesis as published in McCormick. These results suggest that the area ratio used by Reznick and Unnever (equivalent to configuration 1a) is near the optimum for this size ejector (Diameter = 112 mm).

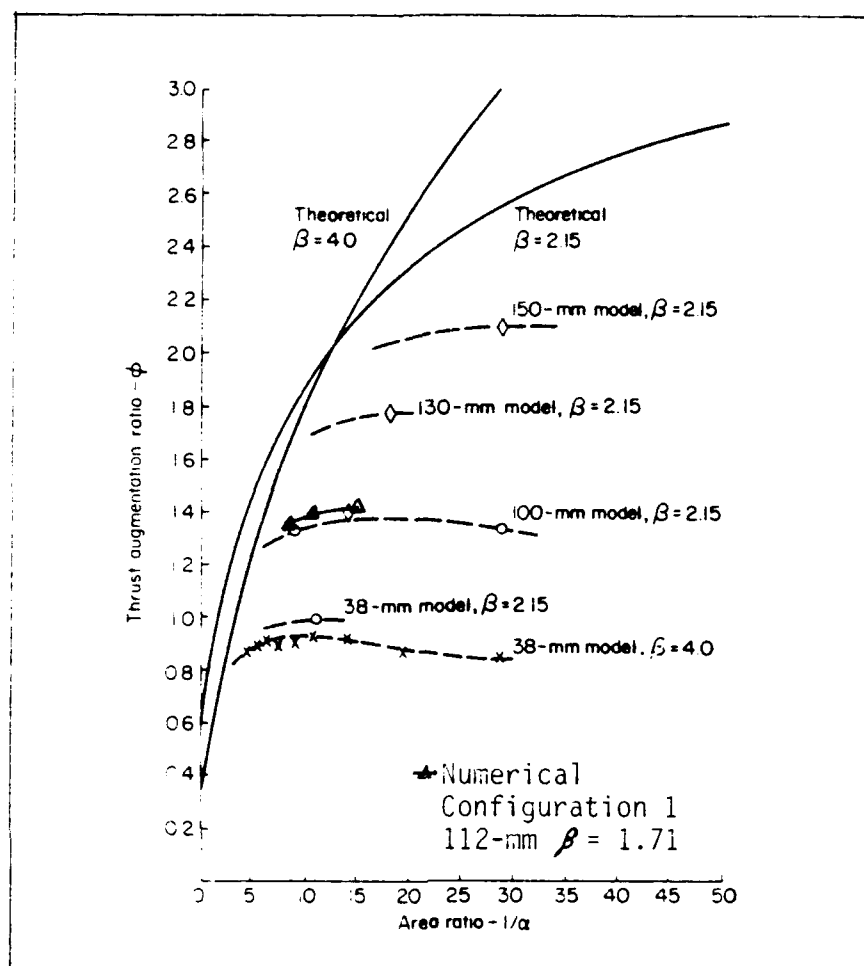


Fig. 36. Augmentation vs. Nozzle Area Ratio ($1/\alpha$)
Numerical and Experimental (9:285)

IV. Conclusions

All primary objectives of this thesis have been met. The numerical model has been shown to provide a reasonable simulation of the flow characteristics through the selected ejector configuration. Although the simulation is not sufficient to permit accurate prediction of actual thrust augmentation values for experimental hardware, all trends appear to be adequately modeled. Taking advantage of the complete knowledge of the flowfield provided by a numerical solution, the dynamics of the computed internal flow were able to be analyzed. Data visualization techniques were able to give us insight into the internal flow of the ejector which could not be measured experimentally. Sufficient flexibility has been incorporated in the code to handle variations of parameters such as injection angle, nozzle position, nozzle to throat area ratio, pressure ratio, as well as inlet and diffuser geometries.

In addition, the secondary objective of exploring the effect of these parameters on thrust augmentation was partially investigated allowing some initial conclusions to be drawn which could affect future experimental hardware design.

1) The area ratio used by Reznick and Unnever is near the optimum and should be sufficient for future experiments. However, if it is within manufacturing capability, some reduction of nozzle area would be beneficial.

2) Future experiments should concentrate on configurations which inject the jet at a location closer to the entrance of the constant area mixing chamber (smaller θ) if possible.

3) Initial indications are that an annular nozzle design should attempt to provide an injection angle approximately $1/4$ of the way between parallel to the wall and tangent to the wall for the selected nozzle location.

V. Suggestions and Recommendations

Any continued research in this area should concentrate on expanding the parametric analysis in the areas of nozzle location as well as inlet and diffuser geometries. Nozzle locations further into the inlet and variations in distance from the wall should be investigated. Larger diffuser ratios should also provide increased augmentation capability and different inlet shapes could optimize the incoming flow. Further analysis of injection angle effects for the new geometries may also be necessary.

Another primary area of research which would be beneficial is application of improved turbulence modeling, better grid refinement, and second-order boundary conditions to improve the numerical model and try to bring the predicted thrust augmentation levels in line with experimental results. It may even be desirable to change to a different solution algorithm to reduce computation time.

Lastly, using the parametric results presented here to design new experimental hardware should result in improved performance and would serve to better validate this model.

Appendix A: Grid Generating Programs and Tables

Appendix A-1: Grid Generating Program EJECGRD

```

PROGRAM      EJEGRD
PARAMETER   (JDIM = 130, LDIM = 115, JARC = 120)
COMMON /THRHT/ THRHT = 1.25, MAR = 101
COMMON /ANFANG/ ANFANG = 1, JARC, MAR, AM(JDIM)
COMMON /AREAS/ AREAS = 1, JARC, MAR, AM(JDIM)
COMMON /ARATS/ ARATS = 1, JARC, MAR, AM(JDIM)
COMMON /DAT/ L1, PS11, L2, PS12, XCVL, KCONE1
COMMON /FARCL/ FARCL = 1, JARC, MAR, AM(JDIM)
COMMON /KSI/ KSI = 1, JARC, MAR, AM(JDIM)
COMMON /NOZ/ NOZ = 1, JARC, MAR, AM(JDIM)

      COMPUTE WALL ARC LENGTH VS X
      J COUNTS HORIZONTALLY (AXIALLY)
      L COUNTS VERTICALLY (RADIALY)

      DIMENSION ARCLEN(JARC), GS(JDIM), XARC(JARC), XP(LDIM),
1 YP(LDIM) SUBSON
      LOGICAL
      XCVL = 3.0
      L1 = 3.5
      PS11 = 0.05235987756
      L2 = 3.5
      PS12 = 0.13962634
      KCONE1 = XCVL + L1 * COS(PS11)

      GENERATE TABLE OF ONE-DIMENSIONAL AREA RATIOS FOR
      SUBSONIC MACH NUMBERS

      CALL ARF

      GENERATE TABLE OF ARC LENGTH ALONG OUTER WALL
      CALL ARCDAT (ARCLEN, XARC, JARC)

      READ VERTICAL DISTRIBUTION OF HORIZONTAL LINES
      CALL READ64

      READ HORIZONTAL DISTRIBUTION OF VERTICAL LINES
      OPEN (7, FILE = 'EJECHRZ', STATUS = 'OLD')
      REWIND 7
      SUBSON = .TRUE.
      DO 1 J = 1, JDIM
      READ (7, 100) GS(J)
      S = GS(J) * ARCLEN(JARC)
      AM = TWIXT(S, ARCLEN, XARC, JARC)

      SUBROUTINES LEFT AND RIGHT DROP THE VERTICAL GRID LINES
      FROM THE SPECIFIED WALL POSITION, AM.

      IF (XW .LE. 0.0) THEN
      CALL LEFT (XW, XP, YP)
      ELSE
      CALL RIGHT (XW, XP, YP)
      END IF

      AT IS THE ARC LENGTH OF THE CURRENT VERTICAL GRID LINE

```

```

C      AR = (AL / THRHT) ** 2
C      JNOZIN = 57
C      JNOZOUT = 69
C      CALL MARF (AR, SUBSON, AM (J))
C      DO 1 L = 1, LDIM
C      AX AND AY ARE THE GRID COORDINATES; SUBSCRIPTS INCREASE
C      DOWNWARD FROM THE WALL.
C      AA IS THE SLOPE OF THE HORIZONTAL GRID LINE.
C      AX(J, L) = XP(L)
C      AY(J, L) = YP(L)
C      AA(J, L) = ANG(L)
C      CONTINUE
C      1 CLOSE (7)
C
C      WRITE FILE FOR JSTAXX
C      CALL FINAL
C      STOP
C
C      100 FORMAT ( 2X, 4E14.7 )
C
C      END
C      SUBROUTINE ARF
C      PARAMETER (GAM = 1.4, MAR = 101, DM = 0.01)
C      COMMON /ARATS/ AMR(NAR), ARAT(NAR)
C      B = 0.5 * (GAM + 1.0) / (GAM - 1.0)
C      A = (2.0 / (GAM + 1.0)) ** B
C      AMR(NAR) = 0.00001
C      ARAT(NAR) = (A / AMR(NAR)) * (1.0 + C * AMR(NAR) ** 2) ** B
C      DO 1 I = 1, NAR
C      K = MAR + I - 1
C      AMR(K) = DM * FLOAT(I - 1)
C      ARAT(K) = (A / AMR(K)) * (1.0 + C * AMR(K) ** 2) ** B
C      1 RETURN
C      CONTINUE
C      END
C      SUBROUTINE FINAL
C      PARAMETER (JDIM = 130, LDIM = 115, JARC = 120)
C      COMMON /ANFANG/ ANFANG = 1, JARC, MAR, AM(JDIM)
C      COMMON /KSI/ KSI = 1, JARC, MAR, AM(JDIM)
C      COMMON /NOZ/ NOZ = 1, JARC, MAR, AM(JDIM)
C      DIMENSION RHO(JDIM, LDIM), RHOE(JDIM, LDIM), ZH(JDIM,
1 RHO(JDIM, LDIM), ZH(JDIM, LDIM), ZH(JDIM, LDIM), ZH(JDIM,
2 ZH(JDIM, LDIM), ZH(JDIM, LDIM)
C      LOGICAL
C      LANIN
C      EQUIVALENCE (F5MACH, XM), (TM, THALL)
C
C      DATA TO, PO / 518.7, 14.698 /
C      DATA TM / 518.7 /
C      DATA CV, RG / 4290.0, 1718 /
C
C      NAMELIST /JIX ALPHA, BETA, CEL, CX, CY, ISMTHX, ISMTHY,
C      1 ISTART, JL, KL, KSTEP, LANIN, MEND, PIN, REV, RL, TINF,
C      2 TTIN, TW, XM

```



```

WRITE (7, 100) BETA, CFL, CX, CY, ISMTHX, ISMTHY, ISTART,
1 JI, KL, KSTEP, LAMIN, NEND, RL, TINF, TM, XM
CLOSE (7)
RETURN

C 100
FORMAT ( ' $JIX', ' BETA', ' F4.1, ' ' /
1 ' CX', ' F7.4, ' ' /
2 ' CY', ' F4.1, ' ' /
3 ' ISMTHX', ' I2, ' ' /
4 ' ISTART', ' I2, ' ' /
5 ' JI', ' I3, ' ' /
6 ' KSTEP', ' I2, ' ' /
7 ' NEND', ' I2, ' ' /
8 ' RL', ' F7.4, ' ' /
9 ' TM', ' F6.1, ' ' /
10 ' XM', ' F5.2, ' ' /
11 ' $END' )

END
SUBROUTINE ARCDAT (ARCLEN, XARC, JARC)
COMMON /DAT/ L1, PSI1, L2, PSI2, XCYL, XCONE1
C
C COMPUTE TABLE OF ARCLEN VS XARC
C
C DIMENSION ARCLEN(JARC), XARC(JARC)
C
ARCLEN(1) = 0.0
XARC(1) = -2.0
ARCLEN(JARC) = 6.14159265 + L1 + L2
XARC(JARC) = XCONE1 + L2 * COS(PSI2)
DARC = ARCLEN(JARC) / (JARC - 1)
DTMETHA = DARC * 2.0
THETA = 0.0
DO 1 J = 2, JARC-1
ARCLEN(J) = ARCLEN(J-1) + DARC
IF (XARC(J-1) .LT. 0.0) THEN
THETA = THETA + DTMETHA
XARC(J) = -2.0 * COS(THETA)
ELSE IF (XARC(J-1) .LT. 3.0) THEN
XARC(J) = XARC(J-1) + DARC
ELSE IF (XARC(J-1) .LT. XCONE1) THEN
XARC(J) = XARC(J-1) + DARC * COS(PSI1)
ELSE
XARC(J) = XARC(J-1) + DARC * COS(PSI2)
END IF
CONTINUE
1 RETURN
END

```

Appendix A-2: Grid Generating Program DEHNEN

2 RETURN
END

```

C
PROGRAM DEHNM
PARAMETER (NMAX = 1000)
DIMENSION XB(NMAX)
CHARACTER FILE * 40

PRINT *, 'NUMBER OF POINTS?'
READ *, N
PRINT *, 'SIZE OF SMALLEST STEP?'
READ *, DX
PRINT *, 'TOTAL SPAN?'
READ *, SPAN
IF (SPAN .LE. 0.0) SPAN = 1.0
N1 = N - 1
DXM1 = 1.0 / FLOAT(N1)
CALL MRX (DX, SPAN, DXM1, CK)
PRINT *, 'FINAL CK =', CK
EKM1 = EXP(CK) - 1.0
PRINT *, 'SMALL THE SMALLEST INCREMENT BE FIRST (1)'
PRINT *, 'OR LAST (2)'
READ *, IGO
IF (IGO .GT. 1) THEN
  DO 1 I = 1, N
    J = 1 - N - I
    B = FLOAT(I - 1) * DXM1
    XB(J) = SPAN * 1.0 - EXP(CK * B) - 1.0 * EKM1
  1 CONTINUE
ELSE
  DO 2 I = 1, N
    B = FLOAT(I - 1) * DXM1
    XB(I) = SPAN * EXP(CK * B) - 1.0 / EKM1
  2 CONTINUE
END IF
PRINT *, 'NAME OF OUTPUT FILE?'
READ *, 100 FILE
OPEN (7, FILE = FILE, STATUS = 'UNKNOWN')
REWIND 7
DO 3 I = 1, N
  WRITE (7, 101) XB (I)
3 CONTINUE
STOP
100 FORMAT (A)
101 FORMAT (2X, E14.7)
END
SUBROUTINE MRX (D, EL, ZETA, CK)
  SOLVE EXPONENTIAL GRID-STRETCHING EQUATION
  BY NEWTON-RAPHSON ITERATION
  CK = 1.0
  DO 1 K = 1, 10
    EK = EXP(CK)
    EKZ = EXP(CK * ZETA)
    FK = EL * (EKZ - 1.0) / (EK - 1.0) - D
    FKP = EL * (ZETA * EKZ - EKZ - 1.0) * EK / (EK - 1.0)
    (EK - 1.0)
    IF (ABS(FK / FKP) .LE. 1.0E-5) GO TO 2
    CK = CK - FK / FKP
  1 CONTINUE
  WRITE (6, *) 'MRX FAILED.'

```

Appendix A-3: Grid Spacing Table EJE CVRT

0.000000E+00
 .227272E-02
 .460363E-02
 .699454E-02
 .946818E-02
 .1196227E-01
 .1464182E-01
 .1718818E-01
 .1990182E-01
 .2268545E-01
 .2554045E-01
 .284684E-01
 .3147297E-01
 .345527E-01
 .377273E-01
 .409531E-01
 .442727E-01
 .476863E-01
 .5118318E-01
 .547700E-01
 .5844818E-01
 .6222136E-01
 .6609136E-01
 .7006045E-01
 .7413136E-01
 .7830727E-01
 .825900E-01
 .8698273E-01
 .9148818E-01
 .9610909E-01
 .1008491E-00
 .1057165E-00
 .1106964E-00
 .1158105E-00
 .121058E-00
 .126329E-00
 .131541E-00
 .136814E-00
 .142131E-00
 .14732E-00
 .152480E-00
 .157436E-00
 .1621682E-00
 .1671436E-00
 .171442E-00
 .175991E-00
 .1807018E-00
 .1854812E-00
 .190263E-00
 .195359E-00
 .196091E-00
 .182468E-00
 .2003418E-00
 .202392E-00
 .2045159E-00
 .2057908E-00
 .2092228E-00
 .2122109E-00
 .215540E-00
 .219451E-00
 .224001E-00

.2393029E+00
 .2394554E+00
 .2425577E+00
 .2507086E+00
 .2594168E+00
 .2683482E+00
 .275091E+00
 .2869050E+00
 .2965423E+00
 .3064268E+00
 .316555E+00
 .3269636E+00
 .3376291E+00
 .3485686E+00
 .3597886E+00
 .3712964E+00
 .383100E+00
 .3952594E+00
 .4076232E+00
 .4203371E+00
 .4334218E+00
 .4468200E+00
 .4605618E+00
 .4746568E+00
 .4891132E+00
 .5039409E+00
 .5191491E+00
 .5347477E+00
 .5507466E+00
 .5671562E+00
 .5839871E+00
 .6012500E+00
 .6189560E+00
 .6371164E+00
 .6557430E+00
 .6748478E+00
 .6944430E+00
 .7145410E+00
 .7351551E+00
 .757282E+00
 .779781E+00
 .797278E+00
 .816789E+00
 .8356479E+00
 .8538532E+00
 .8714057E+00
 .8883053E+00
 .9045521E+00
 .9201460E+00
 .9350871E+00
 .9493754E+00
 .9630108E+00
 .9759934E+00
 .9883231E+00
 .1000000E+01

Appendix A-4: Grid Spacing Table EJECHRZ

.1000000E+04
.2000000E+02
.404115E+03
.612430E+03
.835032E+02
.104308E+01
.126350E+01
.148448E+01
.172009E+01
.195248E+01
.219572E+01
.244090E+01
.269113E+01
.294650E+01
.320713E+01
.347312E+01
.374459E+01
.402164E+01
.430439E+01
.459296E+01
.488745E+01
.518803E+01
.549479E+01
.580786E+01
.612736E+01
.645344E+01
.678623E+01
.712587E+01
.747250E+01
.782626E+01
.818729E+01
.855574E+01
.893181E+01
.931560E+01
.970728E+01
.101070E+01
.104313E+01
.107569E+01
.111266E+01
.115097E+01
.118977E+01
.122829E+01
.126642E+01
.131452E+01
.135267E+01
.138625E+01
.140895E+01
.142481E+01
.143529E+01
.144185E+01
.144593E+01
.144906E+01
.145217E+01
.145725E+01
.146617E+01
.148028E+01
.150073E+01
.152648E+01
.156438E+01
.161174E+01
.166490E+01

.171916E+00
.177454E+00
.183105E+00
.188733E+00
.194759E+00
.200767E+00
.206898E+00
.213155E+00
.219441E+00
.226090E+00
.232710E+00
.239488E+00
.246270E+00
.253078E+00
.260718E+00
.268078E+00
.275594E+00
.283265E+00
.291094E+00
.299083E+00
.307237E+00
.315558E+00
.324053E+00
.332720E+00
.341567E+00
.350595E+00
.359809E+00
.369122E+00
.378410E+00
.388055E+00
.398601E+00
.408803E+00
.419214E+00
.429840E+00
.440856E+00
.451753E+00
.463049E+00
.474570E+00
.486342E+00
.498349E+00
.510403E+00
.523110E+00
.535874E+00
.548907E+00
.562195E+00
.575763E+00
.589104E+00
.603728E+00
.618658E+00
.632885E+00
.647908E+00
.663240E+00
.678873E+00
.694856E+00
.711154E+00
.727785E+00
.744762E+00
.762087E+00
.779768E+00
.797813E+00
.816230E+00

.835025E+00
.854207E+00
.873784E+00
.893763E+00
.914154E+00
.934964E+00
.956203E+00
.977878E+00
.1000000E+01

Appendix B: Flow Solving Program JSIAXK

```

PROGRAM JSIAXK
PARAMETER (MK = 130, MJ = 115)
COMMON /DELTA, DZETA, CV, RC, PR, PRT, GAMMA, DTLM(MJ), GAMH1,
1 CFL, BETA, UINF, RHOINF, CINF, TINF, TM, DT, CX, CY, L, JL, KL,
2 JLM, KLM, ISMTHX, ISMTHY, KSTART(MJ),
COMMON /CGAS, CVIH, CVIAH, GAMMP, GAMMR, GAMHT, RUTNF, REINF,
COMMON /DEP, RHO(MK, MJ), RHOU(MK, MJ), RHOV(MK, MJ), RHOE(MK,
1 MJ),
COMMON /DEPP, RHOP(MK, MJ), RHOPU(MK, MJ), RHOVP(MK, MJ),
1 RHOEP(MK, MJ),
COMMON /DOP, X(MK, MJ), Y(MK, MJ), RY(MK, MJ)
COMMON /ERR, KFE, JFE
COMMON /IBC, PTIN, QZCP, TTIN
COMMON /NELSON, RDET, RDZT, QDET, RMU, SL(MK, MJ)
COMMON /NOZ, KNOZ, JNOZIN, JNOZOUT, JMIN, JMWOUT, JNERIN,
1 JNEROUT, PTNOZ, TTNOZ, ALPHA, EFFNOZ
COMMON /OLD, ROLD(MK, MJ), RUOLD(MK, MJ), RVOLD(MK, MJ),
1 REOLD(MK, MJ), XNOHM
COMMON /PLT, RL, RH, RCV, PINE, KSTEP
COMMON /TV, ETX(MK, MJ), ETY(MK, MJ), ZTX(MK, MJ), ZTY(MK, MJ)
COMMON /TVIS, EP(MK, MJ), CPQPR, CPQPR1
LOGICAL LAMIN, OOPS
NAMELIST /JIX, ALPHA, BETA, CFL, CX, CY, ISMTHX, ISMTHY,
1 ISTART, JL, KL, KSTEP, LAMIN, NEND, PTIN, REV, RL, TINF, TTIN,
2 TM, XM
CALL DROFFILE (0)

CONSTANTS AND PARAMETERS FOR ATR
CV = 4290.0
RC = 1718.0
GAMMA = 1.0
GAMH1 = 1.0
GAMMP = GAMMA / GAMMA
GAMMR = GAMMA * RC
GAMHT = GAMMA / GAMH1
PR = 0.73
PRT = 0.90
RCV = 1.0 / CV
QZCP = 0.5 / (GAMMA * CV)
CPQPR = GAMMA * CV / PR
CPQPR1 = GAMMA * CV / PRT

READ IN THE INPUT DATA
OPEN (5, FILE = 'JIX.DAT', FORM = 'FORMATTED', STATUS = 'OLD')
CALL DDIOFOM ('LABELS')
READ (5, JIX)
CALL DDIOFOM ('LABELS')
CLOSE (5)

GENERATE THE EXIT PLANE (REFERENCE) INFORMATION
CINF = SORT(GAMMA * RC * TINF)
UINF = CINF * XM
RMUINF = 0.71 * CINF

```

```

PINF = RHOINF * RC * TINF
CVIH = TM
CV = TINF * 1.0 + 0.5 * GAMH1 * SORT(PR * XM ** 2)
RHOINF = UINF
RHOINF = (CV * TINF + 0.5 * UINF ** 2)
RL = UINF
JL = 1
KLM = KL - 1
DZETA = 1.0 / JLM
DZETA = 1.0 / NLM

WRITE OUT THE INPUT AND FLOW FIELD INFORMATION
OPEN (6, FILE = 'JIX.OUT', FORM = 'FORMATTED', STATUS = 'NEW')
WRITE (6, 100) XM, REY, TM, RHOINF
WRITE (6, 101) UINF, CINF, TINF, PINF, RMUINF
WRITE (6, 102) DZETA, DZETA, RL
WRITE (6, 103) CFL, CX, CY, BETA
WRITE (6, 104) NEND, JL, KL, LAMIN, TTIN, PTIN
IF (BETA .NE. 0.0) WRITE (6, 105)

MT = 1
TMS1 = 0.0
TMS2 = 0.0

IF (ISTART .EQ. 0) THEN
  READ IN THE GRID POINTS IN CARTESIAN FRAME AND
  INITIALIZE ALL DEPENDENT VARIABLES
  OPEN (1, FILE = 'EJECO', FORM = 'UNFORMATTED', STATUS =
  1 'OLD')
  READ (1) ((X(K, J), K = 1, KL), J = 1, JL)
  1 ((Y(K, J), K = 1, KL), J = 1, JL)
  READ (1) ((RHO(K, J), K = 1, KL), J = 1, JL)
  1 ((RHOU(K, J), K = 1, KL), J = 1, JL)
  2 ((RHOV(K, J), K = 1, KL), J = 1, JL)
  3 ((RHOE(K, J), K = 1, KL), J = 1, JL)
  CLOSE (1)
  ELSE
  READ IN THE RESTART DATA FROM PREVIOUS RUNS
  OPEN (1, FILE = 'JIXPRV', FORM = 'UNFORMATTED', STATUS =
  1 'OLD')
  READ (1) MT, TMS1, TMS2
  READ (1) ((RHO(K, J), K = 1, KL), J = 1, JL)
  1 ((RHOU(K, J), K = 1, KL), J = 1, JL)
  2 ((RHOV(K, J), K = 1, KL), J = 1, JL)
  3 ((RHOE(K, J), K = 1, KL), J = 1, JL)
  4 ((EP(K, J), K = 1, KL), J = 1, JL)
  READ (1) ((X(K, J), K = 1, KL), J = 1, JL)
  1 ((Y(K, J), K = 1, KL), J = 1, JL)
  CLOSE (1)
  END IF

  SOME CONSTANTS FOR EDDY
  RDET = 0.5 / DZETA
  RDET = 0.5 / DZETA

```



```

END
SUBROUTINE BC
PARAMETER (MK = 130, MJ = 115,
COMMON /DETA, DZETA, CV, RC, PR, PRT, GAMMA, DTL(MJ), GAMM1,
1 JLM, BETA, UINF, RHOINF, CINF, TINF, IM, DI, CX, CY, L, JL, KL,
2 JLM, KLM, ISMTX, ISMTY, KSTAR(MJ),
COMMON /CCAS, CXTM, CXTM, GAMMP, GAMMR, GAMMT, RUINF, REINF,
COMMON /DEP, RHO(MK, MJ), RHOUT(MK, MJ), RHOV(MK, MJ), RHOE(MK,
1 MJ),
1 COMMON /DEPP, RHOPI(MK, MJ), RHOUP(MK, MJ), RHOVP(MK, MJ),
COMMON /DOF, X(MK, MJ), Y(MK, MJ), RY(MK, MJ),
COMMON /IBC, PTIM, QZCP, TTIN
COMMON /KNOZ, KNOZ, JNOZIN, JNOZOUT, JNKNIN, JNKNOUT, JNERIN,
1 JNEROUT, PTNOZ, TTNOZ, ALPHA, EFFNOZ
COMMON /PLT, RL, RH, RCV, PINF, KSTEP
COMMON /TV, ETX(MK, MJ), ETY(MK, MJ), ZIX(MK, MJ), ZIY(MK, MJ)
IF (L.EQ. 1) THEN
PREDICTOR SWEEP
UPSTREAM BOUNDARY CONDITIONS.
DO 1 J = 2, JLM
JP = J + 1
JM = J - 1
RHOPI(J, J) = PTIN / (RC * TTIN)
RHOUP(J, J) = RHOVP(J, J)
RHOVP(J, J) = Y(2, J) / Y(1, J)
U = RHOUP(J, J) / RHOPI(J, J)
V = RHOVP(J, J) / RHOPI(J, J)
PSI = ATAN(X(1, JP) - X(1, JM)) / (Y(1, JP) - Y(1, JM))
UPRIME = RHOUP(J, J) * COS(PSI) - RHOVP(J, J) * SIN(PSI)
T = TTIN - QZCP * (U ** 2 - V ** 2)
RHOEP(J, J) = RHOPI(J, J) * (CV * T + 0.5 * (U ** 2 +
V ** 2))
1
IF (UPRIME .LE. 0.0) THEN
E2 = RHOEP(J, J) / RHOPI(J, J)
U2 = RHOUP(J, J) / RHOPI(J, J)
V2 = RHOVP(J, J) / RHOPI(J, J)
T = (E2 - 0.5 * (U2 ** 2 - V2 ** 2)) / CV
RHOPI(J, J) = PTIN / (T * RC)
U = RHOUP(J, J) / RHOPI(J, J)
V = RHOVP(J, J) / RHOPI(J, J)
E = CV * T + 0.5 * (U ** 2 + V ** 2)
RHOEP(J, J) = E * RHOPI(J, J)
ENDIF
DOWNSTREAM BOUNDARY CONDITIONS.
EM = RHOEP(KLM, J) / RHOPI(KLM, J)
UM = RHOUP(KLM, J) / RHOPI(KLM, J)
VM = RHOVP(KLM, J) / RHOPI(KLM, J)
T = (EM - 0.5 * (UM ** 2 - VM ** 2)) / CV

```

```

RHOPI(KL, J) = PTIN / (T * RC)
U = RHOUP(KL, J) / RHOPI(KL, J)
V = RHOVP(KL, J) / RHOPI(KL, J)
E = CV * T + 0.5 * (U ** 2 + V ** 2)
RHOEP(KL, J) = E * RHOPI(KL, J)
CONTINUE
1
ON THE SOLID CONTOUR, NO SLIP FOR U, V,
CONSTANT SURFACE TEMP. AND DP / DN = 0.
DO 2 K = 1, KL
RH = 1.0 / RHOPI(K, JLM)
RHOUP(K, JL) = 0.0
RHOVP(K, JL) = 0.0
RHOEP(K, JL) = RHOPI(K, JLM) - 0.5 * RHOPI(K, JLM) *
((RHOUP(K, JLM) * RH) ** 2 + (RHOVP(K, JLM) * RH) ** 2)
RHOPI(K, JL) = RHOEP(K, JL) / CVIM
ON THE AXIS, ZERO RADIAL GRADIENT.
RHOVP(K, 1) = 0.0
RHOUP(K, 1) = RHOUP(K, 2)
RHOEP(K, 1) = RHOEP(K, 2) - 0.5 * RHOVP(K, 2) ** 2 / RHOPI(K, 2)
RHOPI(K, 1) = RHOPI(K, 2)
CONTINUE
2
PRIMARY NOZZLE BOUNDARY CONDITIONS
KNP = KNOZ + 1
RHNKAR1 = 1.0 / RHOPI(KNOZ, JNERIN)
YNEARI = RHOUP(KNOZ, JNERIN) * RHNKAR1
VNEARI = RHOVP(KNOZ, JNERIN) * RHNKAR1
TNEARI = (RHOEP(KNOZ, JNERIN) * RHNKAR1 - 0.5 *
(UNEARI ** 2 + VNEARI ** 2)) * RCV
PNEARI = RHOPI(KNOZ, JNERIN) * RC * TNEARI
RHNKARO = 1.0 / RHOPI(KNOZ, JNEROUT)
UNEARO = RHOUP(KNOZ, JNEROUT) * RHNKARO
VNEARO = RHOVP(KNOZ, JNEROUT) * RHNKARO
TNEARO = (RHOEP(KNOZ, JNEROUT) * RHNKARO - 0.5 *
(UNEARO ** 2 + VNEARO ** 2)) * RCV
PNEARO = RHOPI(KNOZ, JNEROUT) * RC * TNEARO
SET NOZZLE EXIT PRESSURE TO AVERAGE LOCAL PRESSURE
AND CALCULATE MEAN EXIT VELOCITY
PNOZ = 0.5 * (PNEARI + PNEARO)
IF (PNOZ .GE. 0.95 * PTNOZ) THEN
PNOZ = 0.95 * PTNOZ
ENDIF
TNOZ1 = (PNOZ / PTNOZ) * GAMMP * TTNOZ
TNOZ1 = 507.42
CNOZ = SORT(2.0 / GAMM1 * (TTNOZ / TNOZ1 - 1.0))
ANOZ = SORT(GAMMR * TNOZ1)
VELNOZ = EFFNOZ ** 0.5 * CNOZ * ANOZ
TNOZ = TTNOZ - EFFNOZ * (TNOZ - TNOZ1)
GIVE EXIT VELOCITY A PARABOLIC PROFILE
AND PRESSURE A LINEAR PROFILE
1
ZJMAX = SORT((X(KNOZ, JNOZOUT) - X(KNOZ, JNOZIN))
** 2 + (Y(KNOZ, JNOZOUT) - Y(KNOZ, JNOZIN)) ** 2)

```

```

DO 3 J = JNOZIN, 1, JNOZOUT - 1
  ZJ = SORT (X(KNOZ, J) - X(KNOZ, JNOZIN))
  Z = ZJ + 1, IAX
  VELNOZJ = 6.0 * VELNOZ + Z * (1.0 - Z)
  PNOZJ = PREARI + Z * (PREARO - PREARI)
  TNOZJ = PNOZJ / PTNOZ * GAMMA
  RHNOZJ = PTHOZ / (RC * TNOZ)
  RHOUP(KNOZ, J) = (RHOUP(KNP, J) * ZTX(KNP, J) +
    (ZTX(KNOZ, J) * TAN(ALPHA) * Y(KNP, J) / Y(KNOZ, J) +
    (ZTX(KNOZ, J) * TAN(ALPHA) * Y(KNOZ, J) * TANIALPHA)
  RHOUP(KNOZ, J) = RHOUP(KNP, J) * Y(KNP, J) / Y(KNOZ, J)
  RHOUP(KNOZ, J) = RHOUP(KNP, J) * Y(KNP, J) / Y(KNOZ, J)
  RHOVEL = SORT(RHOUP(KNOZ, J) * Z + RHOUP(KNOZ, J) *
  RHOUP(KNOZ, J) = RHOVEL * COS(ALPHA)
  U = RHOUP(KNOZ, J) / RHOUP(KNP, J)
  V = RHOUP(KNOZ, J) / RHOUP(KNP, J)
  TNOZJ = TTHOZ - QZCP * (U ** 2 + V ** 2)
  TNOZ = TTHOZ - EFFNOZ * (TNOZ - TTHOZ)
  RGAMH1 = 1.0 / GAMH1
  RHOUP(KNOZ, J) = RHNOZ * (TNOZ / TTHOZ) * RGAMH1
  U = RHOUP(KNOZ, J) / RHOUP(KNOZ, J)
  V = RHOUP(KNOZ, J) / RHOUP(KNOZ, J)
  UNOZ = VELNOZJ * COS(ALPHA)
  VNOZ = VELNOZJ * SIN(ALPHA)
  RHOUP(KNOZ, J) = RHOUP(KNOZ, J) * UNOZ
  RHOUP(KNOZ, J) = RHOUP(KNOZ, J) * VNOZ
  RHOUP(KNOZ, J) = RHOUP(KNOZ, J) * (CY * TNOZ
    + D.5 * VELNOZJ ** 2)
  E = CY * TNOZ + D.5 * (U ** 2 + V ** 2)
  RHOUP(KNOZ, J) = E * RHOUP(KNOZ, J)
  CONTINUE

NO SLIP / NO PENETRATION ON NOZZLE SIDES
DO 4 K = 1, KNOZ - 1
  OUTSIDE INNER WALL
  RH = 1.0 / RHOUP(K, JNERIN)
  RHOUP(K, JNNIN) = 0.0
  RHOUP(K, JNNIN) = 0.0
  RHOUP(K, JNERIN) = RHOUP(K, JNERIN) * RH ** 2
    + (RHOUP(K, JNERIN) * RH) ** 2
  RHOUP(K, JNNIN) = RHOUP(K, JNNIN) / CVTM
  OUTSIDE OUTER WALL
  RH = 1.0 / RHOUP(K, JNEROUT)
  RHOUP(K, JNNOUT) = 0.0
  RHOUP(K, JNNOUT) = 0.0
  RHOUP(K, JNEROUT) = RHOUP(K, JNEROUT) * RH ** 2
    + (RHOUP(K, JNEROUT) * RH) ** 2
  RHOUP(K, JNNOUT) = RHOUP(K, JNNOUT) / CVTM
  IGNORES ALL POINTS BLOCKED BY NOZZLE STRUCTURE

```

```

JCL = (JNOZIN + JNOZOUT) * 0.5
DO 4 J = JNNIN + 1, JNNOUT - 1
  RHOUP(K, J) = 0.0
  IF (J.LE.JCL) THEN
    RHOUP(K, J) = RHOUP(K, JNNIN)
  ELSE
    RHOUP(K, J) = RHOUP(K, JNNOUT)
  ENDIF
  CONTINUE
DO 5 J = JNNIN + 1, JNOZIN - 1
  INNER WALL END
  KNER = KNOZ + 1
  RH = 1.0 / RHOUP(KNER, J)
  RHOUP(KNOZ, J) = 0.0
  RHOUP(KNOZ, J) = 0.0
  RHOUP(KNOZ, J) = RHOUP(KNER, J) * 0.5 *
    + (RHOUP(KNER, J) * RH) ** 2
  RHOUP(KNOZ, J) = RHOUP(KNOZ, J) / CVTM
  CONTINUE
DO 6 J = JNOZOUT + 1, JNNOUT - 1
  OUTER WALL END
  KNER = KNOZ + 1
  RH = 1.0 / RHOUP(KNER, J)
  RHOUP(KNOZ, J) = 0.0
  RHOUP(KNOZ, J) = 0.0
  RHOUP(KNOZ, J) = RHOUP(KNER, J) * 0.5 *
    + (RHOUP(KNER, J) * RH) ** 2
  RHOUP(KNOZ, J) = RHOUP(KNOZ, J) / CVTM
  CONTINUE
  OUTSIDE INNER WALL END
  JC = JNNIN
  JNER = JC - 1
  KC = KNOZ
  KNER = KC + 1
  RHKNER = 1.0 / RHOUP(KNER, JC)
  RHJNER = 1.0 / RHOUP(KC, JNER)
  RHOUP(KC, JC) = 0.0
  RHOUP(KC, JC) = 0.0
  RHOUP(KC, JC) = 0.5 * RHOUP(KC, JNER) + 0.5 *
    + RHOUP(KC, JNER) * RHJNER ** 2
  RHOUP(KC, JC) = 0.25 * RHOUP(KC, JNER)
    + RHOUP(KC, JNER) * RHJNER ** 2
    + (RHOUP(KC, JNER) * RHKNER) ** 2
    + (RHOUP(KC, JNER) * RHJNER) ** 2
  RHOUP(KC, JC) = RHOUP(KC, JC) / CVTM
  INSIDE OUTER WALL END
  JC = JNOZOUT
  JNER = JC - 1

```



```

1 UNLARI = RHO(KNOZ,JNERIN) * RHNEARI
  VNLARI = RHOV(KNOZ,JNERIN) * RHNEARI
  TNLARI = RHOE(KNOZ,JNERIN) * RHNEARI - 0.5 *
  (UNLARI ** 2 + VNLARI ** 2) / RCV
  PNLARI = RHO(KNOZ,JNERIN) * RC * TNLARI
  RHNEARO = 1.0 / RHO(KNOZ,JNEROUT)
  UNNEARO = RHO(KNOZ,JNEROUT) * RHNEARO
  VNEARO = RHOV(KNOZ,JNEROUT) * RHNEARO
  TNEARO = RHOE(KNOZ,JNEROUT) * RHNEARO - 0.5 *
  (UNNEARO ** 2 + VNEARO ** 2) / RCV
  PNEARO = RHO(KNOZ,JNEROUT) * RC * TNEARO

SET NOZZLE EXIT PRESSURE TO AVERAGE LOCAL PRESSURE
AND CALCULATE MEAN EXIT VELOCITY
PNOZ = 0.5 * (PNLARI + PNEARO)
IF (PNOZ .GE. (0.95 * PTNOZ)) THEN
  PNOZ = 0.95 * PTNOZ
ENDIF
TNOZ1 = (PNOZ/PTNOZ)**GAMMA * TTNOZ
CNOZ = SORT(2.0/GAMMA*(TTNOZ/TNOZ1-1.0))
ANOZ = SORT(GAMMA * TNOZ1)
VELNOZ = EFFNOZ ** 0.5 * CNOZ * ANOZ
TNOZ = TTNOZ - EFFNOZ * (TTNOZ - TNOZ1)

GIVE EXIT VELOCITY A PARABOLIC PROFILE
AND PRESSURE A LINEAR PROFILE
ZJMAX = SORT((X(KNOZ,JNOZOUT) - X(KNOZ,JNOZIN))
  ** 2 + (Y(KNOZ,JNOZOUT) - Y(KNOZ,JNOZIN)) ** 2)
DO 9 J = JNOZIN + 1, JNOZOUT - 1
  ZJ = SORT((X(KNOZ,J) - X(KNOZ,JNOZIN))
  ** 2 + (Y(KNOZ,J) - Y(KNOZ,JNOZIN)) ** 2)
  Z = ZJ / ZJMAX
  VELNOZJ = 6.0 * VELNOZ * Z * (1.0 - Z)
  PNOZJ = PNEARI + Z * (PNEARO - PNEARI)
  TNOZJ = (PNOZJ/PTNOZ)**GAMMA * TTNOZ
  TNOZ = TTNOZ - EFFNOZ * (TTNOZ - TNOZJ)
  VNOZ = VELNOZJ * COS(ALPHA)
  RHO(KNOZ,J) = PNOZJ / (RC * TNOZJ)
  RHOV(KNOZ,J) = RHO(KNOZ,J) * UNOZ
  RHOE(KNOZ,J) = RHO(KNOZ,J) * VNOZ
  RHOE(KNOZ,J) = RHO(KNOZ,J) * (CV * TNOZ
  + 0.5 * VELNOZJ ** 2)
  RHOMNOZ = PTNOZ / (RC * TTNOZ)
  RHO(KNOZ,J) = (RHO(KNOZ,J) * ZTX(KNP,J) +
  RHOV(KNP,J) * ZTY(KNP,J) * Y(KNP,J) / Y(KNOZ,J))
  / (ZTX(KNOZ,J) + TAN(ALPHA) * ZTY(KNOZ,J))
  RHOV(KNOZ,J) = RHO(KNOZ,J) * TAN(ALPHA)
  RHOV(KNOZ,J) = RHOV(KNP,J) * Y(KNP,J) / Y(KNOZ,J)
  RHOVEL = SORT(RHO(KNOZ,J)**2 + RHOV(KNOZ,J)**2)
  RHO(KNOZ,J) = RHOVEL * COS(ALPHA)
  RHOV(KNOZ,J) = RHOVEL * SIN(ALPHA)
  U = RHO(KNOZ,J) / RHO(KNP,J)
  V = RHOV(KNOZ,J) / RHO(KNP,J)
  TNOZ1 = TTNOZ - QZCP * (U ** 2 + V ** 2)
  TNOZ = TTNOZ - EFFNOZ * (TTNOZ - TNOZ1)

```

```

9 RHO(KNOZ,J) = RHOMNOZ * (TNOZ / TTNOZ) ** RGAMMA1
  U = RHOV(KNOZ,J) / RHO(KNOZ,J)
  V = RHOV(KNOZ,J) / RHO(KNOZ,J)
  E = CV * TNOZ * 0.5 * (U ** 2 + V ** 2)
  RHOE(KNOZ,J) = E * RHO(KNOZ,J)
  CONTINUE

NO SLIP / NO PENETRATION ON NOZZLE SIDES
DO 10 K = 1, KNOZ - 1

OUTSIDE INNER MALL
RH = 1.0 / RHO(K,JNERIN)
RHOV(K,JNMOUT) = 0.0
RHOV(K,JNMOUT) = 0.0
RHOE(K,JNMOUT) = RHOE(K,JNERIN) - 0.5 *
  (RHO(K,JNERIN) * ((RHOV(K,JNERIN) * RH)**2
  + (RHOV(K,JNERIN) * RH)**2)
RHO(K,JNMOUT) = RHOE(K,JNMOUT) / CVTM

OUTSIDE OUTER MALL
RH = 1.0 / RHO(K,JNEROUT)
RHOV(K,JNMOUT) = 0.0
RHOV(K,JNMOUT) = 0.0
RHOE(K,JNMOUT) = RHOE(K,JNEROUT) - 0.5 *
  (RHO(K,JNEROUT) * ((RHOV(K,JNEROUT) * RH)**2
  + (RHOV(K,JNEROUT) * RH)**2)
RHO(K,JNMOUT) = RHOE(K,JNMOUT) / CVTM

IGNORES ALL POINTS BLOCKED BY NOZZLE STRUCTURE
JCL = (JNOZIN + JNOZOUT) * 0.5
DO 10 J = JNMOUT + 1, JNMOUT - 1
  IF (K.NE.KNOZ) THEN
    RHOV(K,J) = 0.0
    RHOV(K,J) = 0.0
    IF (J.LE.JCL) THEN
      RHOE(K,J) = RHOE(K,JNMOUT)
      RHO(K,J) = RHO(K,JNMOUT)
    ELSE
      RHOE(K,J) = RHOE(K,JNMOUT)
      RHO(K,J) = RHO(K,JNMOUT)
    ENDIF
  ENDIF
CONTINUE
DO 11 J = JNMOUT + 1, JNOZIN - 1
  INNER WALL END
  KNER = KNOZ + 1
  RH = 1.0 / RHO(KNER,J)
  RHOV(KNOZ,J) = 0.0
  RHOV(KNOZ,J) = 0.0
  RHOE(KNOZ,J) = RHOE(KNER,J) - 0.5 *
  (RHO(KNER,J) * ((RHOV(KNER,J) * RH)**2
  + (RHOV(KNER,J) * RH)**2)
  RHO(KNOZ,J) = RHOE(KNOZ,J) / CVTM
CONTINUE
DO 12 J = JNOZOUT + 1, JNMOUT - 1

```



```

15  CONTINUE
    ENDIF
    RETURN
    END
    SUBROUTINE EDDY
    PARAMETER (N1 = 130, N2 = 115)
    COMMON / / DETA, DZETA, CY, RC, PR, PRT, GAMMA, DTL(MJ), GAMMA,
    1  CFL, BETA, UINF, RHOINF, CINF, TINF, TM, DT, CA, CV, L, JL, KL,
    2  JLM, KLM, TSMTHX, TSMTHY, KSTART(MJ)
    COMMON / / DEP, RHO(MK, MJ), RHO(MK, MJ), RHO(MK, MJ), RHO(MK, MJ),
    1  MJ
    COMMON / / DOF, X(MK, MJ), V(MK, MJ)
    COMMON / / DV, R(MK, MJ), U(MK, MJ), V(MK, MJ), P(MK, MJ), T(MK, MJ)
    1  MJ
    COMMON / / NELSON, ROET, RDZT, QDET, RMU, SL(MK, MJ)
    COMMON / / NOZ, KNOZ, JNOZIN, JNOZOUT, JNMHIN, JNMHOUT, JNERIN,
    1  JNEROUT, PINOZ, TINOZ, ALPHAZ, EFFNOZ
    COMMON / / TV, ETX(M, MJ), ETY(MK, MJ), ZTX(MK, MJ), ZTY(MK, MJ)
    COMMON / / TVIS, EP(MK, MJ), CPQPR, CPQPR
    1  MJ
    DIMENSION EP(MK, MJ), F(MK, MJ), JMAX(MK), OMEGA(MK, MJ),
    1  UET(MK, MJ), UZT(MK, MJ), VET(MK, MJ), VZT(MK, MJ)
    BALDWIN-LOMAX MODEL OF EDDY VISCOSITY WITH INTERMITTENCY
    CORRECTION.
    THIS VERSION ASSUMES THE SOLID SURFACE TO BE AT THE TOP, J = JL.
    DO 1 J = 1, JL
    DO 1 K = 1, KL
    RR = 1.0 / RHO(J, J)
    U(K, J) = RHO(UK, J) * RR
    V(K, J) = RHO(VK, J) * RR
    CONTINUE
    1  C
    GENERATE THE DERIVATIVES OF VELOCITY
    DO 2 J = 2, JLM
    DO 2 K = 2, KLM
    UET(K, J) = (U(K, J+1) - U(K, J-1)) * RDZT
    VET(K, J) = (V(K, J+1) - V(K, J-1)) * RDZT
    UZT(K, J) = (U(K, J+1) - U(K, J-1)) * RDZT
    VZT(K, J) = (V(K, J+1) - V(K, J-1)) * RDZT
    CONTINUE
    2  C
    GENERATE THE VORTICITY DISTRIBUTION
    DO 3 J = 2, JLM
    DO 3 K = 2, KLM
    OMEGA(K, J) = SORT((ETX(K, J) * VET(K, J) + ZTX(K, J) *
    1  ZTY(K, J) - ETY(K, J) * UET(K, J) - ZTY(K, J) * UZT(K, J))
    2  ** 2)
    CONTINUE
    3  C
    GENERATE THE SURFACE VORTICITY
    DO 4 K = 2, KLM
    OMEGA(K, JL) = SORT((ETX(K, JL) * (V(K, JLM) - V(K, JL)) -
    1  ETY(K, JL) * (U(K, JLM) - U(K, JL)) ** 2) * QDET
    CONTINUE
    4  C
    GENERATE THE INNER VISCOSITY COEFFICIENT

```

```

    KS = KNOZ + 1
    DO 5 K = 2, KS, KLM
    YPB = MIN(SORT(RHO(K, JL) * OMEGA(K, JL) / RMU) *
    1  SL(K, J) / 26.0, 50.0) * (0.40 * SL(K, J) * (1.0 - EXP(
    2  - YPB))) ** 2 * OMEGA(K, J)
    F(K, J) = SL(K, J) * (1.0 - EXP(- YPB)) * OMEGA(K, J)
    CONTINUE
    5  C
    SEARCH THE MAX. EDDY VISCOSITY COEFF. FOR A J.
    DO 7 K = KS, KLM
    DU2MAX = 0.0
    FMAX = 0.0
    JMAX(K) = 0
    DO 6 J = JLM, 2, -1
    DU2MAX = MAX(U(K, J) ** 2 + V(K, J) ** 2, DU2MAX)
    IF (F(K, J) .GT. FMAX) THEN
    1  FMAX = F(K, J)
    JMAX(K) = J
    END IF
    CONTINUE
    6  C
    FMAX = SL(K, JMAX(K)) * F(K, JMAX(K))
    F1 = 0.25 * SL(K, JMAX(K)) * DU2MAX / F(K, JMAX(K))
    FMAX = MIN(FMAX, F1)
    EP(MK, K) = 0.0336 * RHO(K, JMAX(K)) * FMAX
    CONTINUE
    7  C
    GENERATE SURFACE VORTICITY ON NOZZLE WALLS
    DO 8 K = 2, KNOZ
    OMEGA(K, JNMHIN) = SORT((ETX(K, JNMHIN) * (V(K, JNERIN) -
    1  V(K, JNMHIN)) - ETY(K, JNMHIN) * (U(K, JNERIN) -
    2  U(K, JNMHIN))) ** 2) * QDET
    CONTINUE
    DO 9 K = 2, KNOZ
    OMEGA(K, JNMHOUT) = SORT((ETX(K, JNMHOUT) * (V(K, JNEROUT) -
    1  V(K, JNMHOUT)) - ETY(K, JNMHOUT) * (U(K, JNEROUT) -
    2  U(K, JNMHOUT))) ** 2) * QDET
    CONTINUE
    9  C
    FIND INNER VISCOSITY COEFFICIENT FOR K = 2, KNOZ
    JCL = JNMHOUT + (JL - JNMHOUT) / 2
    DO 12 K = 2, KNOZ
    DO 10 J = 2, JNERIN
    YPB = MIN(SORT(RHO(K, JNMHIN) * OMEGA(K, JNMHIN) / RMU) *
    1  SL(K, J) / 26.0, 50.0)
    EP(K, J) = RHO(K, J) * (0.40 * SL(K, J) * (1.0 - EXP(
    2  - YPB))) ** 2 * OMEGA(K, J)
    F(K, J) = SL(K, J) * (1.0 - EXP(- YPB)) * OMEGA(K, J)
    CONTINUE
    DO 11 J = JNEROUT, JCL
    YPB = MIN(SORT(RHO(K, JNMHOUT) * OMEGA(K, JNMHOUT) / RMU)
    1  SL(K, J) / 26.0, 50.0)
    EP(K, J) = RHO(K, J) * (0.40 * SL(K, J) * (1.0 - EXP(
    2  - YPB))) ** 2 * OMEGA(K, J)
    F(K, J) = SL(K, J) * (1.0 - EXP(- YPB)) * OMEGA(K, J)
    CONTINUE
    10  C
    1  C
    1  C

```

```

11 CONTINUE
DO 12 J = JCL, JLM
  YPB = MIN(SORT(RHO(K, J)), OMEGA(K, J)) / RMUJ
  EP(K, J) = RHO(K, J) * (1.0 - EXP(-
  YPB)) * 2 * OMEGA(K, J)
  FIK(J) = SL(K, J) * (1.0 - EXP(- YPB)) * OMEGA(K, J)
12 CONTINUE
C
C FIND MAX EDDY VISCOSITY COEFF FOR K = 2, KNOZ, J .GT. JNMOUT
C
DO 14 K = 2, KNOZ
  DUZMAX = 0.0
  FMAX = 0.0
  JMAX(K) = 0
DO 13 J = JLM, JNMOUT, -1
  DUZMAX = MAX(DUZMAX, J * 2 + V(K, J) * 2, DUZMAX)
  IF (FIK(J) .GT. FMAX) THEN
    FMAX = FIK(J)
    JMAX(K) = J
  END IF
13 CONTINUE
C
C FMAKE = SL(K, JMAX(K)) * FIK, JMAX(K))
  F1 = 0.25 * SL(K, JMAX(K)) * DUZMAX / FIK, JMAX(K))
  FMAKE = MIN(FMAKE, F1)
  EPMAX(K) = 0.0336 * RHO(K, JMAX(K)) * FMAKE
14 CONTINUE
C
C SET THE MAX EDDY VISCOSITY FOR THE OUTER REGION
C
DO 16 K = 2, KNOZ
  ISM = 0
DO 15 J = JLM, JNMOUT, -1
  IF (EPMAX(K) .LE. EP(K, J)) ISM = 1
  IF (ISM .GT. 0) EP(K, J) = EPMAX(K) * RHO(K, J) /
  RHO(K, JMAX(K))
  EP(K, J) = EP(K, J) / (1.0 + 5.5 * (0.3 * SL(K, J) / SL(K,
  JMAX(K))) ** 6)
15 CONTINUE
16 CONTINUE
DO 18 K = KS, KLM
  ISM = 0
DO 17 J = JLM, 2, -1
  IF (EPMAX(K) .LE. EP(K, J)) ISM = 1
  IF (ISM .GT. 0) EP(K, J) = EPMAX(K) * RHO(K, J) /
  RHO(K, JMAX(K))
  EP(K, J) = EP(K, J) / (1.0 + 5.5 * (0.3 * SL(K, J) / SL(K,
  JMAX(K))) ** 6)
17 CONTINUE
18 CONTINUE
C
C FIND MAX EDDY VISCOSITY COEFF FOR K = 2, KNOZ, J .LT. JNMIN
C
DO 20 K = 2, KNOZ
  DUZMAX = 0.0
  FMAX = 0.0
  JMAX(K) = 0
DO 19 J = JNMOUT, 2, -1
  DUZMAX = MAX(DUZMAX, J * 2 + V(K, J) * 2, DUZMAX)
  IF (FIK(J) .GT. FMAX) THEN
    FMAX = FIK(J)
    JMAX(K) = J
  END IF
19 CONTINUE
20 CONTINUE

```

```

C
C FMAX = SL(K, JMAX(K)) * FIK, JMAX(K))
  F1 = 0.25 * SL(K, JMAX(K)) * DUZMAX / FIK, JMAX(K))
  FMAKE = MIN(FMAKE, F1)
  EPMAX(K) = 0.0336 * RHO(K, JMAX(K)) * FMAKE
20 CONTINUE
C
C SET THE MAX EDDY VISCOSITY FOR THE OUTER REGION
C
DO 22 K = 2, KNOZ
  ISK = 0
DO 21 J = JNMOUT, 2, -1
  IF (EPMAX(K) .LE. EP(K, J)) ISK = 1
  IF (ISK .GT. 0) EP(K, J) = EPMAX(K) * RHO(K, J) /
  RHO(K, JMAX(K))
  EP(K, J) = EP(K, J) / (1.0 + 5.5 * (0.3 * SL(K, J) / SL(K,
  JMAX(K))) ** 6)
21 CONTINUE
22 CONTINUE
C
C COMPLETE THE EDDY VISCOSITY MATRIX
C
EP(1, 2) = EP(2, 2)
EP(KL, 2) = EP(KLM, 2)
C
DO 23 K = 1, KL
  EP(K, JLM) = 0.0
  EP(K, 1) = EP(K, 2)
C
DO 24 J = 1, JLM
  EP(KL, J) = EP(KLM, J)
  EP(1, J) = EP(2, J)
C
DO 25 K = 1, KNOZ
  DO 25 J = JNMIN, JNMOUT
    EP(K, J) = 0.0
25 CONTINUE
RETURN
END
SUBROUTINE LETA (J)
  PARAMETER (MK = 130, MJ = 115)
  COMMON // DELTA, DZETA, CV, RC, PR, PRT, GAMMA, DTL(MJ), GAMM1,
  1 CFL, BETA, UINF, RHOINF, CINF, YINF, TN, DT, CX, CY, L, JL, KL,
  2 JLM, KLM, ISMTHK, ISMTHY, KSTART(MJ)
  COMMON /DOF/ X(MK, MJ), Y(MK, MJ), RY(MK, MJ)
  COMMON /FLEUET/ F2(MK, 2), F22(MK, 2), F23(MK, 2), F25(MK, 2),
  1 G21(MK, 2), G22(MK, 2), G23(MK, 2), G25(MK, 2), H(MK),
  2 G21(MK, 2), R(MK, MJ), U(MK, MJ), V(MK, MJ), P(MK, MJ), T(MK,
  1 MJ)
  COMMON /TV/ ETX(MK, MJ), ETY(MK, MJ), ZTX(MK, MJ), ZTY(MK, MJ)
  COMMON /TVIS/ EP(MK, MJ), CPQPR, CPQPRI
  C
  DIMENSION DUZ(MK), DVOR(MK), RK(MK), RLMBD(MK), RMU(MK),
  1 SHU(MK), TAURR(MK), TAUXR(MK), TET(MK), TX(MK),
  2 TY(MK), TZT(MK), UET(MK), UZT(MK), VET(MK), VZT(MK)
  RDET = 1.0 / DELTA

```

```

ROZT = 1.0 / (2.0 * DZETA)
KSP = 2
DO 7 M = 1, 2
C
C
C
FORWARD & BACKWARD DIFFERENCING FOR PREDICTOR & CORRECTOR
C
C
C
JV = L * M + J - 3
JM = J + M - 2
JP = JM + 1
C
DO 1 KV = KSP, KLM
KP = KV + 1
KM = KV - 1
C
C
C
GENERATE THE SHEAR STRESS & HEAT FLUX TERMS
C
C
C
UET(KV) = (U(KV, JP) - U(KV, JM)) * RDET
VET(KV) = (V(KV, JP) - V(KV, JM)) * RDET
TET(KV) = (T(KV, JP) - T(KV, JM)) * RDET
C
UZT(KV) = (U(KP, JV) - U(KM, JV)) * RZT
VZT(KV) = (V(KP, JV) - V(KM, JV)) * RZT
TZT(KV) = (T(KP, JV) - T(KM, JV)) * RZT
C
C
C
GENERATE THE VISCOSITY COEFFS & HEAT CONDUCTIVITY
C
C
C
RMU(KV) = 2.27E - 08 * SQRT(T(KV, JV) ** 3) / (T(KV, JV) +
198.6)
RK(KV) = CPQPR * RMU(KV) + CPQPR * EP(KV, JV)
RMU(KV) = RMU(KV) + EP(KV, JV)
RLMBD(KV) = -(2.0 / 3.0) * RMU(KV)
SMU(KV) = 2.0 * RMU(KV) + RLMBD(KV)
C
C
C
CONTINUE
C
DO 2 KV = KSP, KLM
DUOX(KV) = ETX(KV, JV) * UET(KV) + ZTX(KV, JV) * UZT(KV)
DVDR(KV) = ETY(KV, JV) * VET(KV) + ZTY(KV, JV) * VZT(KV)
C
TAUX(KV) = SMU(KV) * DUOX(KV) + RLMBD(KV) * (V(KV, JV) *
RY(KV, JV) + DVDR(KV)) - P(KV, JV)
TAUR(KV) = SMU(KV) * DVDR(KV) + RLMBD(KV) * (V(KV, JV) *
RY(KV, JV) + DUOX(KV)) - P(KV, JV)
TAUR(KV) = RMU(KV) * (ETX(KV, JV) * UET(KV) + ZTX(KV, JV) *
UZT(KV) + ETY(KV, JV) * VET(KV) + ZTY(KV, JV) * VZT(KV))
C
C
C
CONTINUE
C
IF (JV .NE. J) GO TO 4
JP = J + 1
JM = J - 1
DO 3 KV = KSP, KLM
KVP = KV + 1
KVM = KV - 1
C
DUOX(KV) = ETX(KV, J) * (U(KV, JP) - U(KV, JM)) * (0.5 *
RDET) + ZTX(KV, J) * (U(KVP, J) - U(KVM, J)) * RZT
DVDR(KV) = ETY(KV, J) * (V(KV, JP) - V(KV, JM)) * (0.5 *
RDET) + ZTY(KV, J) * (V(KVP, J) - V(KVM, J)) * RZT
C
H(KV) = (SMU(KV) * V(KV, J) * DV(KV, J) + RLMBD(KV) *

```

```

(DUOX(KV) + DVDR(KV)) - P(KV, J)) * RY(KV, J)
CONTINUE
C
C
C
GENERATE THE HEAT FLUX TERMS
C
C
C
DO 5 KV = KSP, KLM
TX(KV) = ETX(KV, JV) * TET(KV) + ZTX(KV, JV) * TZT(KV)
TY(KV) = ETY(KV, JV) * TET(KV) + ZTY(KV, JV) * TZT(KV)
CONTINUE
C
C
C
GENERATE THE FLUX TERMS
C
C
C
DO 6 KV = KSP, KLM
F21(KV, M) = R(KV, JV) * U(KV, JV)
F21(KV, M) = F21(KV, M) + U(KV, JV) - TAUX(KV)
F23(KV, M) = F21(KV, M) * V(KV, JV) - TAUR(KV)
F23(KV, M) = F23(KV, M) + (CV * T(KV, JV) + 0.5 * (U(KV, JV)
** 2 + V(KV, JV) ** 2)) - RK(KV) * TX(KV) - (U(KV, JV) *
TAUX(KV) + V(KV, JV) * TAUR(KV))
C
G21(KV, M) = R(KV, JV) * V(KV, JV) * Y(KV, JV)
G21(KV, M) = G21(KV, M) + U(KV, JV) - TAUX(KV) * Y(KV, JV)
G23(KV, M) = G21(KV, M) * V(KV, JV) - TAUR(KV) * Y(KV, JV)
G23(KV, M) = G23(KV, M) + (CV * T(KV, JV) + 0.5 * (U(KV, JV)
** 2 + V(KV, JV) ** 2)) - (RK(KV) * TY(KV) + (U(KV, JV) *
TAUR(KV) + V(KV, JV) * TAUR(KV))) * Y(KV, JV)
CONTINUE
C
C
C
END
SUBROUTINE LZETA (J)
PARAMETER LNK = 130, MJ = 115
COMMON /DETA/ DZETA, CY, RC, PR, PRT, GAMMA, DTL(MJ), GAMH1,
1 CFL, BETA, UINF, RHOFIN, CINF, TINF, TH, DT, CX, CY, L, JL, KL,
2 JLM, KLM, ISMTH, ISMTHY, KSTART(MJ)
COMMON /DOF/ X(MK, MJ), Y(MK, MJ), RY(MK, MJ)
COMMON /FLUZZ/ F31(MK), F32(MK), F33(MK), G31(MK),
1 G32(MK), G33(MK), G35(MK)
COMMON /DV/ R(MK, MJ), U(MK, MJ), V(MK, MJ), P(MK, MJ), T(MK,
1 MJ)
COMMON /MONC/ G31N(2), G32N(2), G33N(2), G35N(2)
COMMON /TV/ ETX(MK, MJ), ETY(MK, MJ), ZTX(MK, MJ), ZTY(MK, MJ)
COMMON /TVIS/ EP(MK, MJ), CPQPR, CPQPR1
C
C
C
DIMENSION DUOX(MK), DVDR(MK), RK(MK), RLMBD(MK), RMU(MK),
1 SMU(MK), TAUR(MK), TAUX(MK), TET(MK), TET(MK), TX(MK),
2 TY(MK), TZT(MK), UET(MK), UZT(MK), VET(MK), VZT(MK)
C
RDET = 1.0 / (2.0 * DZETA)
ROZT = 1.0 / DZETA
JP = J + 1
JM = J - 1
KS = 1
KSP = KS + 1
C
DO 1 KK = KS, KLM
C
C
C
FORWARD & BACKWARD DIFFERENCING FOR PREDICTOR & CORRECTOR
C
C
C
KV = KK + L - 1
KM = KK

```



```

C      COMMON /TV/ ETX(MK, MJ), ETY(MK, MJ), ZTX(MK, MJ), ZTY(MK, MJ)
      DO 1 J = 1, JL
        ROLD(K, J) = ABS(RHO(K, J) - ROLD(K, J)) / RHOINF
        RVOLD(K, J) = ABS(RHOU(K, J) - RVOLD(K, J)) / RHUINF
        ROLD(K, J) = ABS(RHOE(K, J) - ROLD(K, J)) / REINF
        RVOLD(K, J) = ABS(RHOE(K, J) - RVOLD(K, J)) / REINF
      CONTINUE
      XNORM = 0.0
      DO 2 J = 1, JL
        DO 2 K = 1, KL
          XNORM = XNORM + ROLD(K, J)**2 + RVOLD(K, J)**2
        CONTINUE
      XNORM = SQRT(XNORM)
      RESET FOR NEXT TIME.
      DO 3 J = 1, JL
        DO 3 K = 1, KL
          ROLD(K, J) = ROLD(K, J)
          RVOLD(K, J) = RVOLD(K, J)
          ROLD(K, J) = ROLD(K, J)
          RVOLD(K, J) = RVOLD(K, J)
          ROLD(K, J) = ROLD(K, J)
          RVOLD(K, J) = RVOLD(K, J)
        CONTINUE
      RETURN
END
SUBROUTINE PAGE(OOPS)
PARAMETER (MK=130, MJ=115)
COMMON // DELTA, DZETA, CY, RC, PR, PRT, GAMMA, DTL(MJ), GAMM1,
      CFL, BETA, UINF, RHOINF, CINF, TINF, TM, DT, CX, CY, L, JL, KL,
      JLM, KLM, ISMTHX, ISMTHY, KSTART(MJ)
      COMMON /DV/ R(MK, MJ), U(MK, MJ), V(MK, MJ), P(MK, MJ), T(MK,
      MJ)
      COMMON /TV/ ETX(MK, MJ), ETY(MK, MJ), ZTX(MK, MJ), ZTY(MK, MJ)
      COMMON /DEP/ RHOMK, MJ, RHOU(MK, MJ), RHOV(MK, MJ), RHOE(MK,
      MJ)
      COMMON /ERR/ KFE, JFE
      PREDICTOR SHEEP
      LOGICAL OOPS
      OOPS = .FALSE.
      L = 1
      GENERATE THREE PAGES OF TEMPORAL VECTOR ARRAYS
      DO 1 JV = 1, JL
        DO 1 KV = 1, KL
          R(KV, JV) = RHO(KV, JV)
          U(KV, JV) = RHOU(KV, JV)
          V(KV, JV) = RHOV(KV, JV)
          T(KV, JV) = (RHOE(KV, JV)/R(KV, JV) - 0.5*(U(KV, JV)**2
          + V(KV, JV)**2))/CV
          IF (T(KV, JV) .LT. 25.0) THEN
            OOPS = .TRUE.
            KFE = KV
            JFE = JV
          RETURN
        CONTINUE
      DO 4 J = 2, JLM
        CALL LETA (J)
        CALL LZETA (J)
        CALL SUM (J)
        CONTINUE
      CALL BC
      RETURN
END
SUBROUTINE PLOTCH
PARAMETER (MK=130, MJ=115)
COMMON // DELTA, DZETA, CY, RC, PR, PRT, GAMMA, DTL(MJ), GAMM1,
      CFL, BETA, UINF, RHOINF, CINF, TINF, TM, DT, CX, CY, L, JL, KL,
      JLM, KLM, ISMTHX, ISMTHY, KSTART(MJ)
      COMMON /DEP/ RHOMK, MJ, RHOU(MK, MJ), RHOV(MK, MJ), RHOE(MK,
      MJ)
      COMMON /DOF/ X(MK, MJ), Y(MK, MJ), RY(MK, MJ)
      COMMON /DV/ R(MK, MJ), U(MK, MJ), V(MK, MJ), P(MK, MJ), T(MK,
      MJ)
      COMMON /NOZ/ KNOZ, JNOZIN, JNOZOUT, JKNIN, JKNOUT, JNERIN,
      JNEROUT, PTNOZ, TTNOZ, ALPHA, EFFNCZ
      COMMON /TV/ ETX(MK, MJ), ETY(MK, MJ), ZTX(MK, MJ), ZTY(MK, MJ)
      COMMON /PLT/ RL, RH, RCV, PINF, KSTEP
      WRITE OUT THE COMPUTED FLOW DATA
      C
      C

```

```

      JFE = JV
      RETURN
END IF
P(KV, JV) = R(KV, JV) * RC * T(KV, JV)
CONTINUE
DO 2 J = 2, JLM
  CALL LETA (J)
  CALL LZETA (J)
  CALL SUM (J)
  CONTINUE
  CALL BC
  CORRECTOR SHEEP
  L = 2
  GENERATE THREE PAGES OF TEMPORAL VECTOR ARRAYS
  DO 3 JV = 1, JL
    DO 3 KV = 1, KL
      R(KV, JV) = RHO(KV, JV)
      U(KV, JV) = RHOU(KV, JV)
      V(KV, JV) = RHOV(KV, JV)
      T(KV, JV) = (RHOE(KV, JV)/R(KV, JV) - 0.5*(U(KV, JV)**2
      + V(KV, JV)**2))/CV
      IF (T(KV, JV) .LT. 25.0) THEN
        OOPS = .TRUE.
        KFE = KV
        JFE = JV
      RETURN
    CONTINUE
  DO 4 J = 2, JLM
    CALL LETA (J)
    CALL LZETA (J)
    CALL SUM (J)
    CONTINUE
  CALL BC
  RETURN
END
SUBROUTINE PLOTCH
PARAMETER (MK=130, MJ=115)
COMMON // DELTA, DZETA, CY, RC, PR, PRT, GAMMA, DTL(MJ), GAMM1,
      CFL, BETA, UINF, RHOINF, CINF, TINF, TM, DT, CX, CY, L, JL, KL,
      JLM, KLM, ISMTHX, ISMTHY, KSTART(MJ)
      COMMON /DEP/ RHOMK, MJ, RHOU(MK, MJ), RHOV(MK, MJ), RHOE(MK,
      MJ)
      COMMON /DOF/ X(MK, MJ), Y(MK, MJ), RY(MK, MJ)
      COMMON /DV/ R(MK, MJ), U(MK, MJ), V(MK, MJ), P(MK, MJ), T(MK,
      MJ)
      COMMON /NOZ/ KNOZ, JNOZIN, JNOZOUT, JKNIN, JKNOUT, JNERIN,
      JNEROUT, PTNOZ, TTNOZ, ALPHA, EFFNCZ
      COMMON /TV/ ETX(MK, MJ), ETY(MK, MJ), ZTX(MK, MJ), ZTY(MK, MJ)
      COMMON /PLT/ RL, RH, RCV, PINF, KSTEP
      WRITE OUT THE COMPUTED FLOW DATA
      C
      C

```

```

1 DIMENSION ARCL(1), CF2(1), CF2(1), PBYPI(1), RHO(1), RHO(1),
2 STANT(1), STANT(1), STANT(1), YBPP(1), YBPP(1), YBPP(1), YBPP(1),
3 CF2(1), RHO(1), RHO(1), RHO(1), RHO(1), RHO(1), RHO(1), RHO(1),

```

```

C
1 JLM = 1
2 GAMMA = 1.0 / UINF
3 RC = 1.0 / UINF
4 DO 2 K = 1, KL
5 IF (K.EQ.1) OR (K.EQ.100) K = 100
6 WRITE(6, 100) K
7 DO 1 J = 1, JLM
8 RH = 1.0 / RHO(K, J)
9 U = RHO(K, J) * RH
10 VV = RHO(K, J) * RH
11 RR = RHO(K, J) * RH
12 UR = RHO(K, J) * RH
13 VR = RHO(K, J) * RH
14 TT = (RHO(K, J) * RH - 0.5 * (UU ** 2 + VV ** 2)) *
15 PP / RCV
16 TR = PP / PINF
17 RP = PP / PINF
18 OCS = 1.0 / SORT(UU ** 2 + VV ** 2) * OCS
19 XM = SORT(UU ** 2 + VV ** 2) * OCS
20 AXH = UU * OCS

```

```

C
1 WRITE(6, 101) J, X(K, J), Y(K, J), RR, UR, AXH, VR, XM,
2 TR, RP
3 CONTINUE
4 END IF
5 PBYPI(K) = RHO(K, JLM) * RC * TM / PINF
6 CONTINUE
7 ARCL(1) = 0.0
8 DO 3 K = 1, KL
9 XBP(K) = X(K, JLM)
10 YBP(K) = Y(K, JLM)
11 CONTINUE

```

```

C
1 DO 4 K = 1, KL
2 XBP(K) = XBP(K) - XBP(K - 1) ** 2 + (YBP(K) -
3 DELS
4 YBP(K) = YBP(K) - YBP(K - 1) * DELS
5 CONTINUE

```

```

C
1 CALCULATE STANTON NUMBER
2 CP = GAMMA * CV
3 STETHY = CP * TINF + (0.5 * UINF * UINF)
4 ENTHL = CP * TM
5 DENF = PR * RHOINF * UINF * (STETHY - ENTHL)
6 DENF = 0.5 * (RHOINF * UINF * UINF)
7 WRITE(6, 102)

```

```

C
1 FIRST ORDER APPROXIMATION
2 DO 5 K = 1, KL
3 DERE1 = (RHO(K, JLM) / RHO(K, JLM)) - (RHO(K, JLM) /
4 RHO(K, JLM)) / DETA

```

```

1 RHO(K) = 2.27E - 08 * SORT(ETX(K, JLM) ** 3) / (ETX(K, JLM) +
2 198.6)
3 ANUM1 = GAMMA * RHO(K) * (SORT(ETX(K, JLM) ** 2 + ETY(K,
4 JLM) ** 2)) / DERE1
5 STANT(K) = - ANUM1 / DENF

```

```

C
1 SECOND ORDER APPROXIMATION
2 DERE2 = ((4.0 * RHO(K, JLM) / RHO(K, JLM)) - (RHO(K, JLM) /
3 (2.0 * DETA)) - (3.0 * RHO(K, JLM) / RHO(K, JLM)) /
4 ANUM2 * GAMMA * RHO(K) * (SORT(ETX(K, JLM) ** 2 + ETY(K,
5 JLM) ** 2)) / DERE2
6 STANT(K) = - ANUM2 / DENF

```

```

C
1 CALCULATE SKIN FRICTION COEFFICIENT
2 FIRST ORDER APPROXIMATION
3 DERE1 = ((RHO(K, JLM) / RHO(K, JLM)) - (RHO(K, JLM) /
4 RHO(K, JLM)) / DETA
5 ANUM1 = RHO(K) * (ETY(K, JLM) * DERE1 - ETX(K, JLM) *
6 CF1(K)) = - ANUM1 / DENF

```

```

C
1 SECOND ORDER APPROXIMATION
2 DERE2 = ((4.0 * RHO(K, JLM) / RHO(K, JLM)) - (RHO(K, JLM) /
3 (2.0 * DETA)) - (3.0 * RHO(K, JLM) / RHO(K, JLM)) /
4 DERE2 * GAMMA * RHO(K) * (SORT(ETX(K, JLM) ** 2 + ETY(K,
5 JLM) ** 2)) / DERE2
6 ANUM2 = RHO(K) * (ETY(K, JLM) * DERE2 - ETX(K, JLM) *
7 CF2(K)) = - ANUM2 / DENF

```

```

C
1 CALCULATE SKIN FRICTION COEFFICIENT
2 SECOND ORDER APPROXIMATION
3 DERE2 = ((4.0 * RHO(K, JLM) / RHO(K, JLM)) - (RHO(K, JLM) /
4 (2.0 * DETA)) - (3.0 * RHO(K, JLM) / RHO(K, JLM)) /
5 DERE2 * GAMMA * RHO(K) * (SORT(ETX(K, JLM) ** 2 + ETY(K,
6 JLM) ** 2)) / DERE2
7 ANUM2 = RHO(K) * (ETY(K, JLM) * DERE2 - ETX(K, JLM) *
8 CF2(K)) = - ANUM2 / DENF

```

```

C
1 DO 6 K = 1, KL
2 WRITE(6, 103) XBP(K), CF1(K), CF2(K), STANT(K), STANT(K)
3 CONTINUE
4 WRITE(6, 104)
5 JLM = JLMIN - 1
6 JIM = JIM - 1
7 JOP = JNOUT + 1
8 JOP2 = JOP + 1
9 DO 7 K = 1, KNOZ
10 XBP(K) = X(K, JNMIN)
11 YBP(K) = Y(K, JNMIN)
12 XBP(K) = X(K, JNOUT)
13 YBP(K) = Y(K, JNOUT)

```

```

C
1 CALCULATE SKIN FRICTION COEFFICIENT
2 SECOND ORDER APPROXIMATION
3 DERE2 = ((4.0 * RHO(K, JLM) / RHO(K, JLM)) - (RHO(K, JLM) /
4 (2.0 * DETA)) - (3.0 * RHO(K, JLM) / RHO(K, JLM)) /
5 DERE2 * GAMMA * RHO(K) * (SORT(ETX(K, JLM) ** 2 + ETY(K,
6 JLM) ** 2)) / DERE2
7 ANUM2 = RHO(K) * (ETY(K, JLM) * DERE2 - ETX(K, JLM) *
8 CF2(K)) = - ANUM2 / DENF

```

```

C
1 DO 6 K = 1, KL
2 WRITE(6, 103) XBP(K), CF1(K), CF2(K), STANT(K), STANT(K)
3 CONTINUE
4 WRITE(6, 104)
5 JLM = JLMIN - 1
6 JIM = JIM - 1
7 JOP = JNOUT + 1
8 JOP2 = JOP + 1
9 DO 7 K = 1, KNOZ
10 XBP(K) = X(K, JNMIN)
11 YBP(K) = Y(K, JNMIN)
12 XBP(K) = X(K, JNOUT)
13 YBP(K) = Y(K, JNOUT)

```

```

C
1 CALCULATE SKIN FRICTION COEFFICIENT
2 SECOND ORDER APPROXIMATION
3 DERE2 = ((4.0 * RHO(K, JLM) / RHO(K, JLM)) - (RHO(K, JLM) /
4 (2.0 * DETA)) - (3.0 * RHO(K, JLM) / RHO(K, JLM)) /
5 DERE2 * GAMMA * RHO(K) * (SORT(ETX(K, JLM) ** 2 + ETY(K,
6 JLM) ** 2)) / DERE2
7 ANUM2 = RHO(K) * (ETY(K, JLM) * DERE2 - ETX(K, JLM) *
8 CF2(K)) = - ANUM2 / DENF

```

```

C
1 DO 6 K = 1, KL
2 WRITE(6, 103) XBP(K), CF1(K), CF2(K), STANT(K), STANT(K)
3 CONTINUE
4 WRITE(6, 104)
5 JLM = JLMIN - 1
6 JIM = JIM - 1
7 JOP = JNOUT + 1
8 JOP2 = JOP + 1
9 DO 7 K = 1, KNOZ
10 XBP(K) = X(K, JNMIN)
11 YBP(K) = Y(K, JNMIN)
12 XBP(K) = X(K, JNOUT)
13 YBP(K) = Y(K, JNOUT)

```

```

C
1 CALCULATE SKIN FRICTION COEFFICIENT
2 SECOND ORDER APPROXIMATION
3 DERE2 = ((4.0 * RHO(K, JLM) / RHO(K, JLM)) - (RHO(K, JLM) /
4 (2.0 * DETA)) - (3.0 * RHO(K, JLM) / RHO(K, JLM)) /
5 DERE2 * GAMMA * RHO(K) * (SORT(ETX(K, JLM) ** 2 + ETY(K,
6 JLM) ** 2)) / DERE2
7 ANUM2 = RHO(K) * (ETY(K, JLM) * DERE2 - ETX(K, JLM) *
8 CF2(K)) = - ANUM2 / DENF

```

```

C
1 DO 6 K = 1, KL
2 WRITE(6, 103) XBP(K), CF1(K), CF2(K), STANT(K), STANT(K)
3 CONTINUE
4 WRITE(6, 104)
5 JLM = JLMIN - 1
6 JIM = JIM - 1
7 JOP = JNOUT + 1
8 JOP2 = JOP + 1
9 DO 7 K = 1, KNOZ
10 XBP(K) = X(K, JNMIN)
11 YBP(K) = Y(K, JNMIN)
12 XBP(K) = X(K, JNOUT)
13 YBP(K) = Y(K, JNOUT)

```

```

C
1 CALCULATE SKIN FRICTION COEFFICIENT
2 SECOND ORDER APPROXIMATION
3 DERE2 = ((4.0 * RHO(K, JLM) / RHO(K, JLM)) - (RHO(K, JLM) /
4 (2.0 * DETA)) - (3.0 * RHO(K, JLM) / RHO(K, JLM)) /
5 DERE2 * GAMMA * RHO(K) * (SORT(ETX(K, JLM) ** 2 + ETY(K,
6 JLM) ** 2)) / DERE2
7 ANUM2 = RHO(K) * (ETY(K, JLM) * DERE2 - ETX(K, JLM) *
8 CF2(K)) = - ANUM2 / DENF

```



```

2      CONTINUE
C      ADDNC      = - DT * ZTY(2, J) * (G33N(2) - G33N(1)) * RDZT
RHOVP(2, J) = RHOVP(2, J) + ADDNC
C      ADDNC      = - DT * ZTY(2, J) * (G35N(2) - G35N(1)) * RDZT
RHOEP(2, J) = RHOEP(2, J) + ADDNC
C
C      IF ((ISMTX .EQ. 0) .AND. (ISMTY .EQ. 0)) RETURN
C      CALL DAMPING (J)
C
C      DO 3 KV = KSP, KLM
C      RHOVP(KV, J) = RHOVP(KV, J) + ADD1(KV)
C      RHOEP(KV, J) = RHOEP(KV, J) + ADD2(KV)
C      RHOVP(KV, J) = RHOVP(KV, J) + ADD3(KV)
C      RHOEP(KV, J) = RHOEP(KV, J) + ADD5(KV)
C      CONTINUE
C
C      ELSE
C      CORRECTOR SHEEP
C      DO 4 KV = KSP, KLM
C      KM = KV - 1
C
C      RHO(KV, J) = 0.5 * (RHO(KV, J) + RHO(KV, J) - DT * ((ETX(KV, J) * (F21(KV, 2) - F21(KV, 1)) + ETY(KV, J) * (F21(KV, 2) - F21(KV, 1)) * RDZT - (ZTX(KV, J) * (F31(KV, 2) - F31(KV, 1)) + ZTY(KV, J) * (F31(KV, 2) - F31(KV, 1)) * RDZT))
C
C      RHO(KV, J) = 0.5 * (RHO(KV, J) + RHO(KV, J) - DT * ((ETX(KV, J) * (F22(KV, 2) - F22(KV, 1)) + ETY(KV, J) * (F22(KV, 2) - F22(KV, 1)) * RDZT - (ZTX(KV, J) * (F32(KV, 2) - F32(KV, 1)) + ZTY(KV, J) * (F32(KV, 2) - F32(KV, 1)) * RDZT))
C
C      RHO(KV, J) = 0.5 * (RHO(KV, J) + RHO(KV, J) - DT * ((ETX(KV, J) * (F23(KV, 2) - F23(KV, 1)) + ETY(KV, J) * (F23(KV, 2) - F23(KV, 1)) * RDZT - (ZTX(KV, J) * (F33(KV, 2) - F33(KV, 1)) + ZTY(KV, J) * (F33(KV, 2) - F33(KV, 1)) * RDZT))
C
C      RHO(KV, J) = 0.5 * (RHO(KV, J) + RHO(KV, J) - DT * ((ETX(KV, J) * (F25(KV, 2) - F25(KV, 1)) + ETY(KV, J) * (F25(KV, 2) - F25(KV, 1)) * RDZT - (ZTX(KV, J) * (F35(KV, 2) - F35(KV, 1)) + ZTY(KV, J) * (F35(KV, 2) - F35(KV, 1)) * RDZT))
C
C      IF ((ISMTX .EQ. 0) .AND. (ISMTY .EQ. 0)) RETURN
C      CALL DAMPING (J)
C
C      DO 6 KV = KSP, KLM
C      RHO(KV, J) = RHO(KV, J) + ADD1(KV)

```

```

6      RHO(KV, J) = RHO(KV, J) + ADD3(KV)
      RHO(KV, J) = RHO(KV, J) + ADD5(KV)
      CONTINUE
      END IF
      RETURN
      END
      SUBROUTINE INSTEP
      PARAMETER (MK = 130, MJ = 115)
      COMMON // DETA, DZETA, CV, RC, PR, PRT, GAMMA, DTL(MJ), GAMMI,
      1 JLM, BETA, UINF, RHOFNF, CINF, TINF, TM, DT, CV, L, JL, KL,
      2 JLM, KLM, ISMTX, ISMTY, KSTART(MJ)
      COMMON /DEP/ RHO(MK, MJ), RHOI(MK, MJ), RHOV(MK, MJ), RHOE(MK, MJ)
      1 MJ)
      COMMON /TV/ ETX(MK, MJ), ETY(MK, MJ), ZTX(MK, MJ), ZTY(MK, MJ)
      COMMON /TVIS/ EP(MK, MJ), CPQPR, CPQPR
      SET UP INITIAL CFL TIME STEP VALUE
      C
      C      DIMENSION C(MK), DTC(MK), U(MK), UET(MK), UZI(MK), V(MK)
      C
      C      DTC(1) = 1.0
      C      GAMM2 = GAMMA * GAMMI
      C      DTCFL = 1.0
      C      RDZT = 1.0 / DZETA
      C      CONST = SORT(2.0 / 3.0)
      C      RPR = 1.0 / PR
      C      TMOGAM = 2.0 * GAMMA
      C      RCG = RC * GAMMA
      C
      C      DO 3 J = 2, JLM
      C      KSP = KSTART(J) + 1
      C      DO 1 K = KSP, KLM
      C      RH = 1.0 / RHO(K, J)
      C      U(K) = RHOI(K, J) * RH
      C      V(K) = RHOV(K, J) * RH
      C      C(K) = SORT(GAMM2 * (RHOE(K, J) * RH - 0.5 * (U(K) * 2
      1 + V(K) * 2)))
      C      TT = C(K) * C(K) / RCG
      C      RMU = 2.27E - 8 * SORT(TT * 3) / (TT + 19 - 6)
      C
      C      UET(K) = ETX(K, J) * U(K) + ETY(K, J) * V(K)
      C      UZI(K) = ZTX(K, J) * U(K) + ZTY(K, J) * V(K)
      C
      C      DT1 = 1.0 / (ABS(UET(K)) * RDET + ABS(UZI(K)) * RDZT +
      2 C(K) * SORT((ETX(K, J) * RDET + ZTX(K, J) * RDZT) * 2))
      C      (ETX(K, J) * RDET + ZTY(K, J) * RDZT) * 2))
      C
      C      DE = RDET * SORT(ETX(K, J) * 2 + ETY(K, J) * 2)
      C      DZ = R * ZT * SORT(ZTX(K, J) * 2 + ZTY(K, J) * 2)
      C      DT2 = 1.0 / (ABS(UET(K)) * RDET + C(K) * DE + RH * DE
      1 (TMOGAM * DE * (RMU * RPR + EP(K, J) * RPR) + CONST * DZ *
      2 (RMU * EP(K, J)))
      C
      C      DT3 = 1.0 / (ABS(UZI(K)) * RDZT + C(K) * DZ + RH * DZ *
      1 (TMOGAM * DZ * (RMU * RPR + EP(K, J) * RPR) + CONST * DE *
      2 (RMU * EP(K, J)))
      C      DTC(K) = MIN(DT1, DT2, DT3)
      C      CONTINUE
      C

```

```

DTMIN = DTC(1)
DO 2 K
  DTMIN = KSP, KLM
  DTMIN = MIN(DTC(K), DTMIN)
CONTINUE
2
C
C
C
DTL(J) = DTMIN * CFL
COMPARE DTMIN BETWEEN ADJACENT PLACES
C
C
C
DTCFL = MIN(DTCFL, DTMIN)
CONTINUE
3
C
C
C
ADJUST DTCFL FOR VISCOUS EFFECT (TRIAL AND ERROR)
DT
RETURN
END
SUBROUTINE TRANS
PARAMETER (MK = 130, MJ = 115)
COMMON // DETA, DZETA, CV, RC, PR, PRI, GAMMA, DTL(MJ), GAMMA1,
CFL, BETA, UINF, RHOINF, CINF, TINF, TH, DT, CX, CY, L, JL, KL,
JLM, KLM, ISMTXK, ISMTXJ, KSTAR(MJ)
COMMON /DOF/ X(MK, MJ), Y(MK, MJ), RY(MK, MJ)
COMMON /NOZ/ KNOZ, JNOZIN, JNOZOUT, JNMW, JNMOUT, JNERIN,
JNEROUT, P1NOZ, T1NOZ, ALPHA, EFFNOZ
COMMON /V/ ETX(MK, MJ), ETY(MK, MJ), ZTX(MK, MJ), ZTY(MK, MJ)
DIMENSION DJ(MK, MJ), ROJ(MK, MJ), XET(MK, MJ), XZT(MK, MJ),
YET(MK, MJ), YZT(MK, MJ)
ROET = 1.0 / (2.0 * DETA)
ROZT = 1.0 / (2.0 * DZETA)
JLM2 = JLM - 1
KLM2 = KLM - 1
GENERATE DX/DETA AND DY/DETA
ONE-SIDED DIFFERENCING FOR J = 1
DO 1 KV = 1, KL
  XET(KV, 1) = (4.0 * X(KV, 2) - X(KV, 3) - 3.0 * X(KV, 1)) *
  ROET
  YET(KV, 1) = (4.0 * Y(KV, 2) - Y(KV, 3) - 3.0 * Y(KV, 1)) *
  ROET
1 CONTINUE
ONE-SIDED DIFFERENCING FOR J = JL
DO 2 KV = 1, KL
  XET(KV, JL) = (4.0 * X(KV, JLM) - X(KV, JLM2) - 3.0 * X(KV,
  JL)) * ROET
  YET(KV, JL) = (4.0 * Y(KV, JLM) - Y(KV, JLM2) - 3.0 * Y(KV,
  JL)) * ROET
1 CONTINUE
2
C
C
C
CENTRAL DIFFERENCING FOR FIELD POINTS
DO 4 JV = 2, JLM
  JP = JV + 1

```

```

JM      = JV - 1
KS      = 1
DO 3 KV = KS, KL
XET(KV, JV) = X(KV, JP) - X(KV, JM) * RDET
YET(KV, JV) = Y(KV, JP) - Y(KV, JM) * RDET
CONTINUE
3
4
C C C C

ONE-SIDED DIFFERENCING FOR J = JNHOUT
JV = JNHOUT
JVP = JV + 1
JVP2 = JV + 2
DO 5 KV = 1, KNOZ
XET(KV, JV) = (4.0 * X(KV, JVP) - X(KV, JVP2)) - 3.0 *
X(KV, JVP) * RDET
YET(KV, JV) = (4.0 * Y(KV, JVP) - Y(KV, JVP2)) - 3.0 *
Y(KV, JVP) * RDET
CONTINUE
5
C C C C

ONE-SIDED DIFFERENCING FOR J = JNHIN
JV = JNHIN
JVM = JV - 1
JVM2 = JV - 2
DO 6 KV = 1, KNOZ
XET(KV, JV) = -(4.0 * X(KV, JVM) - X(KV, JVM2)) - 3.0 * X(KV,
JV) * RDET
YET(KV, JV) = -(4.0 * Y(KV, JVM) - Y(KV, JVM2)) - 3.0 * Y(KV,
JV) * RDET
CONTINUE
6
C C C C

GENERATE DX/DZETA AND DY/DZETA
ONE-SIDED DIFFERENCING FOR K = 1
DO 7 JV = 1, JL
XZT(1, JV) = (4.0 * X(2, JV) - X(3, JV)) - 3.0 *
X(1, JV) * RDT
YZT(1, JV) = (4.0 * Y(2, JV) - Y(3, JV)) - 3.0 *
Y(1, JV) * RDT
CONTINUE
7
C C C C

ONE-SIDED DIFFERENCING FOR K = KL
DO 8 JV = 1, JL
XZT(KL, JV) = -(4.0 * X(KLM, JV) - X(KLM2, JV)) - 3.0 * X(KL,
JV) * RDT
YZT(KL, JV) = -(4.0 * Y(KLM, JV) - Y(KLM2, JV)) - 3.0 * Y(KL,
JV) * RDT
CONTINUE
8
C C C C

CENTRAL DIFFERENCING FOR FIELD POINTS
DO 10 JV = 1, JL
DO 9 KV = 2, KLM
KP = KV + 1
KH = KV - 1
XZT(KV, JV) = X(KM, JV) * RDZT
YZT(KV, JV) = Y(KP, JV) - Y(KM, JV) * RDZT
CONTINUE
9
C C C C

```

```

10 CONTINUE
C
C ONE-SIDED DIFFERENCING FOR K = KNOZ
DO 11 JV = JMIN, JNMOUT
  KS = KNOZ
  KSP = KS + 1
  KSP2 = KS + 2
  XZT(KS, JV) = (4.0 * X(KSP, JV) - X(KSP2, JV) - 3.0 *
1  X(KS, JV)) * RDZT
  YZT(KS, JV) = (4.0 * Y(KSP, JV) - Y(KSP2, JV) - 3.0 *
1  Y(KS, JV)) * RDZT
11 CONTINUE
C
C GENERATE THE INVERSE JACOBIAN OF TRANSFORMATION
DO 13 JV = 1, JL
  DO 12 KV = 1, KL
    DJ(KV, JV) = XET(KV, JV) * YZT(KV, JV) - XZT(KV, JV) *
1  YET(KV, JV)
12 CONTINUE
13 CONTINUE
C
DO 15 JV = 1, JL
  DO 14 KV = 1, KL
    RDJ(KV, JV) = 1.0 / DJ(KV, JV)
14 CONTINUE
15 CONTINUE
C
C GENERATE THE METRICS OF THE COORDINATE TRANSFORMATION
DO 17 JV = 1, JL
  DO 16 KV = 1, KL
    ETX(KV, JV) = YZT(KV, JV) * RDJ(KV, JV)
    ZTX(KV, JV) = - YET(KV, JV) * RDJ(KV, JV)
    ETY(KV, JV) = - XZT(KV, JV) * RDJ(KV, JV)
    ZTY(KV, JV) = XET(KV, JV) * RDJ(KV, JV)
16 CONTINUE
17 CONTINUE
C
C GENERATE THE 1 / R TERM
DO 18 KV = 1, KL
  RY(KV, 1) = 0.0
  DO 18 JV = 2, JL
    RY(KV, JV) = 1.0 / Y(KV, JV)
18 CONTINUE
18 RETURN
END

```

Appendix C: Post-Processing Program AUGMENT

```

PROGRAM AUGMENT
PARAMETER JL = 115, KL = 130, KNOZ = 46)
COMPUTES THE THRUST AUGMENTATION BY INTEGRATING
THE X-MOMENTUM AT THE EXIT COMPARING THE
RESULTING THRUST TO THE ISENTROPIC THRUST.
COMMON /RANDATA/ RJ(JL), U(JL), RHO(JL), RHOREF, UREF
WRITE A HEADER
OPEN (6, FILE = 'EJTHRST', FORM = 'FORMATTED', STATUS = 'NEW')
WRITE(6,100)
WRITE(6,110)
WRITE(6,120)
WRITE(6,130)
WRITE(6,140)
JLM = JL - 1
VELNOZ = 478.725
RHON0Z = 2.465687 E-03
AREAN0Z = 0.9066386 E-02
READ DATA
CALL READDAT
CALCULATE X-MOMENTUM
R = 0.5 * RJ(J)
XMOH = 3.14159 * R * R * RHO(1) * U(1) * U(1)
DO 10 J = 2, JLM
JP = J - 1
JM = J + 1
DELTAR = 0.5 * (RJ(JP) + RJ(JM))
XMOH = XMOH + 6.283185 * RJ(J) * DELTAR * RHO(J) *
U(J) * U(J)
10 CONTINUE
CALCULATE THRUST AND REFERENCE (ISENTROPIC) THRUST
AND GET THRUST AUGMENTATION RATIO
THRST = XMOH
REFTHRST = RHON0Z * VELNOZ * AREAN0Z
PHI = THRST / REFTHRST
OUTPUT THRUST, REFERENCE THRUST AND THRUST
AUGMENTATION RATIO
WRITE(6,150)
WRITE(6,140)
WRITE(6,160) THRST, REFTHRST, PHI
STOP
100 FORMAT ( ' THIS PROGRAM CALCULATES THE THRUST GENERATED' )
110 FORMAT ( ' BY THE EJECTOR AND COMPARES IT TO THE ISENTROPIC' )
120 FORMAT ( ' THRUST OF THE NOZZLE ALONE TO ARRIVE AT A THRUST' )
130 FORMAT ( ' AUGMENTATION RATIO.' )
140 FORMAT ( ' )
150 FORMAT ( 4X, 'X-MOM THRUST', 4X, 'ISEN THRUST', 6X, 'PHI' )

```

```

160 FORMAT ( 3F13.5 )
C
END
SUBROUTINE READDAT
PARAMETER (JL = 115, KL = 130, KNOZ = 46)
COMMON /RANDATA/ RJ(JL), U(JL), RHO(JL), RHOREF, UREF
OPEN (64, FILE = 'EJTEMP', FORM = 'FORMATTED', STATUS = 'OLD')
READ (64,200) RHOREF
READ (64,200) UREF
READ (64,200)
READ (64,200)
READ DATA FOR EXIT PLANE
DO 10 J = 1, JL
READ (64,220) RJ(J), RHO(J), U(J)
RHO(J) = RHOREF
U(J) = U(J) * UREF
10 CONTINUE
FORMAT ( 31X, E15.7 )
FORMAT ( 31X, F10.4 )
FORMAT ( 18X, G11.5, G13.5, G11.5 )
END
C
10
200
210
220
C

```

Bibliography

1. Anderson, D. A., J. C. Tannehill and R. H. Pletcher. Computational Fluid Mechanics and Heat Transfer. New York: Hemisphere Publishing Corporation, 1984.
2. Baldwin, B. S. and H. Lomax. 'Thin Layer Approximation and Algebraic Model for Separated Turbulent Flows,' AIAA Paper 78-257 (January 1978).
3. Hankey, W. L. and J. S. Shang. 'Natural Transition - A Self Excited Oscillation,' AIAA Paper 82-1011 (June 1982).
4. Hasen, Capt. Gerald A. 'Navier-Stokes Solutions for an Axisymmetric Nozzle in a Supersonic External Stream,' AFWAL Technical Report 81-3161 (March 1982).
5. Hill, P. G. and C. R. Peterson. Mechanics and Thermodynamics of Propulsion. Reading, Massachusetts: Addison-Wesley Publishing Company, 1965.
6. Kedem, Maj. Eli. Israeli Air Force. An Experimental Study of Static Thrust Augmentation Using a 2-D Variable Ejector. MS Thesis AFIT/GAE/AA/79D-7. School of Engineering, Air Force Institute of Technology (AU), Wright-Patterson AFB OH, December 1979.
7. Kohlman, D. L. Introduction to V/STOL Airplanes. Ames, Iowa: Iowa State University Press, 1981.
8. Lewis, Capt. William D. US Army. An Experimental Study of Thrust Augmenting Ejectors. MS Thesis AFIT/GAE/AA/83D-13. School of Engineering, Air Force Institute of Technology (AU), Wright-Patterson AFB OH, December 1983.

Bibliography (cont.)

9. McCormick, B. W. Jr. Aerodynamics of V/STOL Flight.
Orlando, Florida: Academic Press, 1967.
10. Olson, L. E., P. R. McGowan and R. W. MacCormack.
'Numerical Solution of the Time-Dependent Compressible
Navier-Stokes Equations in Inlet Regions,' NASA TM-X-
62338 (March 1974)
11. Reznick, Capt. Steven G. An Experimental Study of
Circular and Rectangular Thrust Augmenting Ejectors.
MS Thesis AFIT/GAE/AA/80D-18. School of Engineering,
Air Force Institute of Technology (AU), Wright-
Patterson AFB OH, December 1980.
12. Roache, P. J. Computational Fluid Dynamics.
Albuquerque, New Mexico: Hermosa Publishers, 1972.
13. Shang, J. S., W. L. Hankey, and R. E. Smith. 'Flow
Oscillations of Spike-Tipped Bodies,' AIAA Paper
80-0062 (January 1980).
14. Shang, J. S. and R. W. MacCormack. 'Flow Over a
Biconic Configuration with an Afterbody Compression
Flap,' AFWAL Technical Report 84-3059 (April 1984).
15. Stock, H. W. and W. Haase. 'Determination of Length
Scales in Algebraic Turbulence Models for Navier-Stokes
Methods,' AIAA Journal Vol 27, No 1: 5-14 (January
1989).

Bibliography (cont.)

16. Uhuad, Capt. Generoso C. An Experimental Investigation of a Circular Thrust Augmenting Ejector. MS Thesis AFIT/GAE/AA/86M-3. School of Engineering, Air Force Institute of Technology (AU), Wright-Patterson AFB OH, December 1985.
17. Unnever, Capt. Gregory. An Experimental Study of Rectangular and Circular Thrust Augmenting Ejectors. MS Thesis AFIT/GAE/AA/81D-31. School of Engineering, Air Force Institute of Technology (AU), Wright-Patterson AFB OH, December 1981.
18. Von Kármán, T. "Theoretical Remarks on Thrust Augmentation," Contributions to Applied Mechanics. Reissner Anniversary Volume, Ann Arbor, Michigan, pp 461-468, 1949.
19. Zucrow, M. J. and J. D. Hoffman. Gas Dynamics Vol 1, New York: John Wiley & Sons, 1976.

Vita

Captain Kenneth R. Gage [REDACTED]

[REDACTED] He moved to Branford, Connecticut in 1965 and graduated from Branford High School in 1980. He was accepted to and attended the United States Air Force Academy in Colorado Springs, Colorado, from which he received the degree of Bachelor of Science in Astronautical Engineering and a regular commission in the USAF on 30 May 1984. He then went to Headquarters, USAF Space Division (AFSC) at Los Angeles AFB where he served as a flight operations manager for the Inertial Upper Stage and as an advanced launch systems project officer until entering the School of Engineering, Air Force Institute of Technology, in May 1988.

[REDACTED] [REDACTED] ROAD

[REDACTED]

REPORT DOCUMENTATION PAGE

FORM 487-100-2
FEB 80

1 AGENCY USE ONLY (Leave blank)		2 REPORT DATE December 1990	3 REPORT TYPE AND DATES COVERED Master's Thesis
4 TITLE AND SUBTITLE Numerical Analysis of an Axisymmetric Thrust Augmenting Ejector			5 FUNDING NUMBERS
6 AUTHOR(S) Kenneth R. Gage, Capt, USAF			
7 PERFORMING ORGANIZATION NAME(S) AND ADDRESS(ES) Air Force Institute of Technology, WPAFB OH 45433-6583			8 PERFORMING ORGANIZATION REPORT NUMBER AFIT/GAE/ENY/89D-10
9 SPONSORING MONITORING AGENCY NAME(S) AND ADDRESS(ES) Flight Dynamics Laboratory WRDC/FIMM Wright Research and Development Center Wright-Patterson AFB OH 45433			10 SPONSORING MONITORING AGENCY REPORT NUMBER
11 SUPPLEMENTARY NOTES			
12a DISTRIBUTION AVAILABILITY STATEMENT Approved for public release; distribution unlimited			12b DISTRIBUTION CODE
13 ABSTRACT (Maximum 200 words) Use of an ejector is an effective way to increase the thrust produced by a jet. In this thesis project an axisymmetric ejector concept which has been previously explored by experiment was numerically modeled. An existing axisymmetric, internal flow code based on the explicit MacCormack method was modified to incorporate primary nozzle structure and flow injection within the flowfield. Results were compared qualitatively and quantitatively with experimental results to verify the validity of the model. Internal flow structure, difficult to obtain in experiment, is easily examined. This code may be used for parametric analysis of such ejector performance parameters as primary nozzle location, flow injection angle, diffuser area ratio, nozzle area ratio, and inlet geometry to optimize future hardware configurations.			
14 SUBJECT TERMS Fluid Dynamics Axially Symmetric Flow Air Ejectors Fluid Flow Jet Mixing Flow Computational Fluid Dynamics (CFD)			15 NUMBER OF PAGES 104
			16 PRICE CODE
17 SECURITY CLASSIFICATION OF REPORT Unclassified	18 SECURITY CLASSIFICATION OF THIS PAGE Unclassified	19 SECURITY CLASSIFICATION OF ABSTRACT Unclassified	20 LIMITATION OF ABSTRACT UL

GENERAL INSTRUCTIONS FOR COMPLETING SF 298

The Report Documentation Page (RDP) is used in announcing and cataloging reports. It is important that this information be consistent with the rest of the report, particularly the cover and title page. Instructions for filling in each block of the form follow. It is important to **stay within the lines to meet optical scanning requirements.**

Block 1. Agency Use Only (Leave Blank)

Block 2. Report Date. Full publication date including day, month, and year, if available (e.g. 1 Jan 88). Must cite at least the year.

Block 3. Type of Report and Dates Covered. State whether report is interim, final, etc. If applicable, enter inclusive report dates (e.g. 10 Jun 87 - 30 Jun 88).

Block 4. Title and Subtitle. A title is taken from the part of the report that provides the most meaningful and complete information. When a report is prepared in more than one volume, repeat the primary title, add volume number, and include subtitle for the specific volume. On classified documents enter the title classification in parentheses.

Block 5. Funding Numbers. To include contract and grant numbers; may include program element number(s), project number(s), task number(s), and work unit number(s). Use the following labels:

C - Contract	PR - Project
G - Grant	TA - Task
PE - Program Element	WU - Work Unit Accession No.

Block 6. Author(s). Name(s) of person(s) responsible for writing the report, performing the research, or credited with the content of the report. If editor or compiler, this should follow the name(s).

Block 7. Performing Organization Name(s) and Address(es). Self-explanatory.

Block 8. Performing Organization Report Number. Enter the unique alphanumeric report number(s) assigned by the organization performing the report.

Block 9. Sponsoring/Monitoring Agency Names(s) and Address(es). Self-explanatory.

Block 10. Sponsoring/Monitoring Agency Report Number. (If known)

Block 11. Supplementary Notes. Enter information not included elsewhere such as: Prepared in cooperation with...; Trans. of ..., To be published in When a report is revised, include a statement whether the new report supersedes or supplements the older report.

Block 12a. Distribution/Availability Statement.

Denote public availability or limitation. Cite any availability to the public. Enter additional limitations or special markings in all capitals (e.g. NOFORN, REL, ITAR)

DOD - See DoDD 5230.24, "Distribution Statements on Technical Documents."

DOE - See authorities

NASA - See Handbook NHB 2200.2.

NTIS - Leave blank.

Block 12b. Distribution Code.

DOD - DOD - Leave blank

DOE - DOE - Enter DOE distribution categories from the Standard Distribution for Unclassified Scientific and Technical Reports

NASA - NASA - Leave blank

NTIS - NTIS - Leave blank.

Block 13. Abstract. Include a brief (Maximum 200 words) factual summary of the most significant information contained in the report.

Block 14. Subject Terms. Keywords or phrases identifying major subjects in the report.

Block 15. Number of Pages. Enter the total number of pages.

Block 16. Price Code. Enter appropriate price code (NTIS only).

Blocks 17. - 19. Security Classifications. Self-explanatory. Enter U.S. Security Classification in accordance with U.S. Security Regulations (i.e., UNCLASSIFIED). If form contains classified information, stamp classification on the top and bottom of the page.

Block 20. Limitation of Abstract. This block must be completed to assign a limitation to the abstract. Enter either UL (unlimited) or SAR (same as report). An entry in this block is necessary if the abstract is to be limited. If blank, the abstract is assumed to be unlimited.